Investigating the production of a particulate plant-produced vaccine candidate against African horse sickness

Gloria Luhanga

Dissertation presented for the degree of Master of Science

Department of Molecular and Cell Biology

University of Cape Town

February 2021

Full name: Gloria Luhanga

Student Number: LHNGLO001

Course: MCB5005W

Declaration

I know that plagiarism is wrong. Plagiarism is to use another's work and pretend that it is one's own.

I have used the **Harvard** convention for citation and referencing. Each contribution to, and quotation in, this **Dissertation** from the work(s) of other people has been attributed and has been cited and referenced.

This **Dissertation presented for the degree of Master of Science in the Department of Molecular and Cell Biology** is my own work.

I have not allowed, and will not allow, anyone, to copy my work with the intention of passing it off as his or her own work.

Signature

Signed by candidate

Date: 10 February 2021

Acknowledgments

I would like to take this time to firstly thank my co-supervisor, Dr. Susan Jennifer Dennis for allowing me to experience the best two years as a young researcher. Thank you for all your guidance, advices and tremendous patience. Thank you for all the support throughout this journey and for always making room for me to grow and work independently. I'm blessed to have been one of your students.

I would like to thank my supervisor, Assoc. Prof Inga Hitzeroth and co-supervisor Dr. Ann Meyers for giving me the best guidance and support whenever I needed it.

Thank you to Dr. Alta van Zyl, Dr. Megan Hendriks and Jennifer Wayland for always being willing to help me, even in your busy times. Jennifer "Jenni", a special thank you for the polyclonal rabbit anti-ST-AP205 sera and your assistance with the SpyTag/SpyCatcher work.

Thank you to my fellow Biopharming Research Unit members, it was great getting to know each one of you and working with you.

Thank you to Mohammed Jaffer for the TEM assistance.

Thank you to the Lomonossoff lab for providing the pEAQ-HT expression vector.

Thank you to the National Research Foundation (NRF) for providing funding for this project.

Thank you to my family and friends for your endless love and support. To my dad, Gordon Luhanga for all your sacrifices and my mum, Rose Luhanga for your constant encouragement throughout this journey.

Lastly, my greatest gratitude goes to my Heavenly Father (God) for making it all possible.

"But seek ye first the kingdom of God, and His righteousness; and all these things shall be added you." Matthew 6:33.

Table of Contents

Abstract

African horse sickness (AHS) is a non-communicable, infectious disease that affects equids and is mainly prevalent in sub-Saharan Africa. The disease has a major impact on the economy of the equine industry as well as an emotional impact on horse owners. There are nine known serotypes of African horse sickness virus (AHSV), which is spread by *Culicoides* midges. Currently, a multivalent live attenuated vaccine is the only vaccine licensed for use in South Africa. However, it has the inherent risk of reverting to virulence as well as the possibility of genome segment reassortment between vaccine and outbreak strains. Additionally, it is not DIVA compliant (cannot Differentiate between Infected and Vaccinated Animals). There is therefore a need for a safer and more cost-effective alternative vaccine to protect horses against AHSV.

Virus-like particles (VLPs) that display antigens on their surface may be suitable vaccine platforms. One such display particle is the phage AP205 VLP, which is comprised of AP205 coat proteins. To aid antigen display, studies have utilized the SpyTag (ST) - SpyCatcher (SC) or “plug-and-display” system, a novel conjugation system used to display several antigens fused to AP205 VLPs. This study aimed at displaying the neutralizing epitope of AHSV serotype 5, known as the VP2 domain (dom) (873bp), on phage AP205 VLP particles using the SpyTag/SpyCatcher technology. The display particle vaccine candidates were produced in *Nicotiana benthamiana* plants.

Firstly, AHSV 5 VP2dom was expressed by being linked to either the ST or SC peptide at its C-terminus. Recombinant pEAQ-AHSV 5-VP2dom ST and pEAQ-AHSV 5-VP2domSC plasmid constructs were constructed from the full-length pEAQ-AHSV 5-VP2-SpyTag and pEAQ-AHSV 5-VP2-SpyCatcher clones using in-fusion cloning. The ST/SC constructs were transformed into Stellar™ competent *E. coli* cells and thereafter into *Agrobacterium tumefaciens* AGL-1 cells. Expression time trials were conducted on plants infiltrated with the recombinant *Agrobacterial* strains to examine transient AHSV 5-VP2domST/SC small-scale expression. Expression was detected for AHSV 5 VP2domSC but not AHSV 5 VP2domST using guinea pig anti-AHSV 5 and rabbit anti-ST-AP205 sera.

Secondly, the development of a particle display vaccine candidate was investigated by coupling AHSV 5 VP2domSC to plant-expressed ST-AP205 VLPs. Three coupling techniques, namely *in vitro* coupling of purified products, co-infiltration and co-purification, were deployed to determine the assembly of ST-AP205_AHSV 5 VP2domSC VLPs. *In vitro* coupling involved carrying out separate infiltrations and purification of pEAQ-ST-AP205 VLPs and pEAQ-AHSV 5 VP2domSC in plants and thereafter mixing the purified products. For co-infiltration, pEAQ-ST-AP205 VLPs and VP2domSC recombinant cultures were used together to infiltrate plants and the presence of complex formations was determined. During co-purification, the presence of coupled products was analysed following separate infiltration of plants with pEAQ-ST-AP205 and VP2domSC recombinant *Agrobacterial* strains; the homogenates were then incubated together at different VLP: antigen leaf:weight ratios. From the three coupling techniques, co-purification at a 1:1 VLP: antigen ratio was identified as the best coupling approach based on the quality and quantity of particles visualised by electron microscopy.

These findings indicate the potential of producing an AHSV vaccine candidate in plants, which is ultimately a safer and cheaper alternative to the currently-produced AHSV vaccine. Moreover, this preliminary data may pave the way for developing a vaccine that provides protection against all nine serotypes of AHSV by displaying VP2domSC for other serotypes on the ST-AP205 display particles.

List of Abbreviations and Symbols:

AHS	African horse sickness
BCIP	5-bromo, 4-chloro, and 3-indolylphosphate
bp	base pair(s)
BSA	bovine serum albumin
BTV	bluetongue virus
CP	coat protein
DISA	Disabled Infectious Single Animal vaccine
DISC	Disabled Infectious Single Cycle vaccine
DIVA	Differentiating Infected from Vaccinated Animals
DNA	deoxyribonucleic acid
dpi	days post infiltration
EDTA	ethylenediaminetetra-acetic acid
ELISA	enzyme linked immunosorbent assay
EtBr	ethidium bromide
g	gram(s)
g	gravitational force
h	hour(s)
kb	kilobase(s)
kDa	kiloDalton(s)
kPa	kiloPascal(s)
L	Litre(s)

LAV	live attenuated vaccine
LB	Luria broth
m	milli-
m	meter(s)
M	molecular marker
MES	2-morpholinoethanesulfonic acid
mg	milligram(s)
min	minute(s)
mL	millilitre(s)
mM	millimolar(s)
MVA	modified vaccinia Ankara
n	nano-
O/N	Overnight
OD	optical density
PAGE	polyacrylamide gel electrophoresis
PBS	phosphate buffered saline
PCR	polymerase chain reaction
rpm	revolutions per minute
RT	room temperature
RuBisCO	Ribulose-1,5-bisphosphate carboxylase/oxygenase
S	second(s)
SC	SpyCatcher

SDS	sodium dodecyl sulphate
ST	SpyTag
TBE	Tris-borate-EDTA buffer
T-DNA	transfer-DNA
TEM	transmission electron microscopy
Tris	tris(hydroxymethyl)aminomethane
TSP	total soluble protein
V	Volts
VLP	virus-like particle
µ	micro-
Ω	Ohm (resistance)
%	Percentage
˚C	degrees Celsius
=	equals/is
3’	three prime end
5’	five prime end

Chapter 1: Literature review

1.1 Introduction

African horse sickness (AHS) is the most lethal disease of equids worldwide. The mortality rate ranges from 70-95% depending on the form of the disease (Coetzer and Guthrie, 2004). Mules are less susceptible than horses, with a mortality rate of 50-70%, and other equids like donkeys and zebras are merely reservoirs of the disease. Clinical signs of the disease are seen as a result of damage to the respiratory and pulmonary systems. The most severe form of AHS is the pulmonary form, with a mortality rate of more than 95%, while the cardiac form has a fatality rate of about 50%.

African horse sickness is transmitted by biting midges of the *Culicoides* genus which feed on infected vertebrate hosts (Robin *et al*., 2016). The disease is non-contagious but is infectious. Within Africa, AHS is mainly prevalent in sub-Saharan countries, with occasional outbreaks being reported in Northern Africa. Interestingly, no reports of outbreaks in Madagascar or Mauritius have been made. Other countries outside of Africa have also been affected by AHS namely, the Middle East, South East Asia, the Indian sub-continent, Spain and Portugal (Roy *et al*., 1994b, Howell, 1962). Most recently, May 2020, 500 horses were reported dead from AHS in Thailand (Lesté-Lasserre, 2020). Due to the continuous spread of the disease across this country, including its border areas, vaccination strategies have been put into place to try and reduce AHS spread. The severity and rapid spread of the disease has thereby qualified it to be listed by the Office International des Epizooties (OIE: The World Organization for Animal Health) as a notifiable disease worldwide.

1.2 History of AHS

The severity of the spread of AHS caused a high economic and emotional impact, which drew the attention of horse owners and users in the early years. The first recorded outbreak of the disease occurred in 1327 in Yemen. However, it is believed that the disease originated in Africa, with the earliest documentation being reported in central and southern Africa during the seventeenth century. Here, AHS outbreaks had a significant impact on both civilian and military transport. In South Africa, the disease was only recognized after the importation of horses in 1657. Following this, the first major outbreak was recorded in 1719, in which over 1700 animals died (Mellor and Hamblin, 2004). The largest outbreak in South Africa resulted in the loss of 70 000 horses between the years 1854 -1855. Namibia was also noted as one of the southern African countries with frequent and severe AHS outbreaks (Liebenberg et al., 2015). In 2011, Namibia lost a an estimated 10% of its horse population to AHS (Gordon et al., 2017).

Due to the social impacts of the disease, it has led to the development of veterinary science in affected regions. In South Africa, the first research on African horse sickness virus (AHSV), now known to be the aetiological agent of AHS, was conducted by Alexander Edington in 1891 (Verwoerd, 2012). During his early research, Edington suggested that the disease may be caused by either fungi or microbes. However, in later experiments, it was discovered that the disease was caused by a virus. The evidence to this was his ability to attenuate the AHSV in mice through serial intracerebral passages (Alexander, 1935). This allowed for the conversion of the virulent viscerotropic isolates to a neurotropic strain of the virus, with retention of its immunogenic capacity. Arnold Theiler's research also focused on AHS (Theiler, 1921, Verwoerd, 2012). He identified what he called the 'plurality of immunologically distinct strains' of AHSV. It was apparent to him that immunization with one strain of AHSV could not protect against other strains (Theiler, 1921). This observation was verified in a cross-neutralization test in mice (Howell, 1962). It involved the use of viral antigens from horse blood samples, which were intracerebrally injected into suckling mice. Antibodies from the mice brain tissues were then used for the immunization of both rabbits and guinea-pigs to produce antisera

specific to the isolated virus strains. This and other studies altogether led to the recognition that there are nine distinct serotypes of AHSV (Howell, 1962, McIntosh, 1958).

1.3 African horse sickness virus

1.3.1 Aetiology

African horse sickness virus is a member of the *Orbivirus* genus of the family *Reoviridae*. Orbiviruses are pathogens that normally affect livestock. They were historically classified as arboviruses; viruses that can multiply in both vertebrates and their arthropod vectors (Bordon *et al*., 1971, Spence *et al*., 1984). Viruses of the *Reoviridae* family, including Bluetongue virus (BTV) and AHSV are complex non-enveloped RNA viruses with similar morphological and physicochemical properties. These ±80 nm icosahedral virions are characterized by a core with 10-12 distinct genome segments of linear, double-stranded RNA (dsRNA) (Figure 1.1). The genome segments code for four major proteins (VP2, VP3, VP5, and VP7), three minor proteins (VP1, VP4 and VP6) and four non-structural (NS) proteins (NS1, NS2, NS3/3A, and NS4) (MacLachlan and Guthrie, 2010, Roy, 2008, Scacchia *et al*., 2015, Roy, 2004).

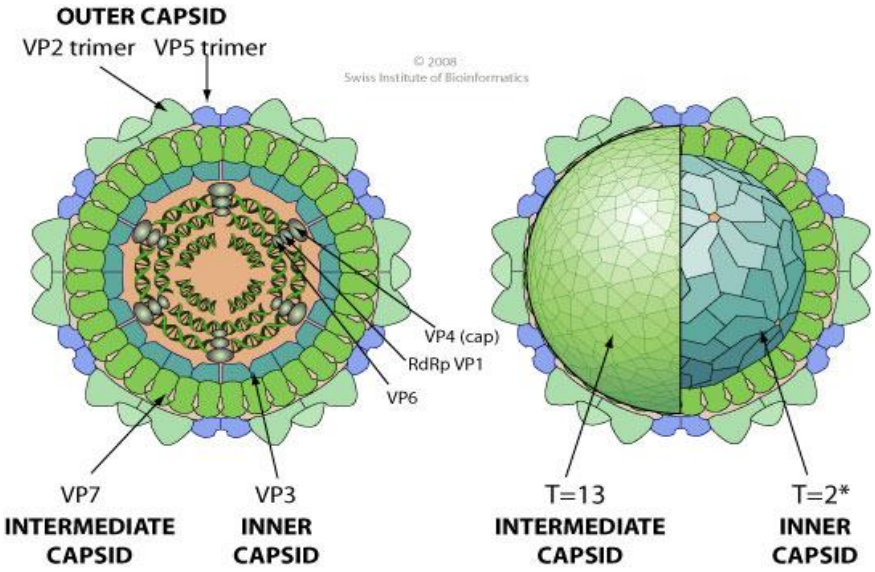

Figure 1.1: AHSV particle structure. Non enveloped, icosahedral, non-turreted virion with a triple capsid structure, about 80 nm in diameter. The intermediate capsid has a T=13 icosahedral symmetry, the inner capsid a T=2* icosahedral symmetry. (Photo retrieved from https://viralzone.expasy.org/106?outline=complete_by_species).

Orbiviruses like AHSV and BTV can be classified based either on having a double-stranded RNA genome or being resistant to certain chemicals such as ether (Bordon *et al*., 1971). The use of chemicals has been used mainly as a stability test for the viruses. Previous studies have shown that AHSV is resistant to both sodium deoxycholate and diethyl ether when the virus was grown in mouse brains. Moreover, a California bluetongue-8 (BT-8) strain of BTV showed no inactivation when the virus was treated with ether and sodium deoxycholate (Studdert, 1965).

Orbiviruses may also be classified according to their serological groups (Gorman *et al*., 1983). Currently, there are thirteen known orbivirus serological groups; where each group is named after the first virus isolated. There is no common generic antigen that has been found. Therefore, each of the viruses is grouped by their ability to share common complement-fixing antigens and are identified through specific reactions in serum-neutralization tests (Gorman *et al*., 1983). For instance, using the complement fixation test, allowed for the identification of AHSV serotype-specific antigens i.e. serotypes 1, 2,

3, 7, 8, and 9 through an antigen-antibody complex using monkey kidney stable host cell line antigens and horse antisera (Ozawa, 1968).

1.3.2 Viral attachment and entry

Viral entry and penetration into host cells leads to irreversible changes to the virus particle. Non-enveloped viruses such as reoviruses, adenoviruses, and picornaviruses depend either on the protein-mediated rupture of endosomes to release the uncoated protein, or the formation of a protein-lined transmembrane pore to translocate the genome into the cytoplasm (Hassan *et al*., 2001). The Orbivirus genus within the *Reoviridae* family comprises of three concentric layers of viral structural protein: outer, intermediate and inner capsid layer containing the genome (Rutkowska *et al*., 2019).

The outer capsid protein VP2, one of the key focus of this study, determines the serotype of the virus as it contains the antigenic determinants which elicit a neutralizing antibody response. This protein also mediates attachment to the host cell receptors during initial host infection (Roy, 2004, Zhang *et al*., 2010). Due to similarities between AHSV and BTV, they share common viral entry and replication mechanisms. Zhang *et al* (2010) have postulated that BTV VP2 attaches to the host cell surface receptors through the tip domain located on the outer-coat VP2 triskelion. This triskelion is an assembly of three VP2 monomers, where each monomer contains a hub, body and tip domain (Figure 1.2 A & B). VP2 attachment is further mediated by the attachment of the sialic acid (SA) - binding domain to a cell surface glycoprotein (Figure 1.2 C), thus implicating that sialic acid plays a role during the infection of host cells. Apart from facilitating in host cell attachment, VP2 capsid protein also determines the serotype of the AHSV virus and is the major target for neutralizing antibodies (Kanai *et al*., 2014).

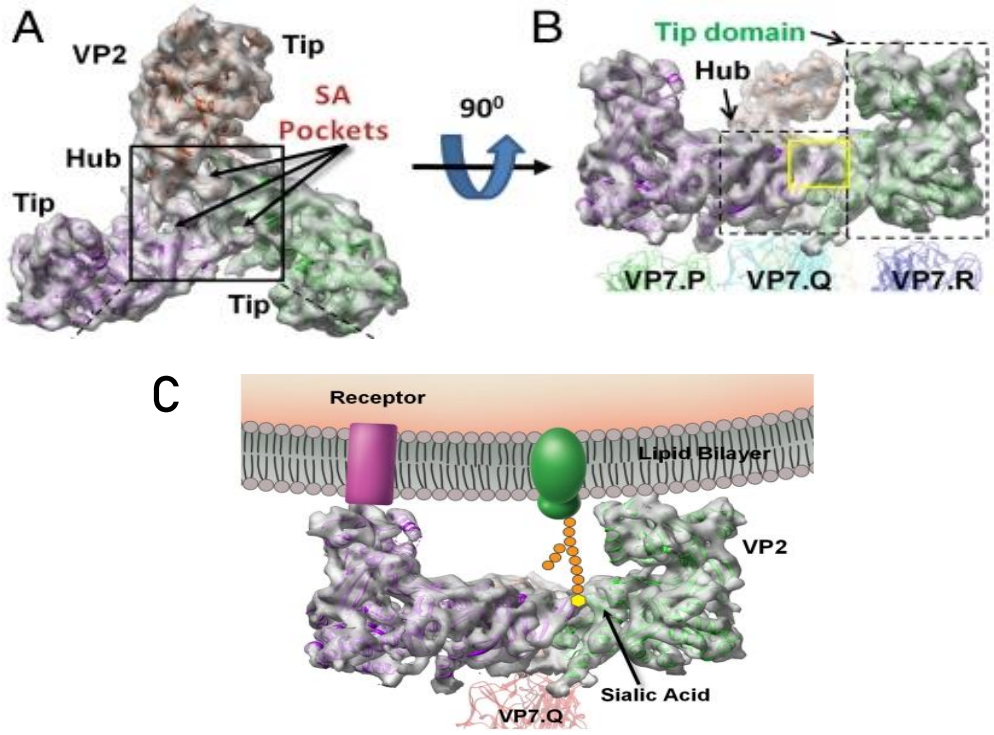

Figure 1.2: Schematic illustration of BTV/AHSV outer capsid protein VP2 and its attachment to the host cell membrane. Top (A) and side (B) views of the density map of a VP2 triskelion shape formed by trimerization of three tip domains and a hub (black box) comprised of three hub domains, the base of which interacts with a Q VP7 trimer. The VP2 SA binding site is indicated by the yellow box. (C) BTV/AHSV VP2 trimers are thought to attach via their tip domains to cell surface receptors and by the SA-binding domain to a cell surface glycoprotein. *Image used with permission from the publisher* (Zhang *et al*., 2010).

African horse sickness virus VP5 is another outer capsid protein, which also exists as a trimer. This capsid protein plays a vital role in host cell attachment, including viral penetration during the initial stages of infection (Hassan *et al*., 2001). It is highly conserved and contains coiled-coil motifs typical of fusion proteins. Cryo-electron microscopic analysis (cryoEM) of BTV virions shows that the VP5 trimer is a globular complex (Figure 1.3). To achieve viral penetration, each of the VP5 trimers is anchored to the membrane by the triplets of the amphipathic and hydrophobic helices. The external surface of VP5 contains 12 additional amphipathic helical regions which may extend to allow contact of the hydrophobic regions with the membrane and destabilize it, thereby

allowing penetration of the virus (Zhang *et al*., 2010). The release of the BTV core into the host cytoplasm is also believed to be dependent on acidic pH. In an *in vitro* study, a pH of 5.0 resulted in complete removal of VP2 and left VP5 exposed to facilitate virion entry into the cell (Huismans *et al*., 1987). Furthermore, it was shown that the addition of compounds that increase the lysosomal or endosomal pH, prevents endocytosed virus particles from entering the cytoplasm (Hassan *et al*., 2001). After penetration, the VP5 protein thereby delivers transcriptionally active core particle comprising of two major structural proteins (VP3 and VP7) and three minor proteins (VP1, VP4, and VP6) including the 10 dsRNA gene segments into the host cytosol (Zhang *et al*., 2010, Roy, 2004).

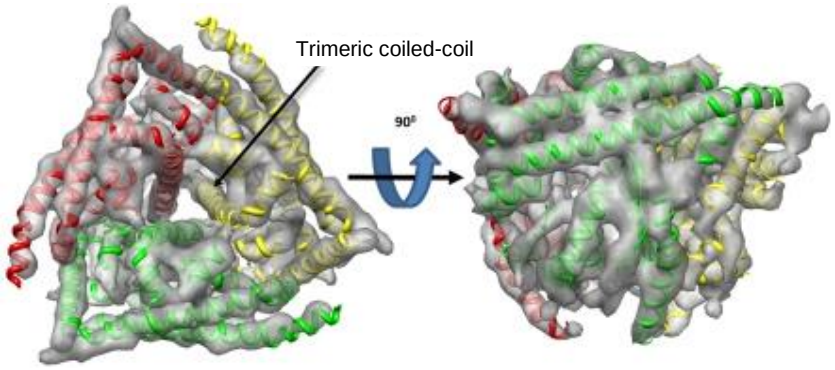

Figure 1.3: Schematic illustration of the fold of VP5. Sixfold averaged density map of the VP5 trimer, viewed from top and side, with an embedded ribbon model. *Image used with permission from the publisher* (Zhang *et al*., 2010).

1.4 Clinical diagnosis

Four different forms of AHS have been described, the per-acute (pulmonary) form, the sub-acute (cardiac) form, acute (mixed) form and subclinical (horse sickness fever) form (Stern, 2011). However, sudden death can also occur without the presence of clinical signs. The pulmonary and mixed form appear to be the most predominant in susceptible horses, with a mortality rate of between 50-95%. Moreover, the pulmonary form has a short incubation period of 3-5 days and affected horses display acute fever (40-42°C),

respiratory distress, coughing, abnormal posture, frothy nasal exudate and redness of conjunctivae (Laegreid, 1994). Almost all horses with this form die within 4-5 days of symptom development.

On the other hand, the cardiac form of AHS has a longer incubation period. The mortality rate of horses ranges from 50-70% and the majority of infected horses die 4-8 days after the onset of the clinical signs. Horses affected with this form display a fever of between 39-41°C, severe depression, oedema of the supraorbital fossae, eyelids, tongue, facial tissues, neck, thorax and shoulders (Demissie, 2013). Death is often caused by cardiac failure. A combination of both the pulmonary and cardiac forms occur frequently. The mortality rate of this mixed form of the disease is roughly 70-80% and affected horses die 3-6 days after onset of signs. In most cases, horses with a mixed form of AHS, display subclinical signs, followed by severe respiratory distress due to the cardiac form (Stern, 2011). However, in some cases, mild respiratory signs are followed by oedema and death due to cardiac failure.

The horse sickness form of AHS is a mild to subclinical disease, characterized by fever (up to 40°C), which is mainly noticeable in the afternoon and lasts for 3 to 5 days. Other symptoms can include congestion of mucous membranes, tachycardia, anorexia and depression (Laegreid, 1994). However, all horses with this form generally recover and death is unusual.

1.5 Prevention and control

There is no specific treatment for AHS. However, preventative measures have been deployed to help prevent animals from contracting AHS. These measures include, decreasing the exposure of horses to biting midges and other insects like mosquitoes and biting flies, which may be carriers of the virus (Mellor and Hamblin, 2004). This is established by stabling all equids in insect-proof housing between dusk and dawn when *Culicoides* are most active. Additionally, the use of insect repellents, insecticides and/or larvicides, may be used as vector control measures. However, despite these good

husbandry practices vaccination of animals remains the most successful method of prevention and control.

1.5.1 Live attenuated vaccines

Alexander Edington was the first to develop an effective attenuated vaccine for horses in 1935 (Verwoerd, 2012). This involved the use of a mouse-adapted strain of AHSV which was inoculated into chicken embryos. The passage of the virus strain through the embryonated eggs resulted in the formation of an attenuated virus, which maintained its immunogenic capacity. The only prophylactic vaccine against AHS registered in South Africa is the freeze-dried polyvalent live-attenuated vaccine (LAV) produced by Onderstepoort Biological Products (OBP). There are two formulations of this vaccine, which are administered three to four weeks apart: a trivalent bottle, containing AHSV-1, 3 and 4 and a tetravalent bottle, containing AHSV-2, 6, 7 and 8. However, AHSV-5 and AHSV-9 are not included. This is because of the residual virulence that was recorded with AHSV-5 in 1993, and AHSV-9 rarely occurs in the southern African regions (Verwoerd, 2012, von Teichman *et al*., 2010). In addition protection is afforded by cross-protection with serotype 1 and 2, serotype 3 and 7, serotype 6 and 9. However, serotype 4 does not cross-react with any of the other serotypes (von Teichman *et al*., 2010).

Although the live attenuated vaccine is the only currently licensed vaccine, it is not registered for use in countries outside of Africa. Furthermore, there are concerns regarding its ability to revert to virulence as well as the possibility of genome segment reassortment between the LAVs (vaccine strains) and wild type AHSV (outbreak) strains (Weyer *et al*., 2016). Moreover, it is not possible to differentiate between vaccinated and infected (DIVA) animals in vaccinated horse populations (Castillo-Olivares *et al*., 2011). There has therefore been an increased interest in the development of new, safer and more effective alternative vaccine candidates over the last 30 years (Aksular *et al*., 2018).

1.5.2 Alternative vaccines strategies

1.5.2.1 Inactivated vaccines

Inactivated vaccines are those comprising of virulent viruses disrupted through the use of physical or chemical agents to reduce their infectivity but maintain their immunogenicity (Dai et al., 2019). Some of the chemicals used to make these inactivated vaccines include formaldehyde, ß-propiolactone, or bromoethylenimine. In early studies, formalin was deployed to produce an inactivated tissue culture vaccine prepared either from viscerotropic or neurotropic AHSV-9. However, it was noted that the serological response in horses was poor (Ozawa and Bahrami, 1966). This posed a concern regarding the production of an AHS inactivated vaccine which would lead to high immunogenicity in horses. To achieve this, Mirchamsy and Taslimi (1968) included an adjuvant (aluminum hydroxide) when administering the inactivated AHSV-9 vaccine and achieved a significantly higher neutralizing antibody titre in horses. In 2016, an inactivated vaccine containing all nine serotypes was developed at the Central Veterinary Research Laboratory (CVRL) in Dubai (Wernery *et al*., 2016). It is administered simultaneously as two shots; The first shot contains five serotypes (1, 4, 7, 8 and 9) and the second shot four serotypes (2, 3, 5 and 6), administered together with an Imject™ Alum adjuvant (aluminum hydroxide and magnesium hydroxide). This inactivated vaccine was used in Kenyan horses and it was observed that no AHS fatalities occurred since 2011 on three premises. Serological follow-up investigations before and after vaccination with CVRL vaccine indicated an increase in antibody levels as compared to the antibody levels from horses previously and regularly vaccinated with the Onderstepoort vaccines.

Although the inactivated vaccine showed promising results in terms of safety and efficacy, it is associated with some drawbacks. Firstly, unlike live virus vaccines, inactivated vaccines do not provide very strong immune responses and require a much higher titre of the virus to be administered in order to provide equivalent protection in equids (Ozawa *et al*., 1967). Secondly, the use of appropriate adjuvants is recommended, and the production cost of this vaccine is also higher than that of live attenuated vaccines.

1.5.2.2 Recombinant vaccines

Recombinant vaccines are those developed through recombinant DNA technology. They are produced using several different expression systems such as bacteria, insects, yeast, plants, mammalian and cell-free systems. These systems are used for the production of proteins that code for protective antigens against pathogens and which are recognized by the host's immune system (Nascimento and Leite, 2012). As the outer capsid layer of AHSV is formed by proteins VP2 and VP5, different strategies may be employed using either one of these structures in an attempt to provide protection against AHSV.

1.5.2.2.1 Subunit vaccines

Subunit vaccines consist of natural substances, such as an antigenic portion of the pathogen rather than the entire microorganism (Foged *et al*., 2015). Over the years, studies have been conducted to produce an effective recombinant subunit vaccine against AHSV (Du Plessis *et al*., 1998, Martínez-Torrecuadrada *et al*., 1996, Roy *et al*., 1996, Stone-Marschat *et al*., 1996). These studies deployed the use of baculovirus- and vaccinia virus-expressed AHSV VP2 to protect horses when challenged with a virulent AHSV strain. However, much variability in the level of protection was observed following immunization with the first-generation baculovirus-expressed AHSV VP2 vaccines. To enhance immunogenicity, the vaccine was administered together with an adjuvant. Some degree of efficacy and safety has been achieved using subunit vaccines (Scanlen *et al*., 2002) and due to the nature of this vaccine, it is easier to differentiate between vaccinated and infected animals, thereby speeding up the process of clearance of horses for international movement (Du Plessis *et al*., 1998).

In recent developments, an avian reovirus muNS-Mi microsphere-based subunit BTV vaccine candidate was able to generate significant levels of neutralizing antibodies in IFNAR (-/-) mice whilst incorporated with VP2, VP7, and NS1 BTV-4 proteins into the microspheres (Marin-Lopez *et al*., 2014). Following this study, it was observed that the combination of this subunit vaccine with recombinant modified vaccinia virus Ankara (rMVA) expressing the same BTV antigens elicited a homotypic and heterotypic immunity and provided protection against homologous and heterologous infection with BTV-4 and BTV-1 (Marin-Lopez et al., 2014).

1.5.2.2.2 Poxvirus- vectored vaccines

Poxvirus-vectored vaccines are recombinant poxviruses that are used as gene delivery carriers. The poxvirus pathogenicity has been altered and can thereby safely express heterologous genes encoding foreign antigens (Nino-Fong and Johnston, 2008). Poxviruses can accommodate large foreign DNA inserts whilst maintaining viral stability, meaning that several antigens from a single pathogen or antigens from different pathogens may be delivered to the host organism to provide protective immunity. However, the main concern with this platform is safety. To overcome this problem, research has focused on producing attenuated vaccinia virus species and using non replicating avipoxvirus vectors in non-avian species; these have proved to be both safe and efficacious (Pastoret and Vanderplasschen, 2003).

1.5.2.2.2.1 Canarypox vaccines

Canarypox vaccine vectors are among those classified under the avipoxvirus genera and are restricted to avian species. Despite the restrictions, attenuated strains are commonly used because these are safe and effective carriers for use in mammalian hosts (Pastoret and Vanderplasschen, 2003). In a challenge study, a recombinant canarypox-vectored vaccine to AHSV 4 (ALVAC®–AHSV4) was shown to elicit serotype-specific neutralizing antibodies in horses (Guthrie *et al*., 2009). Horses were inoculated with two concentrations (high dose) of the vaccine which led to the co-expression of both outer capsid proteins of AHSV 4 (VP2 and VP5). Virus-specific neutralizing antibody titres ranging from 10-80 resulted in a minimal or absent viral replication with a virulent strain of AHSV 4. Following this study, the ALVAC®–AHSV4 vaccine was also shown to induce cell-mediated immunity, as evidenced by the detection of an AHSV4-specific gamma-interferon response in vaccinated horses (El Garch *et al*., 2012).

1.5.2.2.2.2 MVA vaccine

The modified vaccinia Ankara (MVA) strain was developed after more than 570 passages in primary chick embryo fibroblasts (Sutter *et al*., 1994). This resulted in the inability of the virus to replicate at a late stage of morphogenesis in mammalian cells. It was also shown to be non-pathogenic even in immunodeficient animals. Moreover, MVA recombinants were shown to synthesize high levels of foreign protein in human cells, thereby indicating its safety and high efficiency as an expression vector (Sutter and Moss,

1992). A number of studies have been conducted using these recombinant MVA vaccines in horses as candidate vectors for AHSV antigens (Alberca *et al*., 2014, Calvo-Pinilla *et al*., 2014, Calvo-Pinilla *et al*., 2015, Chiam *et al*., 2009, Manning *et al*., 2017).

In a pilot study, recombinant MVA viruses used as vaccines to express AHSV 4 VP2, VP7 or NS3 genes were investigated for their ability to stimulate an immune response against AHSV antigens in horses (Chiam *et al*., 2009). Three recombinant MVA vaccines, MVAVP2, MVAVP7 and MVANS3 were thus successfully generated. After vaccination, it was observed that MVAVP2 initiated a strong virus antigen-specific antibody response, unlike MVAVP7 which was a weaker response, and there was no antibody response from the horses vaccinated with MVANS3. This was also confirmed by Alberca *et al*. (2014), who demonstrated that MVA vaccines expressing AHSV 9 VP2 alone can elicit strong protective immunity, indicating that other co-expressed capsid proteins are not essential for inducing a protective immune response in horses. However, co-expression with VP5 does appear to stabilize the conformation of VP2 thereby enhancing the immunogenicity of VP2-based recombinant vaccines (Rutkowska *et al*., 2019, Guthrie *et al*., 2009).

Furthermore, a follow-up study based on the above work by Chiam *et al*. (2009) investigated whether MVAVP2 would induce a cellular immune response and lead to host protection against AHSV (Castillo-Olivares *et al*., 2011). To achieve this, interferon-α receptor knock-out (IFNAR −/−) mice were used. Interferon-alpha (IFN-α) is involved in the cellular immune response by inducing chemokinesis of T-cells and T-cell migration during viral infection of host cells (Li *et al*., 2018, Le *et al*., 2000). IFNAR −/− mice models challenged with AHSV 4 virus demonstrated clinical signs, lethality, viraemia and pathology similar to those observed in horses. After vaccination with MVAVP2, the mice developed AHSV 4-specific antibodies which provided protective immunity. It was thereby concluded that, although IFN-α plays an important role in the innate immune response against viruses, its absence does not affect the immune responses following MVA vaccination in mice.

Interestingly, it has also been established that protective immunity against AHSV is mainly achieved via a humoral rather than a cell-mediated response (Calvo-Pinilla *et al*., 2014). Using IFNAR −/− mouse models, antibodies induced by the MVAVP2 vaccine resulted in

higher protection against both clinical signs and viraemia in MVAVP2 vaccinated mice unlike the MVA-wildtype vaccinates, which developed clinical signs typical of AHS. Moreover, mice vaccinated with MVAVP2 48 hours post-infection with virulent AHSV 4 showed sufficient clinical immunity associated with antibody induction (Calvo-Pinilla *et al*., 2015). Therefore, passive immunization with MVAVP2 may be used as a potential treatment during initial stages after AHS infection.

To improve the efficiency of the MVAVP2 vaccine, an investigation was conducted using a polyvalent vaccination approach (Manning *et al*., 2017). In order to achieve this, ponies were administered simultaneously and sequentially either with MVAVP2(4) or MVAVP2(9) or both. Simultaneous vaccination of two doses of MVAVP2 serotype 4 and 9 yielded a higher virus-neutralizing antibody titre response against AHSV 4 and AHSV 9 than when each vaccine was administered independently. Interestingly, administration with MVAVP2(9) led to an increased antibody response which would induce protection not only to AHSV 9 but also to AHSV 6. This indicated the possibility of cross-reactive epitopes between these two serotypes. After four months, a boost vaccination with MVAVP2 (5) was administered to the horses and elicited an anamnestic antibody response against AHSV serotype 4, 6, 8 and 9. Thereby, it suggests the possibility that additional sub-dominant cross-reactive epitopes may exist between AHSV serotypes 5, 6, 8 and 9, and also demonstrates the suitability of using MVAVP2 as a polyvalent vaccine mixture to provide protection against more than one serotype.

1.5.2.2.3 Reverse genetics vaccine

Reverse genetics (RG) techniques have been used as an essential tool for developing novel and effective multivalent vaccines. A common feature with most reverse genetics systems is the availability of cloned complementary DNA (cDNA) copies of viral genomes, which can be genetically modified and manipulated, thereby generating live viruses with altered genes (Vermaak *et al*., 2015). The morphology, coding strategy and virus replication cycle of AHSV and BTV are similar but differ only on a genetic and protein level. Therefore, most of the AHSV reverse genetics studies are based on BTV studies (Boyce *et al*., 2008, Kaname *et al*., 2013, Lulla *et al*., 2017, Matsuo *et al*., 2011, van de Water *et al*., 2015, Van Gennip *et al*., 2017, Van Rijn *et al*., 2016). The BTV reverse genetics system focuses on *in vitro* synthesized RNA transcripts generated by T7 RNA

polymerase of cDNA clones from BTV (Boyce *et al*., 2008). During replication, the system utilizes two replication cycles. In the first stage, inner core proteins (VP1, VP3, VP4 and VP6) including non-structural proteins (NS1 and NS2) form the inner layer of the core, whereas in the second stage, VP7 is added to form the stable core particle followed by VP2 and VP5, thereby establishing virion particles (Matsuo and Roy, 2009, Kaname *et al*., 2013). As was seen for BTV, *in vitro* synthesis of synthetic AHSV T7 transcripts resulted in the recovery of infectious AHSV (Kaname *et al*., 2013). This approached utilizes helper plasmids to synthesize the AHSV inner core proteins and non-structural proteins (NS1 and NS2) within permissive cells.

The reverse genetics system has allowed for the development of two platforms to produce defective virus strains, namely: Entry Competent Replication Abortive (ECRA) virus strains, formally known as Disabled Infectious Single-Cycle (DISC) vaccine strains (Matsuo *et al*., 2011) and Disabled Infectious Single Animal (DISA) vaccine strains (Feenstra *et al*., 2014, Paillot, 2020). DISC strains are able to replicate only once in infected cells due to the lack of an essential gene product (VP6). However, they also have the capability to induce both cellular and humoral immune responses. In contrast, the DISA vaccine lacks the gene encoding non-essential NS3/NS3a, which is involved in virus release (Celma and Roy, 2009)

The approach to the use of AHSV DISC vaccine technology aimed at developing a defective-virus vaccine to protect horses against all nine serotypes (Lulla *et al*., 2016). To achieve this, they first used the RG system and AHSV serotype 1, resulting in the production of high viral titres of AHSV 1 within the complemented cell line. Thereafter, they developed a VP6-defective AHSV 1 strain and used it as a backbone in the production of defective-virus vaccines for all nine serotypes. When protective efficiency for each strain was tested in IFNAR−/− mice, complete protection against homologous infection was achieved. Thereby, indicating the suitability of the vaccine strains as vaccine candidates.

On the other hand, the development of the DISA vaccine platform has indicated that the expression of NS3/NS3a is not essential for BTV replication *in vitro* (Feenstra *et al*., 2014). Live attenuated BTV 6 with NS3/NS3a knockout mutants from mammalian cells can

protect sheep against virulent BTV serotypes (Van Gennip *et al*., 2014, Feenstra *et al*., 2014). Accordingly, the AHSV live-attenuated vaccine lacking NS3/NS3a has also shown to be a suitable AHSV DISA platform in developing vaccine candidates for different serotypes.

The incorporation of Seg-2 (encoding serotype-determining VP2 protein) from serotype 1 or 8 into AHSV serotype 4, generated an AHSV4LP LAV strain, and the deletion of NS3/NS3a from AHSV5 formed a DISA5 mutant vaccine. Together, these DISA-based vaccines showed protection against virulent homologous AHSV (Van Rijn *et al*., 2018b). However, the vaccine efficiency should be improved and tested on all the other AHSV serotypes. Moreover, DISA vaccine platforms are serologically DIVA compliant due to the presence or absence of AHSV NS3-directed antibodies (van Rijn *et al*., 2018a).

1.5.2.2.4 Virus-like particles

Virus-like particles (VLPs) are a type of recombinant vaccine formed by self-assembly of structural virus proteins to form a particle that mimics the structural organization and conformation of the actual virus but lacks the infectious genetic material (Noad and Roy, 2003). Thus, VLPs do not have the drawbacks of reversion to virulence, recombination or re-assortment with wild-type or viral vaccine strains, unlike live-attenuated or inactive vaccines. Furthermore, due to the similarities between the structure of VLPs and infectious viruses, VLPs can also induce potent humoral and cellular immune responses without the requirement of adjuvants and are highly immunogenic both in humans and animals (Huang *et al*., 2017). The dense protein arrangement of these 20–200 nm size particles triggers B-cell mediated immune response, stimulates CD4 proliferative responses and cytotoxic lymphocyte (CTL) responses, and also enables lymph node drainage (Brune *et al*., 2016). However, to achieve a desirable protective response, VLPs have to be administered repeatedly at relatively high doses because they cannot replicate themselves. Unlike other subunit vaccines, VLPs are highly immunogenic, thereby making them good candidates that enhance the immune response for poorly immunogenic epitopes.

1.5.2.2.4.1 VLPs as immunogens

Virus-like particles can be produced through the assembly of one or multiple capsid proteins. Although VLPs are suitable vaccine targets, some are assembled as a way of

studying the assembly or architecture of viruses (Noad and Roy, 2003). The BTV was the first member of the *Reoviridae* family for which VLPs were described. Using the four major structural proteins of BTV (VP2, VP3, VP5 and VP7), a BTV VLP system was developed in insect cells and posed as an ideal candidate for a vaccine against BTV. This vaccine was able to elicit a long-lasting protective immune response against virulent BTV challenge in vaccinated sheep (Belyaev and Roy, 1993, Roy *et al*., 1994a, Stewart *et al*., 2013). Recently, co-expression of four major AHSV serotype 9 structural proteins were assembled to form AHS VLPs in insect cells. However, unlike the BTV VLPs, there was a low yield of the assembled particles, thereby preventing quantification (Maree *et al*., 2016).

To overcome the challenges associated with insect cell expression systems in terms of cost production and large-scale productivity, plants have been utilized for both BTV and AHSV VLP production. Previously, BTV VLPs were assembled from the four major structural proteins of BTV serotype 8 in plants. These VLP complexes were able to elicit an immune response and provided protective immunity against challenged sheep with a South African BTV 8 viral strain (Thuenemann *et al*., 2013). Furthermore, transient co-expression of the four capsid proteins of BTV 8 have been tested using different plant expression vectors in the formation of BTV VLPs. This was aimed at improving the production yields and providing flexible platforms for the production of BTV vaccines of other serotypes (van Zyl *et al*., 2016). On the other hand, four AHSV 5 capsid proteins, VP2, VP3, VP5 and VP7 self-assembled to produce homogenous VLPs when transiently expressed in *Nicotiana benthamiana* plants. These plant-produced AHSV-5 VLPs were also shown to elicit strong serotype-specific neutralizing immune responses in guinea pigs and horses (Dennis *et al*., 2018a, Dennis *et al*., 2018b).

1.5.2.2.4.2 VLPs as carrier molecules

To enhance the immunogenic potential of VLPs, foreign antigens must be displayed on the VLP surface at high density (Chackerian, 2007, Frietze *et al*., 2016). This interaction can be achieved by two means, namely genetic fusion or chemical conjugation to the viral coat protein monomers. Genetic fusion of foreign antigens to the viral coat protein leads to an external display of antigens on the surface of the VLP. One advantage of this method is the assurance that the desired antigen can be displayed in the same

conformation and at high density on the VLP as the native virus. However, this strategy is limited by the scope of ligand options and is time-consuming to produce (Smith *et al*., 2013, Chackerian, 2007). Additionally, genetically fusing some antigens directly to the viral coat protein may lead to misfolding of the antigen or capsid protein, thereby affecting the stability and/or assembly of the VLPs. This distortion of the VLPs minimizes their efficiency in triggering an antibody response (Brune *et al*., 2016).

Alternatively, usage of the chemical conjugation strategy prevents the disruption of folding and assembly of foreign antigens when they are attached to preformed VLPs. The antigen to VLP conjugation is achieved using chemical crosslinkers containing various functional moieties that are present on the surface of VLPs, particularly amine or sulfhydryl residues (Jennings and Bachmann, 2008). *In vitro* linkage of the two components is achieved either by covalent bonding, which allows for a permanent linkage between the reactive amino acid side chains on the antigens and the VLPs, or noncovalent bonding, which is reversible. From the 20 canonical amino acids (AAs), some AAs like lysine, cysteine, glutamic acid, aspartic acid, and tyrosine provide reactive side chain moieties that can form biocompatible covalent bonds (Smith *et al*., 2013). The most common covalent method is achieved through the use of hetero-bifunctional chemical cross-linkers with amine- and sulfhydryl-reactive arms. For instance, cysteine-containing antigens can be conjugated to VLPs with surface lysine residues at a high density with up to three peptides per coat protein molecules (Chen and Lai, 2013). On the other hand, the noncovalent VLP functionalization may be achieved through electrostatic protein/protein, protein/nucleotide and protein/metal interactions. Unlike the covalent strategies, however, the noncovalent modification does not result in long-term binding stability.

To address some of the above challenges, a single-stranded RNA phage vaccine carrier has been developed. Once assembled, the *Acinetobacter* phage 205 (AP205) particles are very stable and are robust in tolerating large insertions into the N- or C-terminal termini. These features have made the AP205 VLPs to be attractive carriers of foreign antigens (Shishovs et al., 2016, Tissot et al., 2010a). Conjugation of AP205 particles with protein sequences may be achieved both chemically or using genetic engineering methods (Thrane et al., 2016). Furthermore, a variety of proteins can be attached

including, hormones (angiotensin II, gonadotropin-releasing hormone), cell receptor fragments (CXCR4) and transmembrane proteins (Matrix-2 protein) (Tissot et al., 2010a). Previously, high-density HIV-1 gp41 peptide arrays were displayed on the AP205 VLPs and elicited strong specific humoral responses in mice upon vaccination, even in the absence of an adjuvant (Pastori *et al*., 2012).

1.5.2.3 SpyTag/SpyCatcher technology

Immunoglobulin-like collagen adhesin domain (CnaB2) of FbaB, a fibronectin-binding MSCRAMM domain (microbial surface components recognizing adhesive matrix molecules) is found in the Gram-positive bacterium *Streptococcus pyogenes* (Kang and Baker, 2011). CnaB2 is necessary for phagocytosis-like uptake of the bacteria via endothelial cells (Amelung *et al*., 2011). Once CnaB2 has been split into two, it forms a peptide tag (13 amino acids) and its protein partner (116 amino acids) (Li *et al*., 2014).

The Howarth laboratory based in the University of Oxford, UK developed a technique which takes advantage of the fact that this peptide tag, formally known as SpyTag (ST), spontaneously and irreversibly forms an isopeptide bond with its protein partner SpyCatcher (SC), simply upon mixing (Figure 1.4) (Brune *et al*., 2016, Zakeri *et al*., 2012). Due to the speed and reliability of this ST-SC technology, it is ideal for different applications, including those which rely on protein stability, the formation of Spy Rings and antigen delivery during vaccination. For instance, Spy Rings help increase the flexibility of proteins and prevent them from being denatured by high temperatures or the presence of alkaline substances (Hatlem *et al*., 2019). They are formed from single proteins through the covalent bonding of the N-terminal of ST to the C-terminal of SC, or vice versa. The circularization of enzymes allows for tolerance in extreme conditions and maintains the enzymatic activity. Applicable to my research, however, is the usefulness of this technology for the decoration of virus-like particles (VLPs) to facilitate antigen delivery to the immune system.

Various challenges arise when fusing antigens to VLPs, mainly related to the linkage between the two elements. The formation of both natural and unnatural amino acid bonds may be found between VLPs and antigens. Conjugation can occur via natural amino acid bonds such as amino groups (Lys, N-terminus) or carboxyl groups (Asp, Glu, C-terminus)

and unnatural amino acids, which allows for site-specific modification and stable linkage, but increases the complexity of protein expression and the occurrence of misreading unnatural amino acid codons. Fortunately, the use of the ST/SC technology appears to be a suitable conjugation system that forms covalent bonds between VLPs and antigens (Brune *et al*., 2016).

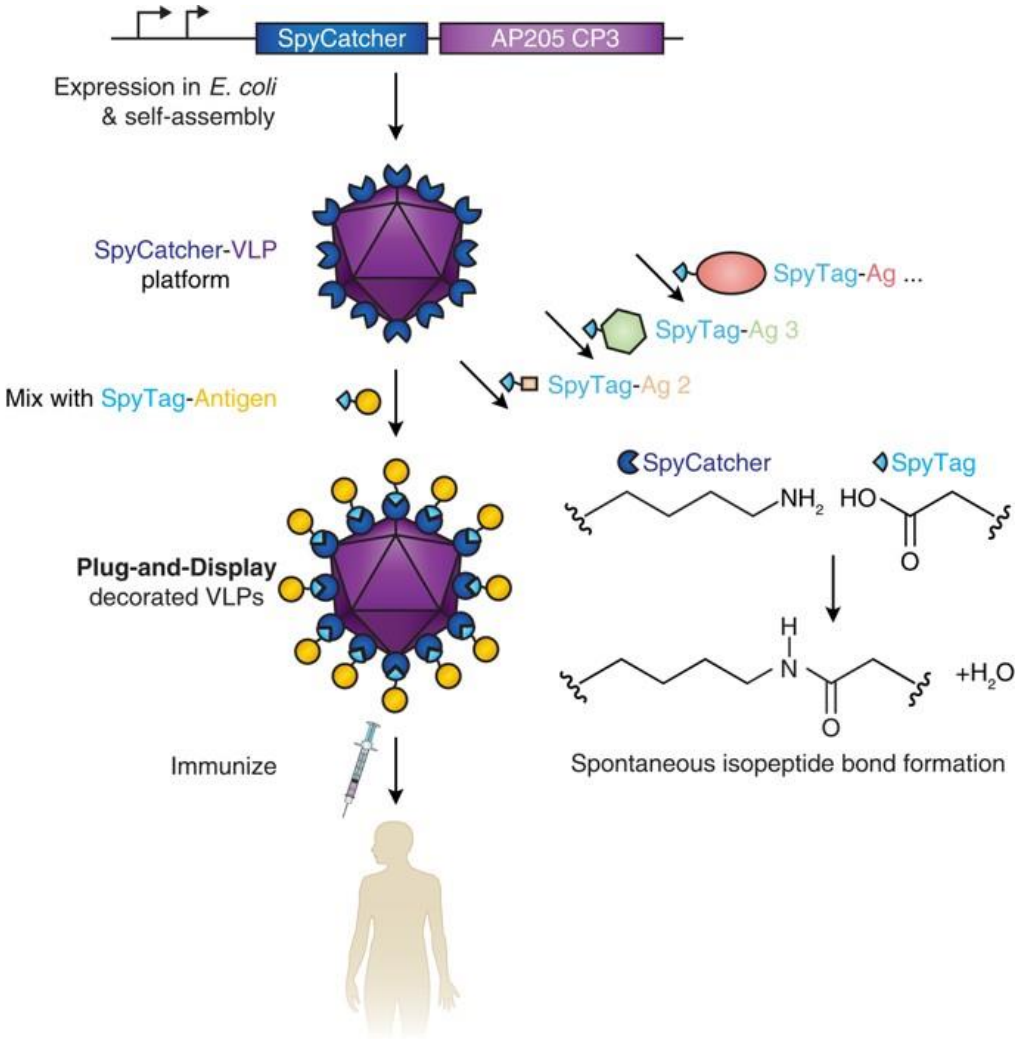

Figure 1.4: Schematic representation of SpyTag/SpyCatcher VLP technology. SpyCatcher (SC) is genetically fused to the AP205 phage coat protein (CP) and expressed in *E. coli* where SC-CP monomers self-assemble to generate VLPs. When mixed with a ST-antigen, a spontaneous isopeptide bond is formed with SC -VLPs, to produce decorated particles for immunization (Brune *et al*., 2016). *Image under the Creative Commons Attribution (CC-BY) license*.

Two independent studies have described the development of Spy-VLPs decorated with antigens and their ability to induce antibody responses. Brune *et al*. (2016) used the SC-VLP to display different immunogenetically-relevant ST-linked malarial protein antigens and ST-linked cancer-related peptides (Brune *et al*., 2016). The SC-VLPs decorated with the malarial protein antigens were able to elicit a strong antibody response after only a single immunization in mice, without requiring an adjuvant. Similarly, Thrane *et al*. (2016) reported on two malaria antigens which were successfully displayed using the Spy-VLP antigen display platform and facilitated strong functional antibody responses. Moreover, the antibody levels against the malarial antigen on the Spy-VLP complex were higher, 6 months post-immunization than those against the uncoupled protein.

1.6 Protein expression systems

1.6.1 Mammalian expression systems

The production of recombinant proteins has commonly been achieved in mammalian cell lines such as Chinese hamster ovary (CHO) cells and prokaryotic cells (mainly *E. coli*). Other expression systems such as yeast, algae and insect cells have also been used although to a lesser extent (Schillberg *et al*., 2019). The use of CHO cells has generally been utilized to produce complex proteins, including therapeutic antibodies because of their ability to carry out post-translational modifications and glycosylation. Over the years, different modifications have been utilized to increase production yields when using these systems. For instance, early production of antibodies yielded about 100 mg/L but has increased to about 5 to 20 g/L antibody titres (Schillberg *et al*., 2019, Pujar *et al*., 2009). Although these systems are suitable for the production of high yields of complex proteins, they are expensive and time-consuming requiring expensive media, and the use of bioreactors for their growth, and are susceptible to contamination with mammalian viruses (Nandi *et al*., 2016).

1.6.2 Bacterial expression systems

The use of prokaryotic cells for protein production is much more efficient and less expensive than mammalian systems. The most suitable prokaryotic host for production is *E. coli*. The first recombinant therapeutic protein produced in *E.coli* was human insulin, which has been commercially produced since 1982 (Baeshen *et al*., 2014). Even though the use of bacteria in production may be cost-effective, this system, like yeast-based systems, is limited to producing mainly simple and non-glycosylated proteins and fragments of antibodies such as scFv or Fab, but may not lead to the formation of full proteins due to limitations in post-translation modification, protein folding and assembly (Mir-Artigues *et al*., 2019).

Despite the existence of these high-performance protein production expression systems, more suitable and cost-effective alternatives are still being explored. The production of plant-made proteins offers several advantages over existing expression systems with regard to increased protein quality and/or yield and reduced manufacturing costs (Ma *et al*., 2003, Schillberg *et al*., 2019, Rybicki, 2010).

1.6.3 Plant-based expression systems

The first report on the use of plants to produce human macromolecules was based on the complete human growth hormone fusion gene, produced in tobacco and sunflower callus tissues (Barta *et al*., 1986). However, no protein expression was observed. A breakthrough occurred in 1989 with the expression of a full-sized and functional IgG in tobacco plants, a demonstration that plants are capable of producing complex and functional mammalian proteins that may be useful pharmaceutically (Hiatt *et al*., 1989). To prove the authenticity of the plant-produced proteins, the human serum albumin was produced and was confirmed to possess similar structures as the native protein, in tobacco and potatoes (Sijmons *et al*., 1990).

Ever since the discoveries, the use of plants as an expression system has become an attractive platform over the traditional expression systems to most researchers. Biologics may be produced at a lower cost in plants while excluding the risk of contamination by

endotoxins and human viral pathogens (Mir-Artigues *et al*., 2019). Normally, a viral-removal or viral-inactivation step is required when mammalian cells are used for protein production, but because plants are unable to replicate human viruses, the risk of contamination with such viruses is removed. Furthermore, plants can carry out all the necessary post-translation modification processes and produce a fully folded and functional protein identical to the original one. For example, a full-sized monoclonal antibody produced in tobacco plants showed the same binding affinity, sensitivity and specificity to tobacco mosaic virus (TMV) as native antibodies (Voss *et al*., 1995). Finally, plants have greater scalability as protein production can be increased by simply growing more plants. However, the use of plants has also led to yield challenges because of the limited space in the plant cells, as this is predominantly occupied by dormant vacuole compartments. Furthermore, the purification of plant-produced recombinant proteins may also be a challenge (Schillberg *et al*., 2019).

There are a variety of plants that can be used for pharmaceutical production. These include leafy crops (tobacco, alfalfa and lettuce), legumes (soybeans and peas), fruits and vegetables (carrots potatoes and tomatoes) and cereals (maize, rice, wheat and barley) (Fischer *et al*., 2004). Leafy crops are advantageous because of their high biomass yields. For example, the use of tobacco plants i.e., *Nicotiana benthamiana* (a small plant from Australia, which can express heterogeneous gene sequences) gained popularity over the years because of its fast scalability and large biomass yields. It is also a non-food crop, thereby this minimizes the risks associated with recombinant protein contamination of food. On the other hand, the use of tobacco also has some disadvantages, such as high nicotine and toxic alkaloid content. Additionally, just like other leafy plants, the recombinant proteins produced by tobacco plants possess a shorter shelf life because of their instability. However, the use of cereal seeds may produce biomolecules that are stable for up to three years and remain protected from proteolytic degradation (Fischer *et al*., 2004).

Recombinant protein expression can be achieved by nuclear transformation and transgenic expression. However, the stability of the transgene within the plant genome may not endure. Alternatively, transient expression has the advantage of quickly verifying

the expression efficiency of transformed constructs (Garabagi *et al*., 2012, Fischer *et al*., 2004). Transient expression is achieved by vacuum infiltration of plants with recombinant *Agrobacterium tumefaciens* strains for transient gene expression. As for stable expression of transgenic cell lines, the transfer DNA (T-DNA) from the bulky tumor-inducing (Ti) plasmid (often greater than 200 kbp) is passed on to the genome of infected cells. Unlike transgene expression, transient expression does not cause the foreign gene to be transferred to future plant generations (Garabagi *et al*., 2012). Many diagnostic and therapeutic proteins have been produced through agroinfiltration of *N. benthamiana* plants. These range from a swine fever vaccine, an Ebola virus vaccine, a Rift Valley fever virus diagnostic antigen and cancer antigens such as human colorectal cancer, just to name a few (Goulet *et al*., 2019).

1.7 Aims of the study

The goal of this study is to display the serotype-specific immunogenic domain of AHSV VP2 on a virus-like particle carrier surface to investigate the potential of developing a multivalent plant-based virus-like particle (VLP) vaccine candidate using a novel conjugation strategy. In this study, the immunogenic region is of prime interest because, from a previous study by Dr. Susan J Dennis (2019) from the Biopharming Research Unit at the University of Cape Town, South Africa observed that the full AHSV VP2 was not suitable for use with the above strategy. Thereby, it is suggested that a smaller VP2 peptide representing the neutralizing epitope would be a more feasible approach. To achieve this aim, the study had the following objectives:

I. Design, synthesis and cloning of the immunogenic region of African horse sickness virus (AHSV) serotype 5 capsid protein VP2 (AHSV VP2dom), tagged with either the SpyTag (ST) or SpyCatcher (SC) peptide into both plant expression vectors.
II. Expression and purification of Spy-tagged AHSV 5 VP2dom in plants
III. Expression of AP205 coat protein (CP) fused to the ST or SC peptide in plants with resultant spontaneous assembly and purification of Spy AP205 VLPs.

IV. Coupling of plant-produced SpyCatcher AHSV VP2dom to SpyTagged AP205 VLPs using the SC/ST conjugation system and purification of the resulting AHSV5 VP2dom- AP205 VLPs.

Chapter 2: Plant-based expression of the immunogenic region of the AHSV 5 VP2 capsid protein gene

2.1: Introduction

The outer capsid protein VP2 is the most variable protein on the African horse sickness virus (AHSV) structure associated with virus neutralization. This variable protein contains the major neutralizing epitopes which induce the serotype-specific immune response (Potgieter *et al*., 2003, Stone-Marschat *et al*., 1996). Antibodies against VP2 have been shown to be protective *in vivo* (Burrage *et al*., 1993), thus making this protein a suitable candidate for vaccine development strategies. Several different studies have been conducted aimed at identifying the location of antibody-binding epitopes on VP2 (Bentley *et al*., 2000, Manole *et al*., 2012, Martínez-Torrecuadrada and Casal, 1995, Martínez-Torrecuadrada *et al*., 2001, Venter *et al*., 2000).

It has been observed that the majority of these neutralizing antibody sites are located in the N-terminal half of VP2. A study of AHSV 4 VP2 showed that the region between amino acids (aa) 254-414 was able to elicit consistently high titres of neutralizing antibodies, while neither the extreme N-terminal (aa 1-199) nor C-terminal (aa 414-1060) domains were found to be immunogenic (Martínez-Torrecuadrada and Casal, 1995). It was later also shown that synthetic peptides derived from aa 321-400, were able to induce neutralizing antibodies against AHSV 4 (Martínez-Torrecuadrada *et al*., 2001).

Most recently, it has been suggested that the major neutralizing antibody sites for VP2 are located between aa 279 and 483 (Manole *et al*., 2012). After mapping aa 279 to 368 to AHSV 4 structure, the authors suggested that the immunogenic epitopes may be located on the tips of the VP2 triskelions (Figure 1.2 A & B), away from contact with VP5 and VP7. The other major immunogenic residues of AHSV 4 VP2 (aa 368 to 403 and aa 450 to 483) (Bentley *et al*., 2000) were mapped to the top of the triskelion hub. Interestingly, all proteins containing an AHSV 4 VP2 fragment 'H' (aa 285 to 413), had the capacity of consistently eliciting neutralizing antibodies in mice and rabbits (Martínez-

Torrecuadrada and Casal, 1995). A combination of sub fragments ‘a’ (321–339) and ‘b’ (374–403) of fragment H brought about a more effective neutralizing activity, although it was not known whether this effect was synergistic or additive from the two epitopes (a and b) (Martínez-Torrecuadrada et al., 2001). Remarkably, aa 340 to 360 have been associated with tissue tropism and virulence (Potgieter *et al*., 2009). The virulence of the virus is believed to correspond with its affinity for certain tissues of the host, thereby, suggesting that outer capsid protein VP2 is involved in cell entry as well as the triggering of apoptosis (Potgieter *et al*., 2009).

For vaccine development, VLPs have become a popular platform used to display pathogen-specific antigens. These highly immunogenic and self-assembling particles can mimic the structural organisation of the actual virus but exclude any genetic material. This approach is also favourable because unlike the currently available vaccine, it does not have the drawbacks of reversion to virulence or genome segment reassortment and it is DIVA compliant (Noad and Roy, 2003).

Displaying proteins on the surface of VLPs allows the presentation of multiple antigenic epitopes with conformation similar to the native antigens (Charlton Hume *et al*., 2019). The novel SpyTag/SpyCatcher (ST/SC) platform (Zakeri *et al*., 2012) allows the conjugation of antigens on assembled VLPs, forming an irreversible isopeptide bond. Recently, Dr. Susan J Dennis from the Biopharming Research Unit at the University of Cape Town, South Africa attempted to use the ST/SC platform to display the full AHSV VP2 on the surface of AP205 VLPs (Dennis, 2019). However, Spy-tagged AHSV VP2 appeared to be cleaved during the coupling process thus preventing display of the full VP2 antigen on the surface of plant-produced SC AP205 VLPs. A smaller VP2 peptide, representing the major neutralisation epitopes, may be a more feasible approach.

This chapter focuses on the design, cloning and transient expression of the region of VP2, believed to contain the antigenic determinants responsible for eliciting a neutralizing antibody response against AHSV 5 (further known as the VP2 dom (domain)), linked to either the ST or SC peptide at its C-terminus. The resulting constructs were cloned into the pEAQ-*HT* plant transient expression vector and expressed in *Nicotiana benthamiana* plants.

2.2: Materials and Methods

2.2.1 Primer design and in-fusion cloning of the AHSV 5 VP2 antigenic domain linked to SpyTag or SpyCatcher into pEAQ-*HT*™

Full-length pEAQ-AHSV5-VP2-SpyTag and pEAQ-AHSV5-VP2-SpyCatcher clones, generated by Dr. Susan J Dennis (2019), were used to design primers (Inqaba Biotechnical Industries (Pty), Muckleneuk, Pretoria, SA) (Table 2.1, Figure 2.1), with the aid of CLCbio Workbench 6.2 (Qiagen). AHSV5-VP2dom-SpyTag and AHSV5-VP2dom-SpyCatcher constructs were created from the full-length clones through two separate Polymerase Chain Reaction (PCR) reactions. The first reaction involved the amplification of two fragments, AHSV 5 VP2dom fragment and SpyTag (ST)-or SpyCatcher (SC)-linker fragment, using the designed primers (FP1 with RP1 and FP2 with RP2, or FP5 with RP5, respectively). VP2dom is a 873 bp sequence from position 1957 to 2829 of the pEAQ-AHSV5-VP2 region, which contains the putative antigenic region. The second reaction was carried out to fuse the two fragments, using the VP2dom forward primer (FP 1) and ST or SC reverse primer (RP2 or RP5, respectively).

The primers included a *SmaI* site at the 5' end and an *XhoI* site at the 3' end of the VP2dom ST/SC sequence and a 6 x histidine (His) at the 5' end of the VP2dom sequence upstream from the *SmaI* site. ST or SC sequence was included at the 3’ end of VP2dom such that the VP2dom and ST/SC sequences were separated by a short glycine/serine linker (GGS) sequence (Appendix A: Figure 1 & 2 - AHSV 5 VP2domSC). DNA was amplified by an initial denaturation step at 98 °C for 30 seconds followed by 35 cycles of denaturation at 98 °C for 10 s, annealing at 60 °C for 30 s and elongation at 72 °C for 30 s (60 s per 1000 bp DNA) and a final elongation step at 72 °C for 10 min.

Table 2.1: Sequences of the vector-specific primers used for PCR amplification to confirm the successful cloning of AHSV genes. HisTag is bolded, *SmaI* site is single underlined, *XhoI* is double underlined, and linker is dashed underlined.

Primer	**5' – 3' sequence**
Forward primer (FP 1)	5' -**CACCATCACCATCAT**CCCGGGAAACTTCGCTTTGGTCTTCTATACCCGCATT
Reverse primer (RP 1)	5' -TCCAGATCCTCCTCCAGCAGTTCCAGATCCAATACTAGCAGCATTTGTACCCTTT
Forward primer (FP 2)	5' -GGATCTGGAACTGCTGGAGGAGGATCTGGAAGTGCTCATATTGTTATGGTAGAT
Reverse primer (RP 2)	5' -GTTAAAGGCCTCGAGCTACTTTGTCGGTTTGTAAGCATCTACCATA
Forward primer (FP 5)	5' -GGATCTGGAACTGCTGGAGGAGGATCTGGATCTGGAGCTATGGTTGATACTCT
Reverse primer (RP 5)	5' -GTTAAAGGCCTCGAGCTAAATGTGAGCATCCCCTTTTGT
pEAQ-*HT* – Forward primer	5' -TTCTTCTTCTTGCTGATTGG
pEAQ-*HT* – Reverse primer	5' -CACAGAAAACCGCTCACC

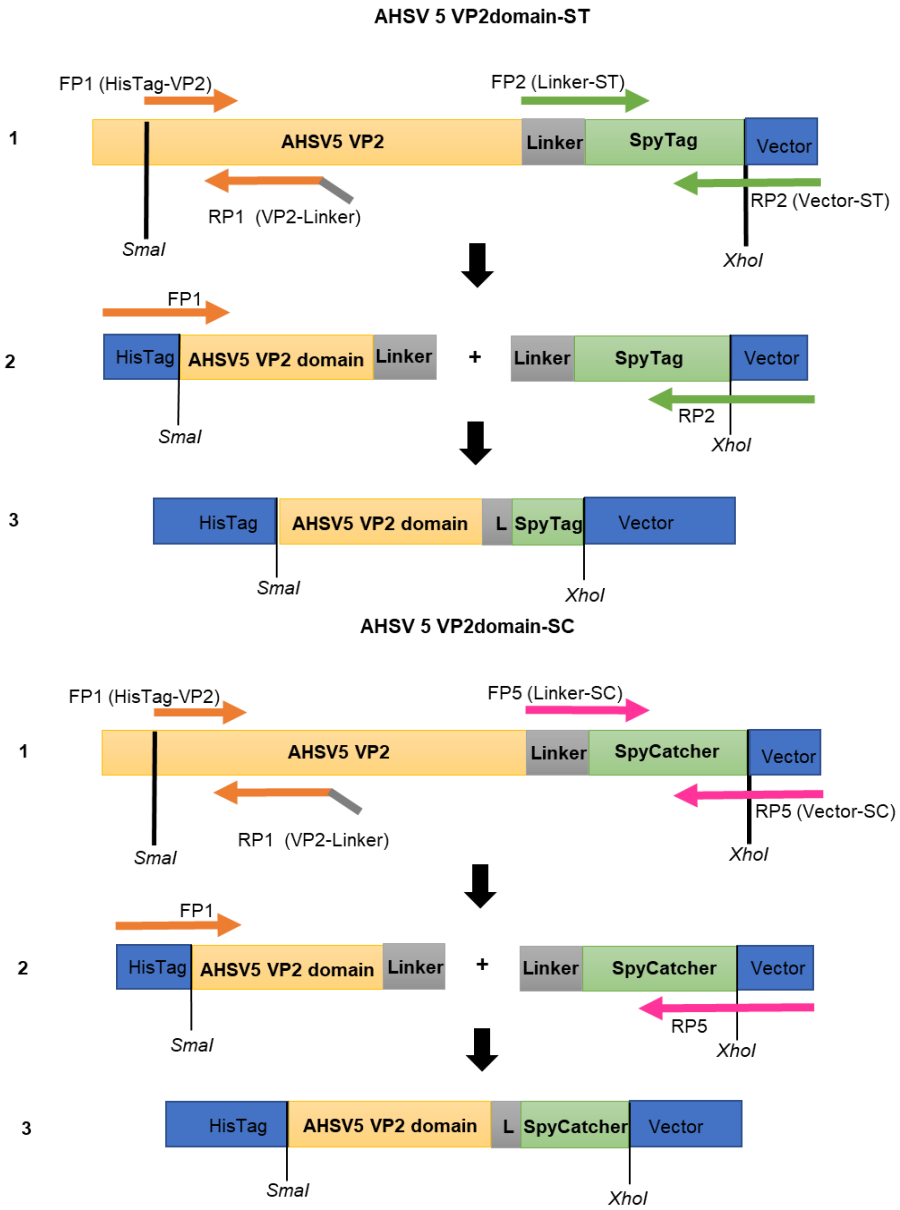

Figure 2.1: Schematic representation of the constructs created for *Agrobacterium*-mediated expression of Spy-tagged AHSV serotype 5 VP2 dom in *N. benthamiana*. Step 1 illustrates plant codon-optimized genes for AHSV-5 VP2 (yellow box) separated from SpyTag (A) or SpyCatcher (B) sequences (green box) by a glycine/serine (GGS) linker sequence (grey box) and 15 bp vector (blue box) overlap at the 3' of ST/SC. Primers FP1 and RP1 (orange arrows) amplify the AHSV5 VP2 dom fused to 15 bp vector at 5' and linker at 3' end. (A) Primers FP2 and RP2 (green arrows) amplify SpyTag sequence fused to linker at 5' and 15 bp at 3'. (B) Primers FP5 and RP5 (pink arrows) amplify SpyCatcher sequence fused to linker at 5' and 15 bp at 3'. Step 2 shows two separate constructs amplified using designed primers. Primer FP1 and RP2 (A) or RP5 (B) are used to fuse the two constructs. Step 3 displays the final AHSV5-VP2domST (A) and AHSV5-VP2domSC (B) constructs. Both constructs were synthesized with a 6 x His (blue box) at the opposite end to the ST or SC peptide.

Recombinant AHSV 5 VP2domST and AHSV 5 VP2domSC genes were inserted into the pEAQ-*HT*™ vector using the in-fusion HD® cloning kit (Clontech Laboratories, Inc. Mountain View, CA, USA). To perform this, the pEAQ-*HT* vector was firstly linearized using enzymes (*SmaI* and *XhoI*) and separated on 1% w/v agarose TBE (89 mM Tris base, 89 mM boric acid and 2 mM EDTA [pH 8]) gel containing 2.5 mg/mL ethidium bromide (EtBr) and visualised under long-wavelength ultraviolet (UV) illumination. O'GeneRuler™ 1kb DNA ladder (Fermentas, Waltham, MA, USA) was used as a molecular weight marker on this and all further agarose gels. Linearized vector DNA was excised from the agarose gels and purified using a Macherey-Nagel™ NucleoSpin™ Gel and PCR Clean-up Kit (Macherey-Nagel, Duren, Germany) following the manufacturer's instructions. The in-fusion cloning reaction was set-up by combining the linearised vector and AHSV5-VP2domST/SC insert in one tube and incubated for 15 min at 50 °C to produce pEAQ-AHSV5-VP2domST and pEAQ-AHSV5-VP2domSC constructs (Figure 2.1).

These pEAQ plasmid constructs were transformed into Stellar™ competent *E. coli* cells (E. cloni™, Lucigen, Middleton, WI, USA). Transformed cells were selected on Luria Bertani (LB) media plates supplemented with kanamycin (50 µg/mL) by incubation for 16 hrs at 37 °C.

Colony PCR using pEAQ vector-specific primers (Table 2.1), was used to confirm successful transformations. In the presence of a DNA insert, these primers will amplify an AHSV5-VP2domST and AHSV5-VP2domSC insert of 984 bp and 1293 bp, respectively and a vector sequence of ±270 bp. A microtip amount of colony material was resuspended in 10 µL double distilled water (ddH_2O) by pipetting up and down to dissolve. The PCR reactions consisted of 5 µL resuspended colony material, 200 µM dNTPs, 1 µM of each primer, 25 mM $MgCl_2$, 1 x Green GoTaq® Reaction Buffer and 1 unit of GoTaq® DNA polymerase (Promega, Madison, WI, USA). Cloned DNA was amplified by an initial denaturation step at 95 °C for 5 min followed by 30 cycles of denaturation at 95 °C for 30 s, annealing at 51 °C for 30 s and elongation at 72 °C for 90 s (±60 s per 1000kb DNA) and a final elongation step at 72 °C for 7 min. The amplified products were separated on

1% w/v agarose TBE gels containing 2.5 mg/mL EtBr and visualised under short wavelength UV light.

Transformed cell colonies were inoculated into 5 mL LB broth supplemented with 50 µg/mL kanamycin and incubated with agitation for 16 hrs at 37 °C. Purification of the plasmid constructs was achieved using the QIAprep® Spin Miniprep kit (Qiagen, Hilden, Germany) according to the manufacturer's instructions. Recombinant pEAQ-AHSV clones were verified by digestion of ±500 ng DNA with 1 unit each of *AgeI* and *XhoI* restriction enzymes per reaction for 2 h at 37°C followed by separation of the DNA fragments on 1% w/v agarose TBE gels containing 2.5 mg/mL EtBr.

2.2.2 Transformation of *Agrobacterium tumefaciens*

Agrobacterium tumefaciens AGL 1 (AGL-1) were made electrocompetent using a previously described method (Shen and Forde, 1989). The pEAQ-*HT* recombinant plasmids (±400 ng each) were electroporated into 100 µL electrocompetent AGL-1 cells at 1.8 kV, 25 µF, and 200 Ω as described previously (Maclean *et al*., 2007) The cells were supplemented with 900 µL of LB media, and the mixture was transferred to a microcentrifuge tube and incubated with agitation at 27°C for 2 h. Following the incubation step, 35 µL of cells were spread plated onto LB media plates containing kanamycin (50 µg/mL) and carbenicillin (25 µg/mL). The plates were incubated for 16 hrs at 27°C.

2.2.3 Confirmation of recombinant *Agrobacterium* constructs

Successful transformations were confirmed by colony PCR using pEAQ vector-specific primers as described in 2.2.1. To ensure long-term maintenance of the recombinant *Agrobacterial* strains, single recombinant colonies were inoculated into 10 mL LB broth supplemented with 50 µg/mL kanamycin and 25 µg/mL carbenicillin and incubated with agitation for 16 hrs at 27°C. Seed stocks of each recombinant strain were then prepared by mixing 500 µL bacterial culture with 500µL 50% glycerol and freezing at -80°C.

2.2.4 Small-scale *Agrobacterium*-mediated transient protein expression in *N. benthamiana*

Starter cultures of the recombinant *Agrobacterial* strains were prepared by inoculating 10mL LB broth supplemented with 50 µg/mL kanamycin and 25 µg/mL carbenicillin with a 1 mL glycerol stock and grown by incubating with agitation for 16 hrs at 27 °C. These starter cultures were used to inoculate 50 mL LB media supplemented with 50 µg/mL kanamycin and 25 µg/mL carbenicillin and 200 µM acetosyringone and grown by incubating with agitation for 16 hrs at 27 °C. The 50 mL culture were then used to inoculate 500 mL LB media supplemented with 50 µg/mL kanamycin and 25 µg/mL carbenicillin and 200 µM acetosyringone and grown by incubating with agitation for 16 hrs at 27 °C. An *Agrobacterium* tumefaciens recombinant containing the empty pEAQ-*HT*™ vector was used as a negative control. The optical density at 600 nm wavelength light (OD_{600}) of the cultures were measured and appropriate volumes were diluted (or combined and diluted for expression) in resuspension solution (10 mM MES, pH 5.6, 10 mM $MgCl_2$, 100 µM acetosyringone) to the desired optical density and incubated for 1 h at 22 °C to allow the acetosyringone to induce expression of the *vir* genes.

The AHSV *Agrobacterial* suspensions were diluted to OD_{600} = 0.25, 0.5 or 1.0. For small-scale expression, the top 5 leaves of 10 five-week-old *N. benthamiana* plants were infiltrated with the relevant recombinant *Agrobacterial* strains by applying a vacuum of 98kPa. Plants were grown at 22 °C under 16 hrs / 8 hrs light / dark cycles until harvested.

2.2.5 Protein extraction and analysis

Expression of AHSV 5 VP2dom-ST and SC was monitored by harvesting the top 3 infiltrated leaves on days 3, 5 and 7 post infiltration (dpi). The leaves were weighed and homogenized in 2 volumes of PI buffer (1 x PBS [137 mM NaCl, 10 mM Na_2HPO_4, 2.7 mM KCl, 2 mM KH_2PO_4, pH 7.4] containing Complete™, EDTA-free protease inhibitor cocktail [Roche, Basel, Switzerland]) using an Ultra-turrax® juice extractor. Homogenates were incubated at 4 °C for 30 min with gentle shaking and then clarified by centrifugation at 25931 x *g* (13 000 rpm) for 20 min at 4 °C using the Beckman Coulter Avanti™ J-25i

Centrifuge. Crude plant extracts were filtered through one layer of Miracloth™ (Merck, Darmstadt, Germany) and spun again.

To analyse protein expression 200 µL crude plant extracts were mixed with 50 µL sample application buffer (Sambrook *et al*. 1989) and denatured at 95 °C for 10 min. Total soluble protein (TSP) amounts were determined in a Bradford assay against a BSA standard curve and corrected for background. Protein samples (40 µL per gel lane) were separated by electrophoresis for ±2 h at 120 V through 10% SDS polyacrylamide gels and then transferred onto BioTrace™ NT Nitrocellulose Transfer Membrane (Pensacola, FL, United States) using a Trans-blot® SD semi-dry transfer cell (Bio-Rad, Irvine, CA). at 15 volts (V) for 1 hr 20 min. Colour Pre-stained Protein Standard, Broad Range Protein Ladder (New England Biolabs, Ipswich, MA) was used as a molecular weight marker.

For western blot analysis, the membranes were incubated in blocking buffer (5% non-fat dairy milk in 1 x PBS containing 0.1% Tween®-20 [PBS-T]) and then probed O/N at 4 °C in primary antibody. To optimise protein detection, western blots were analysed using different antisera, including anti-AHSV 5 sera from VLP-vaccinated horses (Dennis, 2019), mouse anti-histidine sera (Sigma-Aldrich, Missouri, United States), anti-AHSV 5 sera from guinea pigs (Dennis *et al*., 2018a) and rabbit anti-AP205 sera (this antibody binds to AP205, obtained it from Jennifer Wayland, Biopharming Research Unit, University of Cape Town, SA). Protein detection was best seen using anti-AHSV 5 guinea pig sera and this was used for all further experiments.

Guinea pig anti-AHSV 5 serum was diluted (1: 3000 or 1: 5000) in blocking buffer. After four washes with blocking buffer for 15 min each, the membranes were incubated in blocking buffer containing goat anti-guinea pig alkaline phosphatase-conjugated secondary antibody (Sigma-Aldrich, St Louis, MO, USA) at a 1:5000 dilution for 1 hr at 37 °C. The membranes were then washed four times with 1 x PBS-T for 15 min each and the presence of proteins was detected by the addition of 5-bromo-4-chloro-3-indolyl-phosphate substrate (BCIP, 1-component, KPL, Milford, MA, USA).

2.3 Results

2.3.1 In-fusion cloning of the AHSV 5 VP2dom SpyTag/SpyCatcher gene into pEAQ-*HT*™

Transient expression in plants of the major antigenic region of AHSV serotype 5 outer capsid protein VP2 fused to either the SpyTag or SpyCatcher peptide, was investigated. This was achieved by PCR amplification of the desired AHSV5-VP2-SC and AHSV 5-VP2domST sequences from the full-length pEAQ-AHSV5-VP2-SpyTag and pEAQ-AHSV5-VP2-SpyCatcher clones, followed by in-fusion cloning into the pEAQ-*HT*™ plant transient expression vector to produce pEAQ-AHSV5-VP2domST and pEAQ-AHSV5-VP2domSC constructs (Figure 2.2 A & B).

Successful cloning was confirmed by colony PCR and gel electrophoresis of the amplified products. DNA bands of ±0.98 kb (0.71 + 0.27 kb vector sequence) and ±1.29 kb, (1.02 + 0.27 kb vector sequence), representing the correct sizes of AHSV VP2domST (Figure 2.2 A, lanes 2 & 3) and AHSV VP2domSC (Figure 2.2 B, lanes 1, 2 & 4) respectively, were visualised.

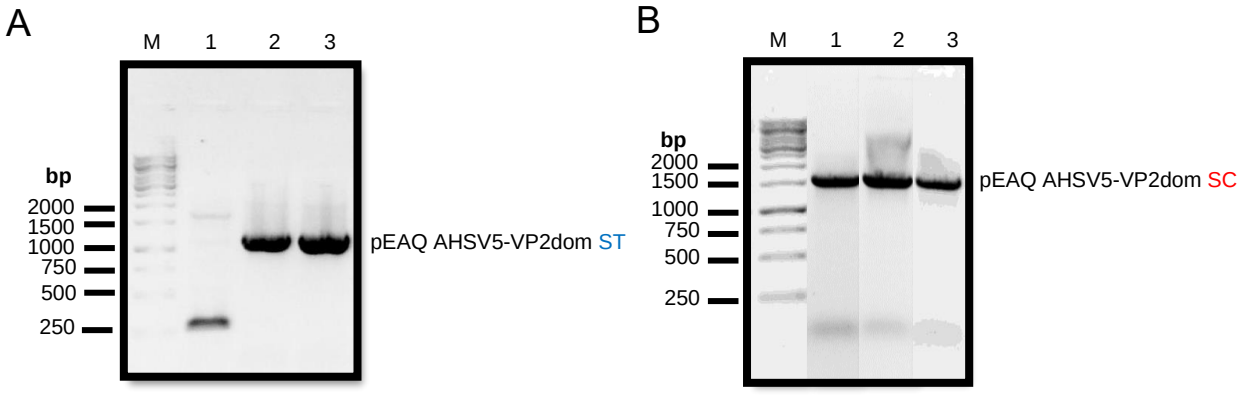

Figure 2.2: Confirmation of successful in-fusion cloning and transformation of recombinant AHSV strains into *E. coli* by colony PCR amplification. PCR of the AHSV recombinants amplified a ±0.98 kb fragment (A, lane 2 & 3) for pEAQ-AHSV5-VP2domST and a ±1.29 kb fragment (B, lanes 1-3) for pEAQ-AHSV5-VP2domSC. Transformation with the pEAQ plasmid lacking gene was used as a negative control (A, lane 1). The size of molecular weight markers (M) is indicated adjacent to each gel.

The colonies in lane 2 (Figure 2.2 A) and lane 3 (Figure 2.2 B) were selected for electroporation into *Agrobacterium* AGL 1. Successful transformations were confirmed by colony PCR by the presence of a ±0.98 kb (Figure 2.3 A, lanes 1 to 5) and a ±1.29 kb (Figure 2.3 B, lanes1 to 6)- sized DNA band, representing AHSV5-VP2domST and AHSV5-VP2domSC, respectively.

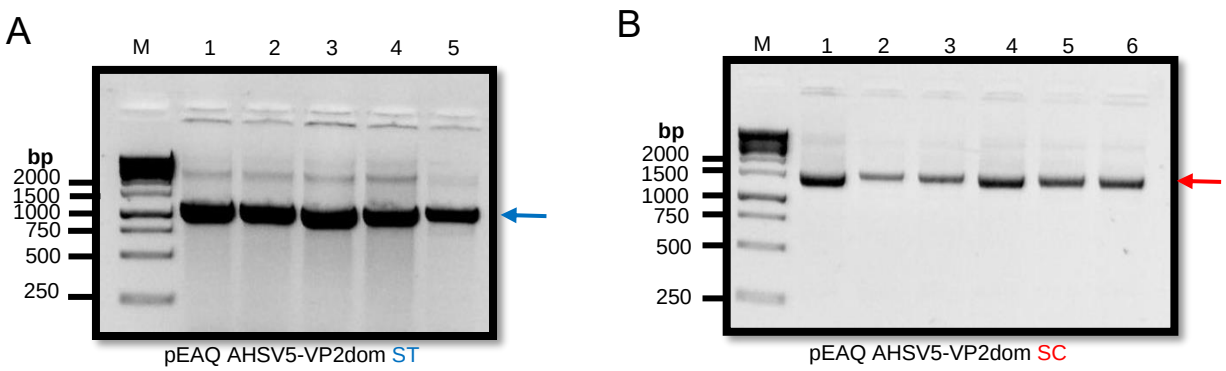

Figure 2.3: Colony PCR of *Agrobacterium* AGL 1 transformed with recombinant AHSV strains *Agrobacterium*. Colony PCR amplification using the pEAQ vector-specific primer set was used to verify the successful transformation of AHSV capsid protein genes into *Agrobacterium* AGL 1 (A and B). PCR of the AHSV recombinants amplified a ±0.98 kb fragment (A, lanes 1-5, blue arrow) for pEAQ-AHSV5-VP2domST and a ±1.29 kb fragment (B, lanes 1-6, red arrow) for pEAQ-AHSV5-VP2domSC. The size of molecular weight markers (M) is indicated adjacent to each gel.

2.3.2 Small-scale expression of AHSV 5 VP2dom SpyTag/SpyCatcher proteins in *Nicotiana benthamiana*

After successfully cloning AHSV 5 VP2domST/SC into the pEAQ-*HT*™ vector and transforming the recombinants into *Agrobacterial* cells, small-scale transient expression studies were carried out. Tests were done to determine the optimal expression conditions by comparing infiltration at different optical densities (OD_{600}) and harvesting leaves at different days post-infiltration (dpi).

Recombinant AHSV *Agrobacterial* suspensions were diluted to OD_{600} of 0.25, 0.5 and 1.0 and then introduced into five-week-old *N. benthamiana* plants by vacuum infiltration. Infiltrated plants were monitored over 7 days and leaves were harvested on days 3, 5,

and 7 post-infiltration (Figure 2.4). All infiltrated leaf tissue exhibited chlorosis with time, especially by 7dpi. Moreover, there was no major physiological difference over time in leaves infiltrated at OD_{600} of 0.25, 0.5 and 1.0 (results not shown)

Figure 2.4: Physiological effects of small-scale expression of recombinant AHSV VP2domST/SC AGL-1 strain and time-trials. Physiological changes of leaves were monitored after 3, 5, 7 dpi, at OD_{600} value of 0.5.

Proteins were separated by SDS-PAGE and their expression analysed by western blot. Approximately 106 µg of TSP was loaded into each well on the gel (Figure 2.5).

To optimise protein detection, horse anti-AHSV 5 sera (1:2000 and 1:5000) and mouse anti-histidine sera (1:2000) were used on western blots. No detection was observed to indicate the presence of expressed recombinant AHSV 5 VP2domST/SC protein at OD_{600} = 0.25 and 0.5 (results not shown). Therefore, the western blots were repeated using two additional antisera: a polyclonal AHSV 5 antiserum raised in guinea pigs (1:5000) and

anti-SpyTag AP205 raised in rabbits (1:500). Little to no yield of Spy-Tag VP2dom was detected with either of these antisera (Figure 2.5, A & B), but VP2dom linked to the SpyCatcher tag (Figure 2.5, C), which has an expected band size of 48kDa, was detected using the guinea pig anti-AHSV 5 sera (1:5000).

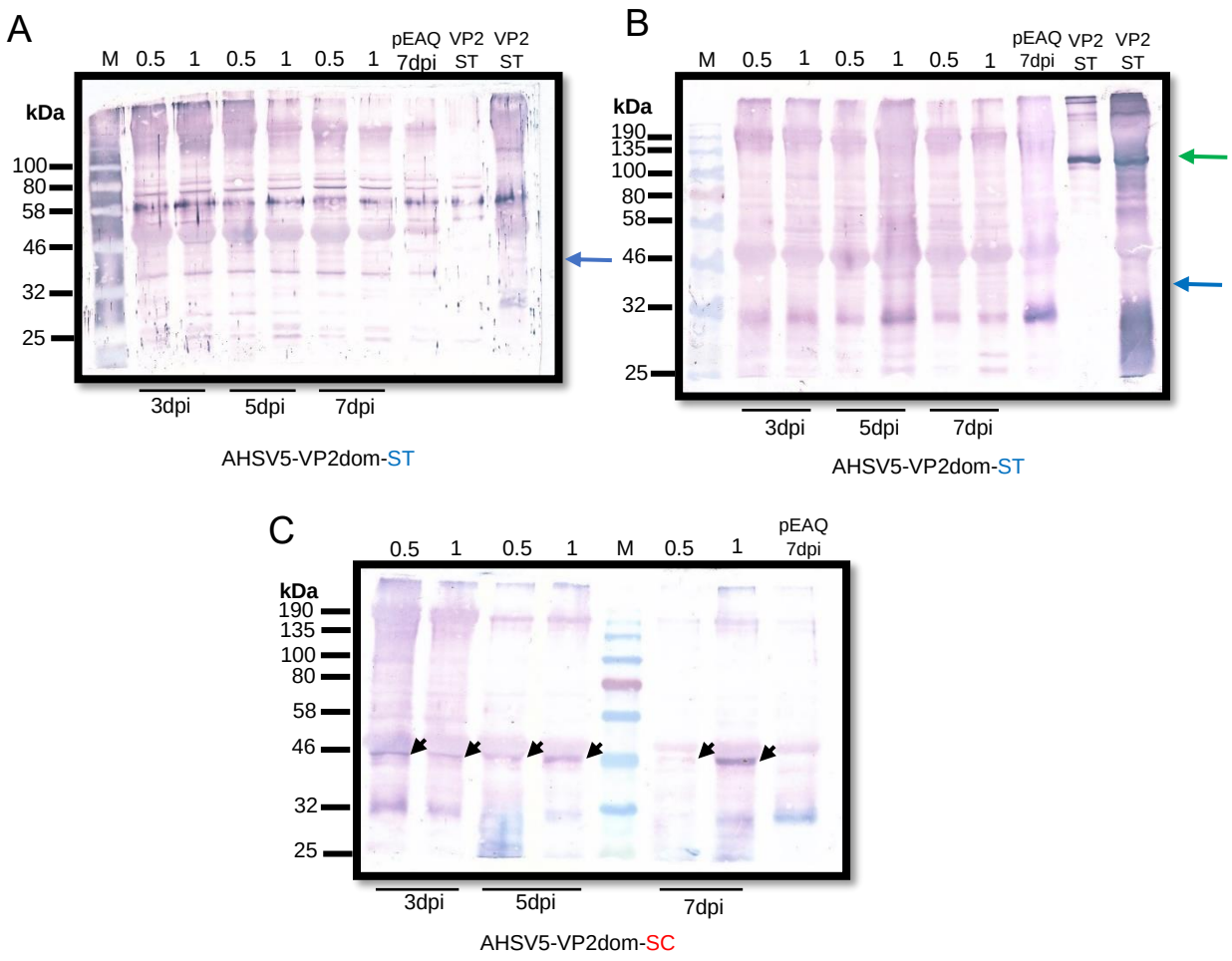

Figure 2.5: Optimization of plant-based expression of recombinant AHSV-5 VP2domST/SC proteins. Crude leaf extracts obtained from plants infiltrated with *Agrobacterium* AGL-1 containing pEAQ-AHSV 5 VP2domST and pEAQ-AHSV 5 VP2domSC at OD_{600}=0.5 & 1.0, and harvested 3-, 5- and 7-days post infiltration, were analysed by western blot. Crude extract from a plant infiltrated with the empty pEAQ expression vector was used as a negative control. A) Guinea pig anti-AHSV 5 sera (1:5000) and B) rabbit anti-ST-AP205 sera (1:500), which proved unable to detect AHSV-5 VP2domST (37kDa, blue arrow), was used as the primary antibody. The green arrow represents full-length VP2 ST protein, used as a positive control. C) AHSV-5 VP2domSC protein (48 kDa) was indicated by black arrowheads after detection with guinea pig anti-AHSV 5 sera (1:5000). M: colour pre-stained protein standard, broad range (New England Biolabs, Massachusetts, USA) was used as a molecular weight marker.

To enhance detection of recombinant AHSV-5 VP2domST/SC proteins, guinea pig anti-AHSV 5 serum was used at a dilution of 1:3000 instead of 1:5000 (Figure 2.6). The repeated western blot analysis indicated that the highest AHSV-5 VP2domSC protein yield was noted at 5dpi, rather than at 7dpi. However, AHSV-5 VP2domST was not detected.

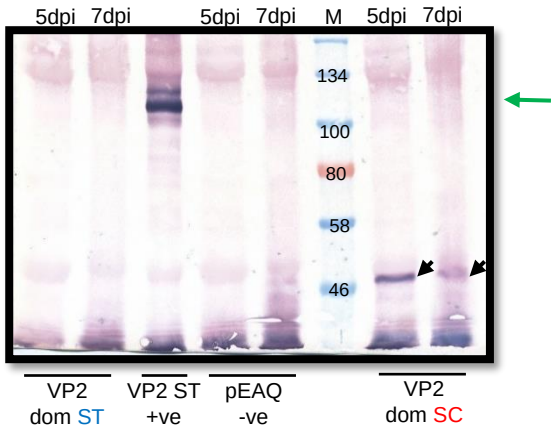

Figure 2.6: Optimization of plant-based expression of recombinant AHSV-5 VP2domST/SC proteins. Crude leaf extracts obtained from plants infiltrated with *Agrobacterium* AGL-1 containing pEAQ-AHSV5 VP2domST and pEAQ-AHSV5 VP2domSC at OD_{600} = 1.0, and harvested 5- and 7-days post infiltration, were analysed by western blot. Crude extract from a plant infiltrated with the empty pEAQ-*HT* expression vector was used as a negative control. Anti-AHSV 5 sera (1:3000) was used as the primary antibody and detected AHSV-5 VP2domSC (48kDa, black arrowheads). However, AHSV-5 VP2domST protein (37 kDa) was not detected. The green arrow represents full-length VP2 ST protein, used as a positive control. M: colour pre-stained protein standard, broad range (New England Biolabs, Massachusetts, USA) was used as a molecular weight marker.

2.4 Discussion

Virus-like particles have become an attractive platform in aiding with the delivery of conformational epitopes. To achieve efficient and stable immobilization of the antigens on the VLP surface, large antigens have been coupled to VLPs using the SpyTag / SpyCatcher conjugation system. This involves the interaction of a highly reactive SpyTag (ST) peptide with the SpyCatcher (SC) protein through the formation of an isopeptide bond.

Target proteins or antigens can be genetically fused to the ST peptide and thereafter efficiently bound to a SpyCatcher conjugated protein on the VLP surface to induce an immune response when used as a vaccine. It is also possible to achieve a reverse combination of the conjugating peptides in that the ST is incorporated onto the VLP surface, and SC is fused to the antigen. The fusion of SC domain to the malaria transmission-blocking vaccine antigens Pfs25 and Pfs48/45, resulted in increased expression in a bacterial system (Singh *et al*., 2017, Thrane *et al*., 2016). Moreover, Peyret *et al*. (2020) reported the successful assembly of tandem Hepatitis B virus (HBV) core protein (tHBcAg) VLPs displaying green fluorescent protein (GFP) in plants using this ST/SC platform. Here, it was more efficient to fuse ST to GFP and SC to tHBcAg VLP, rather than vice-versa.

The VP2 outer capsid protein is the most variable AHSV antigen and is the determinant of the AHSV serotype believed to bear most of the virus neutralisation epitopes identified thus far (Aksular *et al*., 2018, Bentley *et al*., 2000, Burrage *et al*., 1993). These features have made this protein the prime focus of AHSV vaccine development. Previously, the ST/SC platform was used in an attempt to display the full AHSV VP2 (±3.2kb) on the surface of the AP205 VLPs (Dennis, 2019). However, coupling of the large full-length VP2 antigen to the VLP surface was not a success. Therefore, it was of interest to investigate whether a smaller VP2 peptide representing the neutralizing epitopes could be conjugated to AP205 VLPs using the ST/SC technology.

This chapter focuses on the cloning and expression of the AHSV serotype 5 VP2 neutralizing epitope region, known as the VP2 dom (873 bp) fused to either ST or SC.

The AHSV 5 VP2domST and SC constructs, were successfully assembled by PCR amplification and in-fusion cloning into the pEAQ-*HT*^{TM} vector. The presence of these constructs transformed into *E. coli* and subsequently into *A. tumefaciens* was confirmed by colony PCR.

Analysis of small-scale expression of both recombinant proteins in *N. benthamiana* demonstrated expression of AHSV 5 VP2domSC (Figure 2.5 C and 2.7), but no expression of AHSV 5 VP2domST using guinea pig anti-AHSV5 or anti-ST-AP205 sera in western blots (Figure 2.5 A and 2.6 B). It is possible that the antibody concentrations used were unable to detect the AHSV 5 VP2domST protein. This could have been studied further by investigating alternative antibody dilutions but, the focus was shifted to optimising the detection of the AHSV 5 VP2domSC protein. This was considered of greater value due to the availability of the readily made and optimised ST-AP205 VLPs which Dr. Susan J Dennis (2019) expressed in both *N. benthamiana* and *E. coli*, and to which the AHSV 5 VP2domSC could be coupled. The coupling experiments are described in the next chapter.

In this study, the SpyCatcher peptide was only fused to the C-terminus of AHSV 5 VP2dom antigen because neutralizing antibody sites of the VP2 protein are believed to be located in the N-terminal half of VP2 (Martínez-Torrecuadrada and Casal, 1995, Martínez-Torrecuadrada *et al*., 2001). However, it would be worth investigating whether protein expression yield could be improved when SC is fused to N-terminus of VP2dom or if there would not be a significant difference. Additionally, it would be interesting to observe if there is a difference in antibody neutralization when the SC is attached to either the N- or C-terminus of the protein in future studies.

From the optimisation experiments, it was observed that in western blot analyses, anti-AHSV 5 sera used at a dilution of 1: 3000 was suitable for the detection of AHSV 5 VP2domSC produced from leaves infiltrated at OD_{600} = 1.0, (Figure 2.6). On the contrary, despite genetic inclusion of a Histidine tag (His-tag) at the N-terminus of VP2dom, no detection by anti-His antibody was observed (results not shown). This could be due to the cleavage of the His-tag during expression (S Dennis personal communication).

The best expression of AHSV 5 VP2domSC protein was seen on day 5 post infiltration (dpi) (Figure 2.6) and appeared to be reduced at 7 dpi. However, this is not surprising seeing that some studies have indicated similar observations (Shah *et al*., 2013, Zahmanova *et al*., 2020). It has also been suggested that protein expression could have been affected by gene silencing, one of the protective mechanisms deployed by plants against excess or abnormal gene expression or viral invasion (Bhaskar *et al*., 2009, Yu *et al*., 2019). Protein expression may also be affected by infiltration with bacterial cultures that are too concentrated, as this may cause excessive tissue damage in plants and thereby decrease protein expression (Norkunas *et al*., 2018). This hypothesis may be supported by the leaf chlorosis/yellowing observed in infiltrated regions of leaves at 7 dpi as compared to those at 5 dpi (Figure 2.4). Further possibilities are that with time, a higher accumulation of recombinant protein in the agroinfiltrated leaves may cause visible cell death in the infiltrated areas (Kanagarajan *et al*., 2012). With this in mind, in all further experiments, AHSV 5 VP2domSC protein was harvested at 5 dpi in *N. benthamiana* plants.

Chapter 3: Coupling of AHSV 5 VP2domSC to ST-AP205 VLPs

3.1: Introduction

To protect horses against African horse sickness (AHS), new and effective candidate vaccines have been under development. Currently, the only prophylactic vaccine against AHS registered in South Africa is the polyvalent live-attenuated vaccine (LAV) (Verwoerd, 2012). However, this vaccine has the possibility of genome segment reassortment between the live attenuated viruses (vaccine strains) and wild type AHSV (outbreak) strains. Furthermore, it can revert to virulence and it is a challenge to differentiate between vaccinated and infected (DIVA) animals. There has therefore been a need to develop a vaccine that is safer, cost-effective and more advantageous than the LAV.

Most recently (October 2020), an inactivated monovalent LAV for serotype 4 (AHSV4LP) was formulated with different adjuvants and studied as a prototype vaccine to observe its safety and efficacy with regard to local reactions (Van Rijn *et al*., 2020). As compared to LAVs, the safety and its relation to vaccine spread and DIVA compatibility, the inactivated vaccines were shown to be more favourable. However, inflammatory reactions were a problem, even in the presence of the different adjuvants and it had a slow onset of protection which may therefore not be suitable during an emergency. Furthermore, inactivated vaccines are not very economical, as a subsequent boost vaccination needs to be administered to ensure an adequate antigen response (Dennis *et al*., 2019, Rodríguez *et al*., 2020, Zientara *et al*., 2015).

Kanai *et al*. (2014) demonstrated that recombinant VP2 proteins of all nine AHSV serotypes have the potential to be used as safe subunit vaccines for AHS either individually or in a multi-serotype cocktail in guinea pigs. However, it was observed that cocktail formulations containing the genetically related VP2 proteins from serotypes 3 and 7, or 5 and 8, did not increase the neutralizing antibody (nAb) titres against their related serotypes, and no nAbs were detected against unrelated serotypes. Furthermore, there

was a strong difference in the nAb titres against each VP2 protein after immunization with either a cocktail or with a single VP2 protein. In another study, complete clinical protection was achieved after a single vaccination of polyvalent AHSV vaccines using either baculovirus-produced sub-unit VP2 or Modified Vaccinia Ankara (MVA)-VP2 vaccines in mice (Aksular *et al*., 2018). However, although this vaccine may be cost-effective, the protective efficacy needs to be investigated further.

The use of reverse genetics has demonstrated promising results of protective efficacy against AHSV, comparable to the LAV. In 2016, Lulla *et al* produced replication-deficient virus strains for all AHSV serotypes, coated with immunogenic capsid proteins (Lulla *et al*., 2016). These defective AHSV particles were able to replicate in complemented cell lines to obtain titres similar to those of the wild-type AHSV serotype. To evaluate the protective efficiency of defective viruses, vaccinated groups of IFNAR−/− mice showed significantly decreased levels of viremia when compared to the control (unvaccinated) groups. Similar results were observed when the replication-abortive AHSV strains were assessed in ponies (Lulla *et al*., 2017), indicating the suitability of these deficient viruses as animal vaccines.

Another interesting vaccine approach has been the use of virus-like particles (VLPs) for the display of pathogen-specific antigens. Such VLPs are highly immunogenic and act as scaffolds to display the antigenic determinants of these pathogens, thereby making them highly suitable vaccine candidates (Dennis *et al*., 2019, Syomin and Ilyin, 2019). Some of the ways in which antigens may be displayed on VLPs include chemical conjugation, genetic fusion, and most recently, through the use of the “plug-and-display” AP205-SpyTag: SpyCatcher protein conjugation system (Brune *et al*., 2016, Frietze *et al*., 2016). The AP205 coat protein (CP) retains the ability to assemble into VLPs even when fused to either the SpyTag (ST) or SpyCatcher (SC) peptide at either its N- or C-terminus. Thus, the antigen of interest, if fused to the corresponding Spy partner, can be coupled to the AP205 VLP and displayed on its surface by irreversible bond formation between the SpyTag and SpyCatcher peptides. Previously, several antigens have been successfully displayed using this system namely, the malarial antigen target in the pre-erythrocytic stage circumsporozoite protein (CSP), the malaria transmission-blocking vaccine target

antigens Pfs25 and Pfs47, and enterotoxigenic *Escherichia coli* endotoxins (Brune *et al*., 2016, Govasli *et al*., 2019, Janitzek *et al*., 2016, Molina-Cruz *et al*., 2013, Palladini *et al*., 2018, Yenkoidiok-Douti *et al*., 2019).

The promising results observed from the use of the ST/SC technology is an indication that this VLP conjugation approach may play a key role in the development of a potential VP2 AHSV 5 vaccine. As previously mentioned, Dr. Susan J Dennis from the Biopharming Research Unit (BRU) attempted to display the full-length AHSV 5 VP2 antigen on the surface of AP205 VLPs with the aid of the ST/SC platform (Dennis, 2019). Unfortunately, conjugation of the full VP2 protein was unsuccessful due to the large size of this protein. Here, the aim was to develop a particle display vaccine candidate by coupling a smaller VP2 peptide (VP2 domain) representing the major VP2 neutralisation epitopes fused to the SC peptide, to plant expressed ST-AP205 VLPs. It is hoped that successful use of this technology may pave the way towards the development of a multivalent AHSV VP2 vaccine which could potentially provide protection against all nine serotypes of the virus.

3.2: Materials and Methods

3.2.1 Large scale infiltration, expression and purification of AHSV 5 VP2domSpyCatcher

In the previous chapter, it was established that protein expression was only observed when recombinant AHSV 5 VP2dom was fused at its N-terminus to the SC peptide, but not to the ST peptide. Guinea pig anti-AHSV 5 sera (1:3000), detected expression best when plants were infiltrated at OD_{600} = 1.0, and leaves were harvested 5 dpi.

A. tumefaciens-mediated large-scale infiltration was performed as described in section 2.2.4 at optical density (OD_{600}) 1.0, using 20 – 25 *N. benthamiana* plants. The top 3 to 4 infiltrated leaves of each plant were harvested at 5 dpi and protein was extracted as described in section 2.2.5 using 1 x PBS (pH 7.4). Crude plant lysates were clarified by centrifugation at 25931 x *g* (13 000 rpm) for 20 min at 4 °C and AHSV 5 VP2domSC extracts were purified as described below (section 3.2.1.1, 3.2.1.2 and 3.2.1.3). Thereafter, samples were analysed by western blot using guinea pig anti-AHSV 5 sera diluted (1: 3000) in blocking buffer (as in 2.2.5). Alkaline phosphatase (AP) -conjugated goat anti-guinea pig (1: 5000) sera was used as the secondary antibody.

3.2.1.1 Protein purification by Ammonium sulphate $(NH_4)_2SO_4$ precipitation

AHSV 5 VP2domSC was purified from crude plant lysates by ammonium sulphate $(NH_4)_2SO_4$ precipitation (10 - 80% in 10% incrementing steps). The amount of solid $(NH_4)_2SO_4$ required was calculated using the online tool at https://www.encorbio.com/protocols/AM-SO4-new.htm. In each case, the protein was precipitated at 4 °C for 30 min followed by centrifugation at 25931 x *g* (13 000 rpm) for 20 min at 4 °C. Protein pellets were resuspended in 1/2th volume 1 x PBS.

3.2.1.2 Protein purification by pH precipitation

Alternatively, AHSV 5 VP2domSC protein was purified from crude plant lysates by pH precipitation. The pH was adjusted to 5 using hydrochloric acid to precipitate out RuBisCO and other plant proteins from the crude extracts and the supernatant was clarified by centrifugation at 25931 x *g* (13 000 rpm) for 20 min at 4 °C. The pH was then adjusted to 7.4 (pH of 1 x PBS) using sodium hydroxide (NaCl). The desired protein was precipitated

by centrifugation at 25931 x *g* (13 000 rpm) for 20 min at 4 °C and resuspended in 5 mL 1 x PBS. Pellet and supernatant samples were collected after each pH adjustment and 50 µL samples were denatured for 10 min at 95 °C for western blot analysis. Empty vector control (pEAQ-*HT*™ vector) sample was also analysed alongside AHSV 5 VP2domSC protein.

3.2.1.3 Extraction buffer determination

A. tumefaciens-mediated large-scale infiltration was performed as described in section 2.2.4 at optical density (OD_{600}) 1.0, using 20 – 25 *N. benthamiana* plants. The top 3 to 4 infiltrated leaves of each plant were harvested at 5 dpi and protein was extracted as described in section 2.2.5 comparing 5 buffers: 1. 1 x PBS (pH 7.4), 2. Tris base 100mM (pH 7.5), 3. Tris-HCl 100mM / Triton X-100 1% (pH 7.5), 4. Tris-HCl 100Mm / Triton X-100 1% (pH 8.0) and 5. Bicine 50mM / NaCl 20mM (pH 8.4). Crude plant lysates were clarified by centrifugation at 15344 x *g* (10 000 rpm) for 20 min at 4 °C and samples from both the pellet and supernatant were analysed by western blot using guinea pig anti-AHSV 5 sera (1: 3000) diluted in blocking buffer (as in 2.2.5). The supernatant was clarified again by centrifugation at 25931 x *g* (13 000 rpm) for 20 min at 4 °C and analysed by western blot.

3.2.2 ST-AP205 VLP purification from *N. benthamiana*

ST-AP205 VLPs were expressed and purified according to methods optimised by Dr. Susan J Dennis (2019) from the Biopharming Research Unit. The ST-AP205 CP recombinant *Agrobacterial* strain was cultured and used to infiltrate 20 five-week-old *N. benthamiana* plants as described in section 2.2.4. Plants were infiltrated at an OD_{600} of 0.25 by applying a vacuum of 98kPa.

The top 3 to 4 infiltrated leaves were harvested at 4 dpi and homogenised in 2 volumes of 1 x PBS (pH 7.4) using a Moulinex™ juice extractor. Homogenized leaf pulp was incubated with the extracted juice at 4°C for 1h with gentle agitation. The crude extract was filtered through 4 layers of MiraCloth™ (Merck, Darmstadt, Germany) and clarified twice firstly by centrifugation at 15344 x *g* (10 000 rpm) for 30 min at 4°C, followed by centrifugation at 25931 x *g* (13 000 rpm) for 20 min at 4°C

The ST-AP205 VLPs were then further purified by ultracentrifugation through a discontinuous iodixanol (Optiprep™, Sigma Aldrich, St Louis, MO, USA) density gradient. Iodixanol solutions (23%, 29% and 35% in 1 x PBS (pH 7.4) extraction buffer) were prepared and used to create a 7 mL step gradient (2, 3 and 2 mL respectively) and layered under 30 mL clarified plant extract. The gradients were centrifuged at 175000 x *g* (32 000 rpm) for 2 h at 4°C in an SW32 Ti rotor (Beckman, Brea, CA). Fractions (500 µL) were collected from the bottom of the tubes and 50 µL of each fraction was evaluated by SDS-PAGE followed by Coomassie blue staining, and by western blot analysis using ST-AP205 antiserum, raised in rabbits and diluted (1: 20 000) in blocking buffer. Protein expression was detected with AP-conjugated goat anti-rabbit sera diluted in blocking buffer (1: 10 000).

3.2.2.1 Transmission electron microscopy (TEM)

To visualise VLPs, glow-discharged copper grids (mesh size 200) were floated on 20 µL density gradient fractions for 5 min and then washed on five drops of sterilised water, successively. Particles were negatively stained for 30 s with 2% uranyl acetate and then imaged using a Technai G2 transmission electron microscope (TEM).

3.2.2.2 Gel Densitometry

The plant produced ST-AP205 VLP iodixanol gradient fractions were quantified by SDS-PAGE and evaluated by Coomassie blue staining. These samples were electrophoresed alongside serially diluted bovine serum albumin (BSA) (Sigma-Aldrich, St Louis, MO, USA) of known concentration. The SynGene reader (GeneTools version 3.07.03 software) was used to determine the amount of protein in individual bands and quantification of the VLPs was extrapolated from the BSA standard curve.

3.2.3 *In vitro* coupling of ST-AP205 VLPs and AHSV 5 VP2domSC

ST-AP205 and AHSV 5 VP2domSC proteins were purified as described in section 3.2.2 and 3.2.1.1, respectively. AHSV 5 VP2domSC protein was purified using $(NH_4)_2SO_4$ (30%, 40% and 60% salt concentrations) and protein pellets were stored at -20°C. Two methods were investigated to achieve coupling of AHSV 5 VP2domSC to ST-AP205. The first method involved the use of purified products i.e., purified Spy-tagged VLPs and purified SpyCatcher VP2 antigen at different ratios. These were mixed into two 400 µL

reactions. The first reaction comprised 40 µL ST-AP205 VLPs and 360 µL SC VP2. The second reaction mix comprised 80 µL ST-AP205 VLPs and 320 µL SC VP2. The second method involved mixing purified ST-AP205 VLPs (200 µL) with AHSV 5 VP2domSC-containing crude leaf extract (20 mL). Reactions were incubated O/N at 4°C with gentle agitation to allow coupling to occur.

3.2.4 ST-AP205 and AHSV 5 VP2domSC co-infiltration

N. benthamiana plants were co-infiltrated with pEAQ-ST-AP205 and pEAQ-AHSV 5 VP2domSC AGL-1 recombinants at OD_{600} 0.25 and 1, respectively (section 2.2.4 and 3.2.2). The top 3 to 4 infiltrated leaves of each plant were harvested at 4 dpi and protein was extracted as described in section 2.2.5 using 1 x PBS (pH 7.4) with a slight modification: ST-AP205 and VP2domSC homogenates were incubated for 3 ½ h at 4°C with gentle agitation. Crude plant lysates were then clarified by centrifugation at 25931 x *g* (13 000 rpm) for 20 min at 4 °C.

3.2.5 ST-AP205 and AHSV 5 VP2domSC co-purification

An additional strategy involving co-purification was also used to investigate potential coupling of ST-AP205 to AHSV 5 VP2domSC. This method (3.2.5.1) involved comparing three VLP: antigen ratios (1:1, 1:2 and 1:3) to determine the ratio which would indicate the highest yield of coupled product.

N. benthamiana plants were separately infiltrated with recombinant pEAQ-ST-AP205 and pEAQ-AHSV 5 VP2domSC *Agrobacterial* strains as described in section 3.2.2 and 2.2.4, respectively. Leaves were harvested at 4 dpi and then leaves expressing ST-AP205 and AHSV 5 VP2domSC were mixed at three different ST-AP205:AHSV 5 VP2domSC infiltrated leaf weight ratios (1:1, 1:2 and 1:3) and homogenised. Homogenates were incubated for 3 ½ h at 4°C with gentle agitation to allow for coupling, filtered through four layers of MiraCloth™ (Merck, Darmstadt, Germany) and then spun at 25931 x *g* (13 000 rpm) for 20 min at 4°C. Alternatively, leaves expressing ST-AP205 and AHSV 5 VP2domSC were mixed at a 1:1 ratio and homogenised. Homogenates were incubated for 2 h at 4°C with gentle agitation to allow for coupling and spun at 15344 x *g* (10 000

rpm) for 20 min at 4°C. The crude extract was filtered through one layer of MiraCloth™ (Merck, Darmstadt, Germany), spun again at 25931 x *g* (13 000 rpm) for 20 min at 4°C and then filtered again through one-layer MiraCloth™. Crude extract was incubated O/N at 4°C with gentle agitation.

For all coupling methods (3.2.3, 3.2.4 and 3.2.5), ST-AP205/VP2domSC crude extract was purified by ultracentrifugation through a discontinuous iodixanol density gradient as described in section 3.2.2. Fractions (500 µL) were collected from the bottom of the tubes and 50 µL reactions were evaluated for complex formation by western blot analysis with guinea pig anti-AHSV 5 sera (pre-absorbed and diluted 1:1000) and polyclonal rabbit anti-ST-AP205 sera (diluted 1: 20 000).

Pre-absorption was carried out to remove plant proteins from the antisera. To pre-absorb the antisera, leaves from a healthy plant were homogenised in two volumes of 1 x PBS containing protease inhibitor and centrifuged at 15344 x *g* (10 000 rpm) for 10 min. Plant supernatant was added to the nitrocellulose membrane and incubated for 2 h at room temperature (RT) with gentle shaking. The supernatant was poured off and the membrane was incubated in blocking buffer containing 5% milk for 1 hour at RT, with 4 x changes of blocking buffer. Antiserum (100 µL) was diluted in 100 mL blocking buffer with milk. This was added to the membrane and incubated for 3 ½ h at RT with shaking. Pre-absorbed antiserum was aliquoted in 10 mL amounts and store at -20 °C.

3.3 Results

3.3.1 Large scale expression and purification of AHSV 5 capsid protein

3.3.1.1 Protein purification by Ammonium sulphate $(NH_4)_2SO_4$ precipitation

Following expression and extraction, as described in section 3.2.1, AHSV 5 VP2domSC protein was purified by $(NH_4)_2SO_4$ precipitation (10 - 80%, in 10% incrementing steps). From three purification repeats, most of the desired protein was observed to precipitate at a concentration of 40% - 50% $(NH_4)_2SO_4$ (Figure 3.1, Appendix B: Figure 3) as indicated by a 48kDa protein detected by western blot analysis (Figure 3.1). No major difference in protein detection was observed when analysing dialysed versus undialysed purified VP2domSC protein samples (Appendix B: Figure 3).

Although AHSV 5 VP2domSC was precipitated by $(NH_4)_2SO_4$ precipitation, the AHSV antigen appeared to co-migrate with RuBisCO plant protein (55kDa - indicated by yellow arrow in Figure 3.1) on the gel. The majority of AHSV 5 VP2domSC was detected in the 40% fraction and no protein was detected in the 50% and 60% fractions indicating that most protein precipitated out at 40% (Figure 3.1).

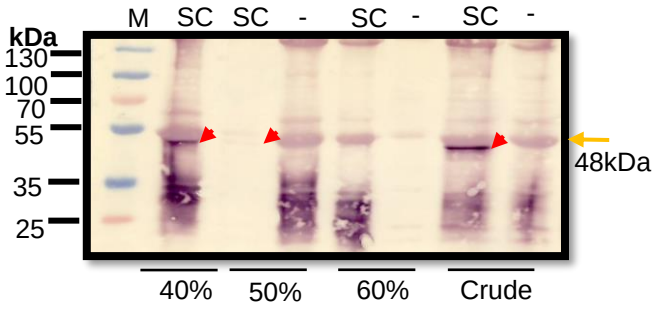

Figure 3.1: Purification of AHSV 5 VP2domSC protein by ammonium sulphate precipitation. Equal volumes of clarified crude plant extract and purified fractions were loaded in each lane. $(NH_4)_2SO_4$ precipitated leaf extract from plants infiltrated with an *Agrobacterial* recombinant containing an empty pEAQ-*HT* expression vector (-) was used as a negative control. Guinea pig anti-AHSV 5 sera (1:3000) was used as the primary antibody and AP-conjugated goat anti-guinea pig (1: 5000) sera was used as the secondary antibody to detect AHSV-5 VP2domain SC protein (SC; 48kDa). Crude extract from plants infiltrated with the VP2domSC *Agrobacterial* recombinant was used as a positive control. Red arrowheads indicate AHSV-5 VP2doSC protein. Yellow arrow indicates RuBisCO plant protein (55kDa). M: PageRuler Plus Prestained Protein Ladder (Fermentas UAB, Vilnius, Lithuania) was used as a molecular weight marker.

3.3.1.2 Protein purification by pH precipitation

After clarification of AHSV 5 VP2domSC, an attempt was made to separate the AHSV protein from the co-migrating RuBisCO plant protein. Both pellet and supernatant of plant crude extract and pH adjusted samples were analysed by western blot analysis using AHSV 5 antiserum diluted (1: 3000) in blocking buffer (Figure 3.2, Appendix B: Figure 4). The VP2domSC protein precipitated out of solution and was found mainly in the pellet, after adjusting the pH to 5.0. However, the band appeared to be slightly higher in the pH 5.0 pellet sample. No VP2domSC protein was detected at pH 7.4 in either pellet or supernatant. The 55 kDa RuBisCO band was less intense in the sample collected after using the pH drop method, suggesting that this step helped in decreasing the amount of co-migratory RuBisCO.

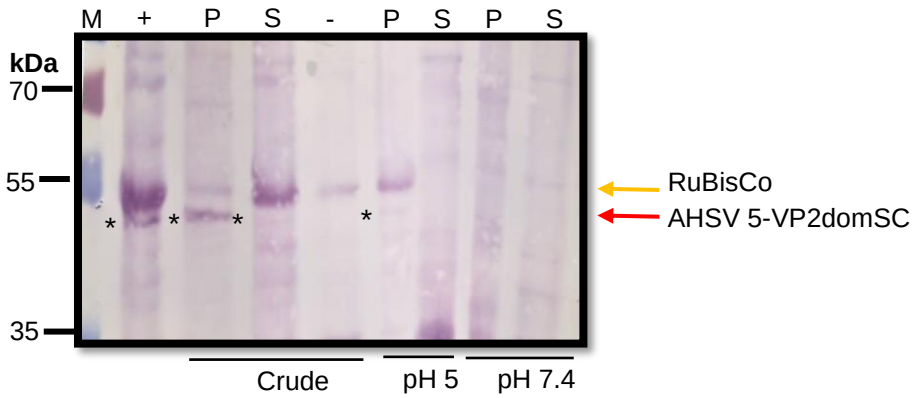

Figure 3.2: Purification of AHSV 5 VP2domSC protein by pH precipitation. Equal volumes of clarified pellet (P) and supernatant (S) plant crude extract and purified fractions were loaded in each lane. Empty pEAQ-*HT* expression vector (-) was used as a negative control. Guinea pig anti-AHSV 5 sera (1:3000) was used as the primary antibody and AP-conjugated goat anti-guinea pig (1: 5000) sera was used as the secondary antibody to detect AHSV-5 VP2domSC protein (SC; 48kDa). Crude extract from plants infiltrated with the VP2domSC *Agrobacterial* recombinant was used as a positive control. Asterisks and red arrow indicate AHSV-5 VP2domSC protein. Yellow arrow indicates RuBisCO plant protein (55kDa). M: PageRuler Plus Prestained Protein Ladder (Fermentas UAB, Vilnius, Lithuania) was used as a molecular weight marker.

3.3.1.3 Optimum extraction buffer determination

Five extraction buffers were compared to determine the optimal buffer for protein extraction. It was hoped that maximising the extraction of the desired protein would render enough protein available after protein purification for successful *in vitro* coupling of

purified products. Approximately 6 g each of infiltrated leaf tissue was used to extract AHSV 5 VP2 SC protein using the different extraction buffers namely, Tris base 100mM (pH 7.5), Tris-HCl 100mM / Triton X-100 1% (pH 7.5), Tris-HCl 100Mm / Triton X-100 1% (pH 8.0), Bicine 50mM / NaCl 20mM (pH 8.4), and 1 x PBS (pH 7.4); the standard protein extraction buffer used for previous AHSV 5 VP2 SC extractions. Equal volumes of pellet and supernatant extracts were analysed by western blot analysis using AHSV 5 antiserum diluted (1: 3000) in blocking buffer, to observe a 48kDa protein (Figure 3.3).

When comparing pellet and supernatant extracts, most of the desired protein was observed in the pellet (Figure 3.3 B), after extraction with Tris-HCl / Triton X-100 (pH 8.0) buffer (Figure 3.3 A & C). Moreover, there were more non-specific bands detected in all AHSV 5 VP2domSC pellet samples, including crude supernatant from the first clarification step as compared to supernatant obtained after the second clarification step (Figure 3.3 C). The second clarification step aimed at reducing the presence of these non-specific proteins in the extract. Although this was achieved, there was also a reduction in the total desired protein, as seen by the lower band intensity.

Additionally, more of the desired protein from the second clarification step was detected when using Tris or Bicine / NaCl as the extraction buffer than when Tris-HCl / Triton X-100 (pH 7.5), Tris-HCl / Triton X-100 (pH 8.0) and 1 x PBS extraction buffers were used (Figure 3.3 C).

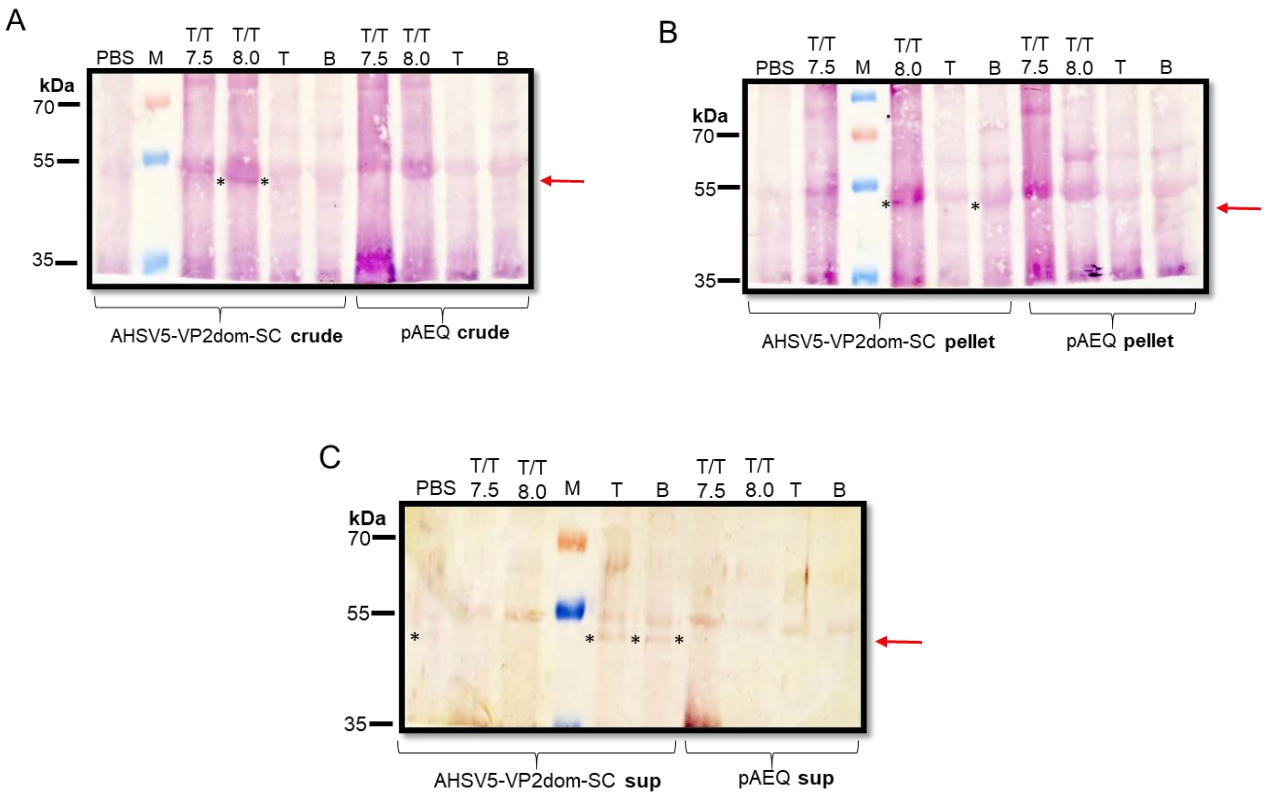

Figure 3.3: Optimum extraction buffer determination of AHSV 5 VP2domSC protein. Equal volumes of plant extracts were loaded in each lane. (A) Protein in supernatant after the first clarification. (B) Protein in pellet. (C) Protein in supernatant after the second clarification. pEAQ: empty pEAQ-*HT* expression vector was used as a negative control. Guinea pig anti-AHSV 5 sera (1:3000) was used as the primary antibody and AP-conjugated goat anti-guinea pig (1: 5000) sera was used as the secondary antibody to detect AHSV-5 VP2domSC protein (SC; 48kDa, asterisks and red arrows). M: PageRuler Plus Prestained Protein Ladder (Fermentas UAB, Vilnius, Lithuania) was used as a molecular weight marker. PBS - phosphate buffer saline, T/T - Tris and Triton X-100, T - Tris base, B - Bicine, Sup - Supernatant.

3.3.2 ST-AP205 VLP purification

An overnight culture of pEAQ-ST-AP205/AGL was used to vacuum infiltrate *N. benthamiana* plants at OD_{600} 0.25. Leaves were harvested at 4 dpi and purification of ST-AP205 VLPs was achieved by ultracentrifugation through a discontinuous iodixanol density gradient. Gradient fractions (50 µL) were analysed by SDS-PAGE then Coomassie blue staining and western blot (Figure 3.4 A) and quantified by gel

densitometry using a BSA standard (Figure 3.4 B). ST-AP205 protein was observed in fractions 2 to 8 (figure 3.4 A).

ST-AP205 CP can be identified on SDS PAGE gels in its monomeric (16.5 kDa), dimeric (33 kDa), trimeric (49.5 kDa) or tetrameric (66 kDa) forms. In this figure, only the ST-AP205 CP trimer is not observed (Figure 3.4 A). Fractions 5 to 7 were selected for further purification, as less background plant protein was present in these fractions and ST-AP205 CP monomer band was quantified by gel densitometry against known bovine serum albumin (BSA) standards. The yield of ST-AP205 CP obtained from fractions 3-6 was 70 µg/mL, 58 µg/mL, 86.2 µg/mL and 145.2 µg/mL, respectively.

TEM evaluation of fraction 5 showed the presence of numerous fully formed particles with an estimated average diameter of ±28.4 nm per field of view (Figure 3.4 C & D).

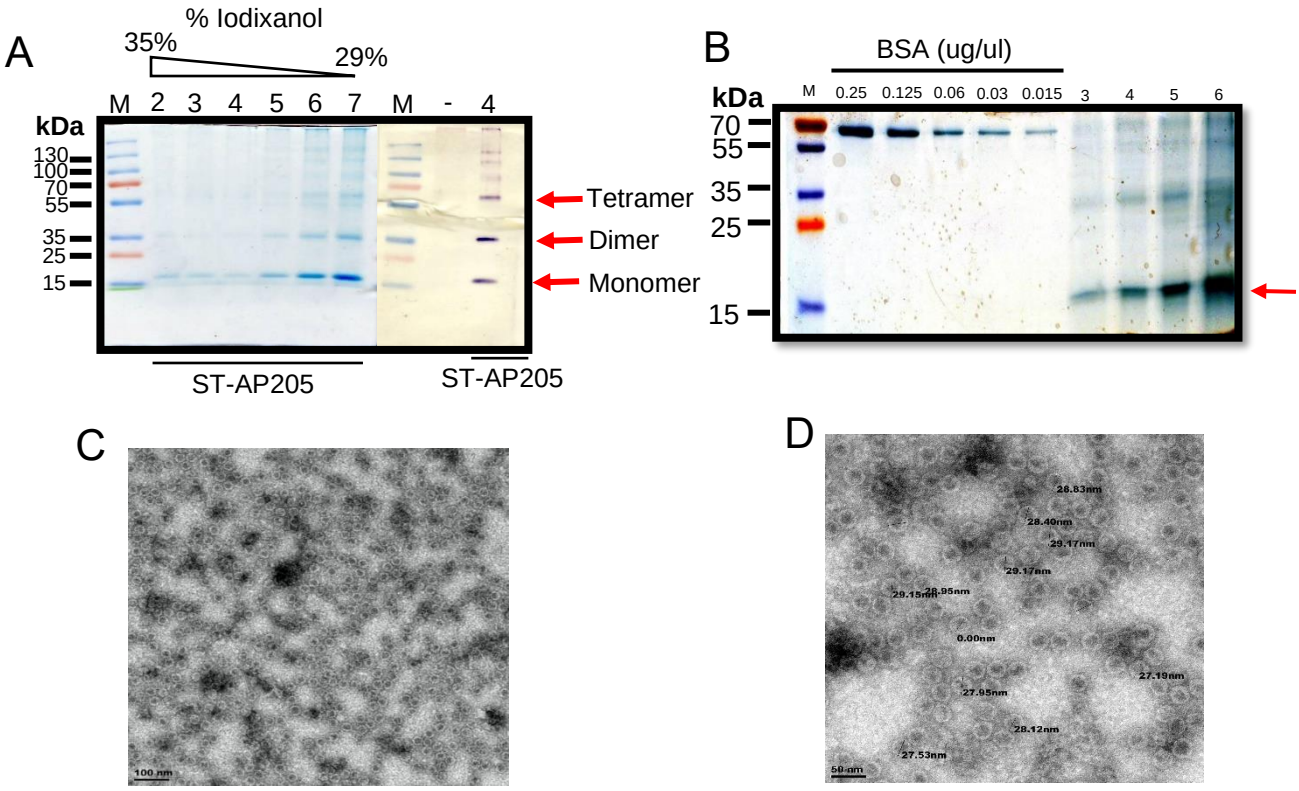

Figure 3.4: Purification of ST-AP205 VLPs expressed in *N. benthamiana* plants. (A) Coomassie blue-staining and western blot of fractions (2–7), retrieved following iodixanol density gradient ultracentrifugation of crude lysate from leaves infiltrated with the pEAQ-ST-AP205/AGL recombinant. Arrows indicate the ST-AP205 protein in its different aggregate forms, monomer (16.5 kDa), dimer (33 kDa) and tetramer (66 kDa). RuBisCo (66kDa) protein was observed below ST-AP205 tetramer in both experimental and pEAQ-*HT* negative control fractions. Gradient fractions from lysate of plants infiltrated with an *Agrobacterial* recombinant containing an empty pEAQ-*HT* expression vector (-), was used as a negative control (B) Quantification of purified ST-AP205 protein fractions 3 - 6 by gel densitometry using a BSA standard. M: PageRuler Plus Prestained Protein Ladder (Fermentas UAB, Vilnius, Lithuania) was used as a molecular weight marker (C-D) Images by TEM revealed the presence of purified ST-AP205 VLPs (±28.4 nm), fraction 5. Scale bars: 100 nm (C) and 50 nm (D).

3.3.3 ST-AP205 VLPs and AHSV 5 VP2domSC coupling

Three different methods of coupling were tested to determine the one that would produce the highest yield of coupled product. These different coupling methods included: *In vitro* coupling of purified ST-AP205 VLPs and AHSV 5 VP2domSC, *in planta* coupling following co-infiltration of *N. benthamiana with* ST-AP205 and AHSV 5 VP2domSC *Agrobacterial*

recombinants, and *in vitro* coupling of ST-AP205 and AHSV 5 VP2domSC by combining leaves infiltrated with ST-AP205 and AHSV 5 VP2domSC *Agrobacterial* recombinants and co-purifying the expressed proteins.

3.3.3.1 *In vitro* coupling of purified ST-AP205 VLPs and AHSV 5 VP2domSC

In vitro coupling involved carrying out separate infiltrations of *N. benthamiana* with either the pEAQ-ST-AP205 or pEAQ-AHSV 5 VP2domSC *Agrobacterial* recombinants at OD_{600} 0.25 or 1.0, respectively. The expressed protein was purified (3.2.2 and 3.2.1.1) and *in vitro* coupling was performed through two coupling methods to observe ST-AP205_AHSV 5 VP2domSC complex formation (Figure 3.5 A & B).

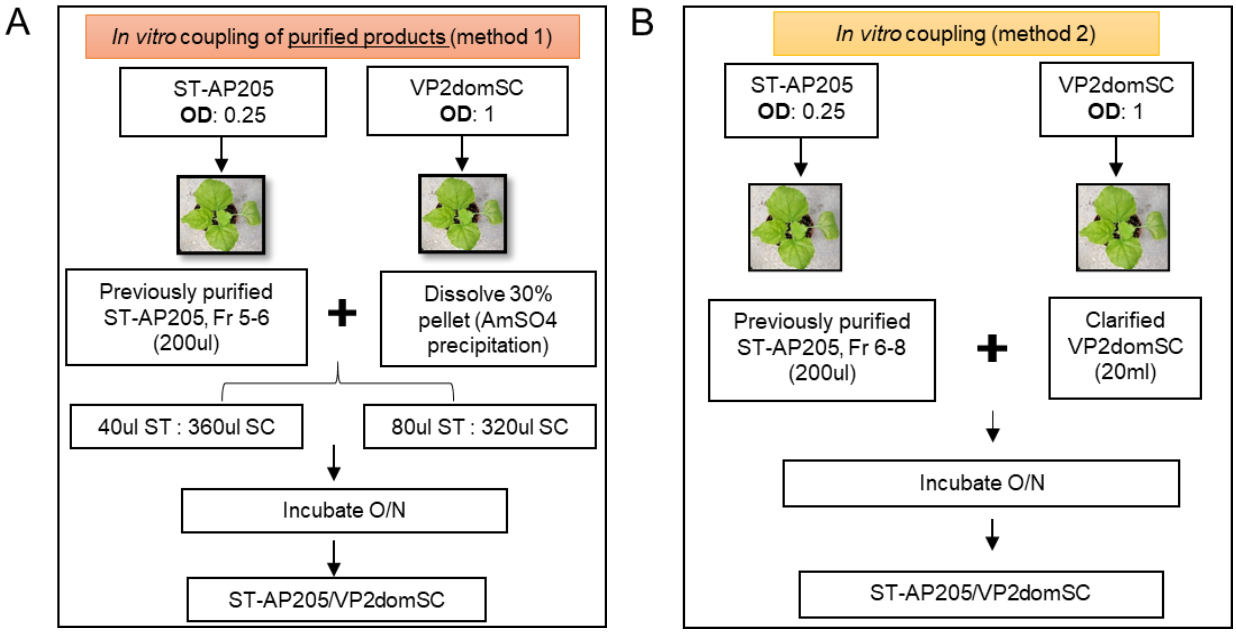

Figure 3.5: Schematic representation of ST-AP205 VLP and AHSV 5 VP2domSC *in vitro* coupling methods. (A) *In vitro* coupling method 1 involved the use of purified ST-AP205 VLPs and purified VP2domSC crude to obtain coupling. (B) *In vitro* coupling method 2 involved the use of purified ST-AP205 VLPs and VP2domSC present in infiltrated crude plant lysate to obtain coupling. Upon mixing, ST-AP205 and SpyCatcher VP2 were incubated O/N at 4 °C to mature particles.

The first *in vitro* coupling method (method 1) involved mixing 40 µL of purified ST-AP205 VLPs (fraction 6) with 360 µL $(NH_4)_2SO_4$ purified AHSV 5 VP2-SC (40:360) or 80 µL of purified ST-AP205 VLPs (fraction 5 & 6) with 320 µL $(NH_4)_2SO_4$ purified AHSV 5 VP2-SC

(80:320). Both fractions 5 and 6 of ST-AP205 VLPs in 80:320 ratio were used because there was not enough fraction 6 available; fraction 6 contained less non-specific protein (results not shown). Plant produced ST-AP205 VLPs were purified by iodixanol density gradient ultracentrifugation and stored at 4° C for about 2 weeks before use, whilst plant expressed AHSV 5 VP2-SC was purified by 30% AHSV 5 VP2-SC precipitation. Formation of coupled products was analysed by western blot using pre-absorbed guinea pig anti-AHSV 5 sera (1: 1000) (Figure 3.6) and polyclonal rabbit anti-AP205 (1: 20 000) (results not shown). Successful coupling was demonstrated by the detection of a 64.5kDa band (red arrow, 16.5 kDa ST-AP205 monomer + 48 kDa VP2domSC). Better coupling was observed when the proteins were combined at a ratio of 80:320 µL (Figure 3.6 B) than 40:360 µL (Figure 3.6 A), as seen by the band intensity. Moreover, there appeared to be less uncoupled VP2domSC (blue arrow) in the 80:320 µL than 40:360 µL coupling ratio.

The second *in vitro* coupling method involved the use of fractions 6-8 of purified ST-AP205 VLPs (200 µL) and crude extract containing AHSV 5 VP2domSC (200 mL). Fractions 6-8 of ST-AP205 VLPs were used because there was not enough fraction 6 available; fraction 6 contained less non-specific protein (results not shown). ST-AP205VLPs were purified by iodixanol density gradient ultracentrifugation. Complex formations were evaluated by western blot analysis using pre-absorbed guinea pig anti-AHSV 5 sera. The presence of complex formation was determined by the detection of a 64.5kDa band (red arrowheads, 16.5 kDa ST-AP205 monomer + 48 kDa VP2domSC). Fractions 6 – 8 were selected because fully formed particles were expected in the 29% iodixanol density gradient fraction. Coupling of purified products was mainly evident in gradient fractions 7 and 8 (Figure 3.6 B) as opposed to gradient fractions 5 and 6 (Figure 3.6 A) where only very faint bands were observed. Coupling may be less efficient with this second method compared to the first *in vitro* coupling method used above, as demonstrated by differing band intensities.

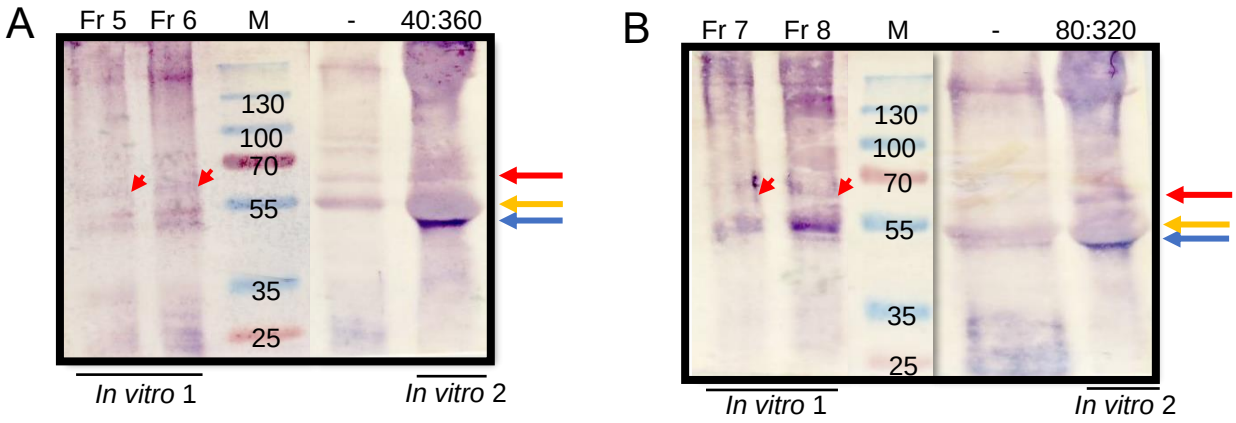

Figure 3.6. Analysis of ST-AP205 VLP and AHSV 5 VP2domSC complex formation by *in vitro* coupling on western blot using pre-absorbed guinea pig anti-AHSV 5 sera. (A) The first and second *in vitro* coupling methods showing fraction 5 & 6 and 40:360 coupling ratio, respectively. (B) The first and second *in vitro* coupling methods showing fractions 7 & 8 and 80:320 coupling ratio, respectively. Red arrows and arrowheads indicate ST-AP205/VP2domSC complex formation (16.5 kDa ST-AP205 monomer + 48 kDa VP2domSC). Blue arrows indicate the VP2domSC proteins (48 kDa). Yellow arrows indicate RuBisCO plant protein. Empty pEAQ-*HT* expression vector (-) was used as a negative control. M: PageRuler Plus Prestained Protein Ladder (Fermentas UAB, Vilnius, Lithuania) was used as a molecular weight marker.

3.3.3.2 ST-AP205 and AHSV 5 VP2domSC co-infiltration

Here, the aim was to investigate whether coupling would occur *in planta* and how effective it might be compared to *in vitro* coupling. *N. benthamiana* plants were co-infiltrated with pEAQ-ST-AP205 and pEAQ-AHSV 5 VP2domSC *Agrobacterial* recombinants at OD_{600} 0.25 and 1.0, respectively. Expressed protein was purified by ultracentrifugation through a discontinuous iodixanol density gradient. Complex formation was determined by western blot analysis using pre-absorbed guinea pig anti-AHSV 5 and polyclonal rabbit anti-AP205 sera (Figure 3.7).

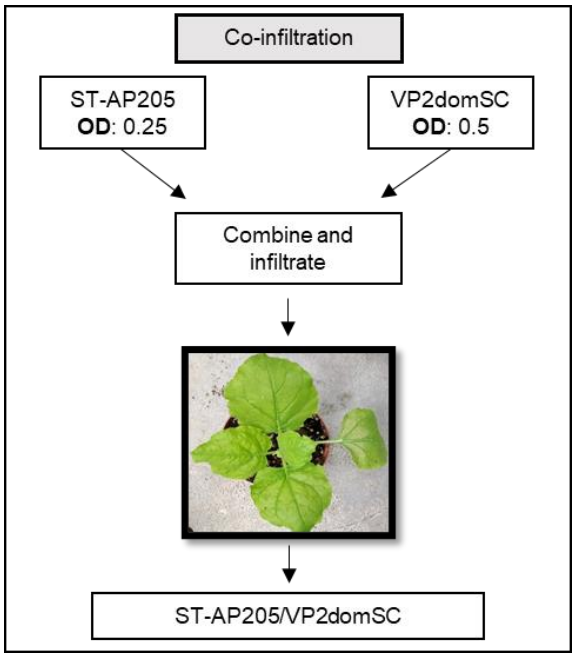

Figure 3.7: Schematic representation of co-infiltrated ST-AP205 VLP and AHSV 5 VP2domSC. *In planta* coupling of ST-AP205 VLPs/VP2domSC after co-infiltrating the two cultures in *N. benthamiana.*

Following co-expression, ST-AP205 VLP/VP2domSC coupled products (16.5 kDa ST-AP205 monomer + 48 kDa VP2domSC, Figure 3.8 A, red arrowheads) were detected by pre-absorbed guinea pig anti-AHSV 5 sera with an increasing band intensity from fractions 6 - 8 (29% iodixanol density gradient). Uncoupled VP2domSC (blue arrow, 48kDa) was faintly noted in fraction 8, directly below the RuBisCO protein band (yellow arrow, 55kDa)

Coupled ST-AP205/VP2domSC products (Figure 3.8 B, red arrow, 16.5 kDa and 48 kDa) were also observed with polyclonal rabbit anti-AP205 sera in the 29% iodixanol density gradient fractions. ST-AP205 proteins in different conformations namely: monomeric, dimeric and tetrameric were detected in fractions 2 – 8, including uncoupled ST-AP205 (positive control). However, the monomer, dimer and tetramer uncoupled ST-AP205 proteins appeared to migrate slightly faster than the conformations in the experimental lanes (fraction 2 – 8), possibly due to the cleavage of ST from AP205 VLP after long-term storage.

TEM evaluation indicated the presence of particles with an estimated average diameter of ±29.4 nm per field of view (Figure 3.8 C & D), fraction 7.

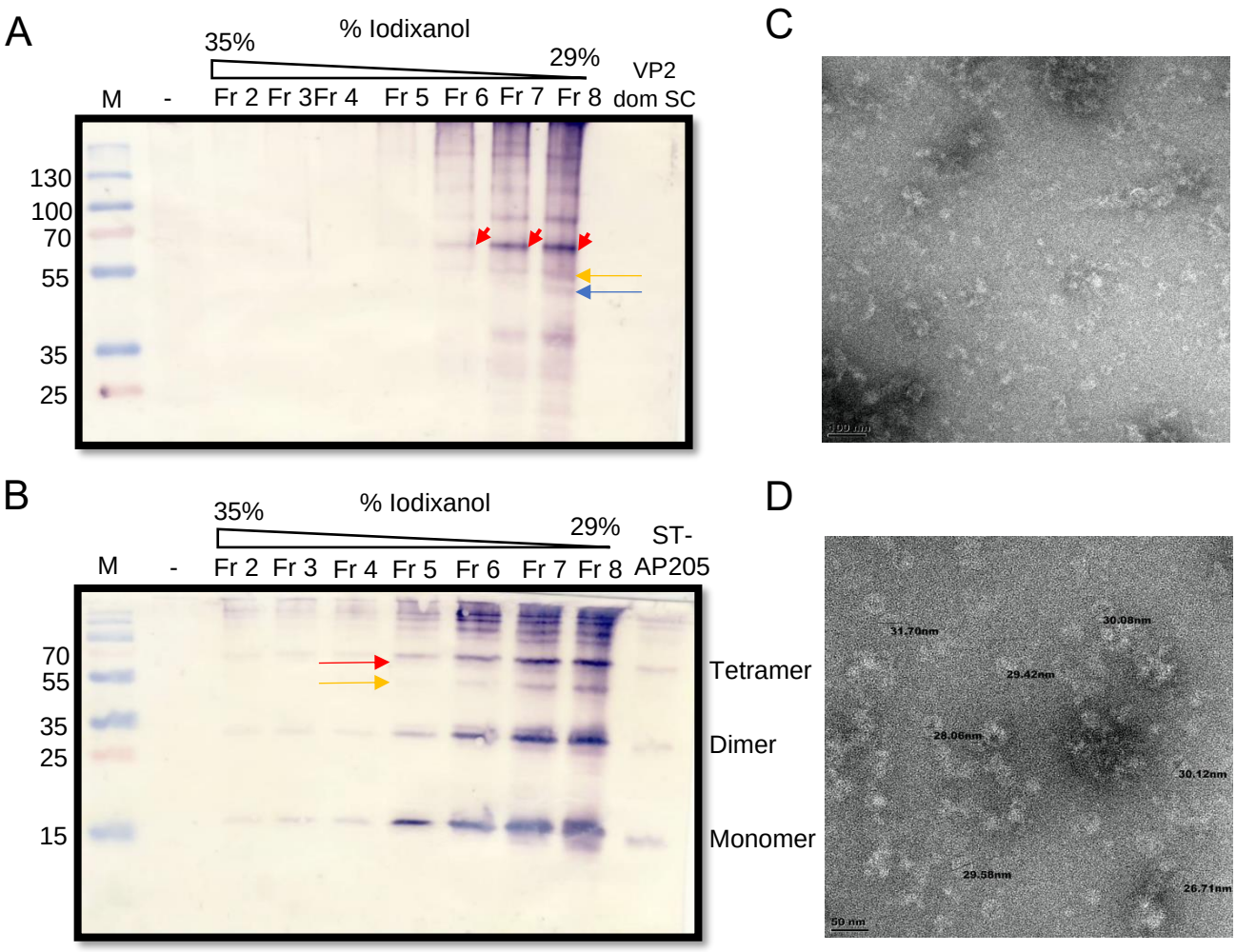

Figure 3.8: Analysis of ST-AP205 VLP and AHSV 5 VP2domSC complex formation after co-infiltration and expression in *N. benthamiana*, detected by western blotting using pre-absorbed guinea pig anti-AHSV 5 (A) and polyclonal rabbit anti-AP205 sera (B). (A) Coupling analysis of ST-AP205 VLP/VP2domSC is indicated by red arrowheads (16.5 kDa and 48 kDa). Blue arrow indicates uncoupled VP2domSC protein (48kDa). (B) ST-AP205 VLP/VP2domSC complex formation is indicated by the red arrow. ST-AP205 protein conformations namely monomer (16.5 kDa), dimer (33 kDa) and tetramer (66 kDa) are indicated to the right of the gel. Yellow arrows indicate RuBisCO plant protein. Empty pEAQ-*HT* expression vector (-) was used as a negative control. M: PageRuler Plus Prestained Protein Ladder (Fermentas UAB, Vilnius, Lithuania) was used as a molecular weight marker. (C-D) Images by TEM revealed the presence of purified VLPs (±29.4 nm), fraction 7. Scale bars: 100 nm (C) and 50 nm (D).

3.3.3.3 ST-AP205 and AHSV 5 VP2domSC co-purification

Lastly, it was investigated whether coupling would occur when *N. benthamiana* plants were infiltrated separately with the pEAQ-ST-AP205 and pEAQ-AHSV 5 VP2domSC *Agrobacterial* recombinants and the crude extracts were combined and incubated prior to purification.

3.3.3.3.1 Initial method for ST-AP205 and AHSV 5 VP2domSC co-purification

To determine the highest yield of coupled product through co-purification, homogenates were incubated at different VLP: antigen leaf weight ratios, namely 1:1, 1:2 and 1:3 (Figure 3.9). ST-AP205/VP2domSC crude extract was purified by ultracentrifugation through a discontinuous iodixanol density gradient. Complex formation was determined by western blot analysis using pre-absorbed guinea pig anti-AHSV 5 and polyclonal rabbit anti-ST-AP205 sera.

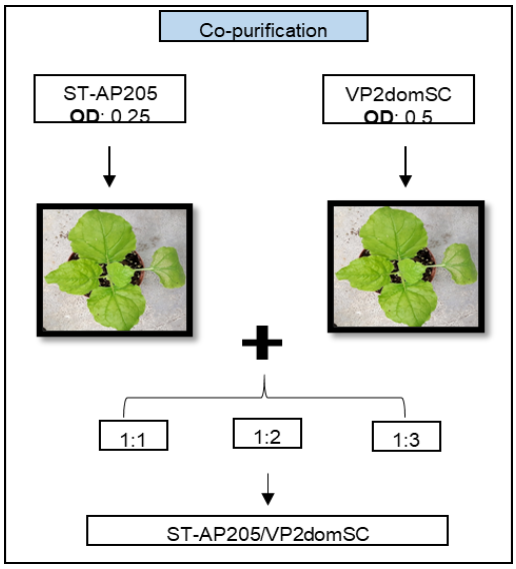

Figure 3.9: Schematic representation of ST-AP205 VLP and AHSV 5 VP2domSC co-purification. Constructs infiltrated separately in *N. benthamiana* and thereafter co-purified to result in coupling.

Coupled ST-AP205 VLP_AHSV 5 VP2domSC products (16.5 kDa ST-AP205 monomer + 48 kDa VP2domSC, Figure 3.10 A-C, red arrow and arrowheads) were detected by western blot when probed with pre-absorbed guinea pig anti-AHSV 5 for all three ST-AP205 VLP:AHSV 5 VP2domSC ratios (1:1, 1:2 and 1:3). Based on the band intensities

of the ST-AP205/VP2domSC complexes, the highest yield of coupled product was observed when infiltrated leaves were mixed in a 1:3 leaf weight ratio (Figure 3.10 A), followed by a 1:2 leaf weight ratio (Figure 3.10 B). However, gradient fractions from the crude lysates resulting from leaves mixed in a 1:3 leaf weight ratio were not properly collected and some sample was lost during sample collection. Therefore, these fractions could not be accurately compared with those obtained from 1:1 or 1:2 ST-AP205 VLP:AHSV 5 VP2domSC leaf weight ratios. Fraction 4, 1:2 was not included in Figure 3.10 B. Uncoupled VP2domSC (blue arrow, 48kDa) was faintly noted in 1:3 ratio, fraction 2 but not in the positive control.

No ST-AP205:VP2domSC complexes were detected in all three VLP: antigen ratios with polyclonal rabbit anti-ST-AP205 sera (Figure 3.10 C). However, ST-AP205 proteins in different aggregate forms (monomeric, dimeric and tetrameric) were detected in experimental lanes (Figure 3.10 C), including uncoupled ST-AP205 (positive control). However, the monomer, dimer and tetramer uncoupled ST-AP205 proteins appeared to be slightly lower than expected.

Images by TEM evaluation showed the presence of particles with an estimated average diameter between ±27.8nm to ±31.3nm per field of view (Figure 3.10 D - G), fraction 6 to 7. On average, particles in 1:1 ratio, fraction 6 appeared to be bigger (±31.3nm) and fully formed relative to the particles in 1:1, fraction 7, or those in the 1:2 ratio (fraction 6 & 7).

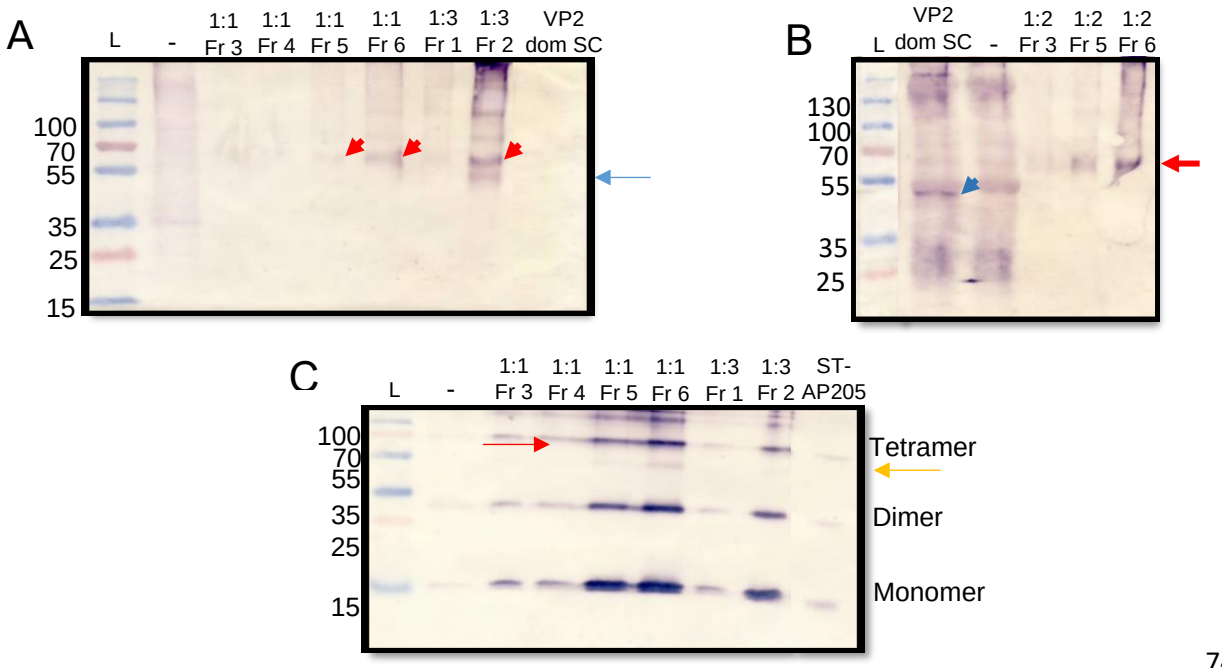

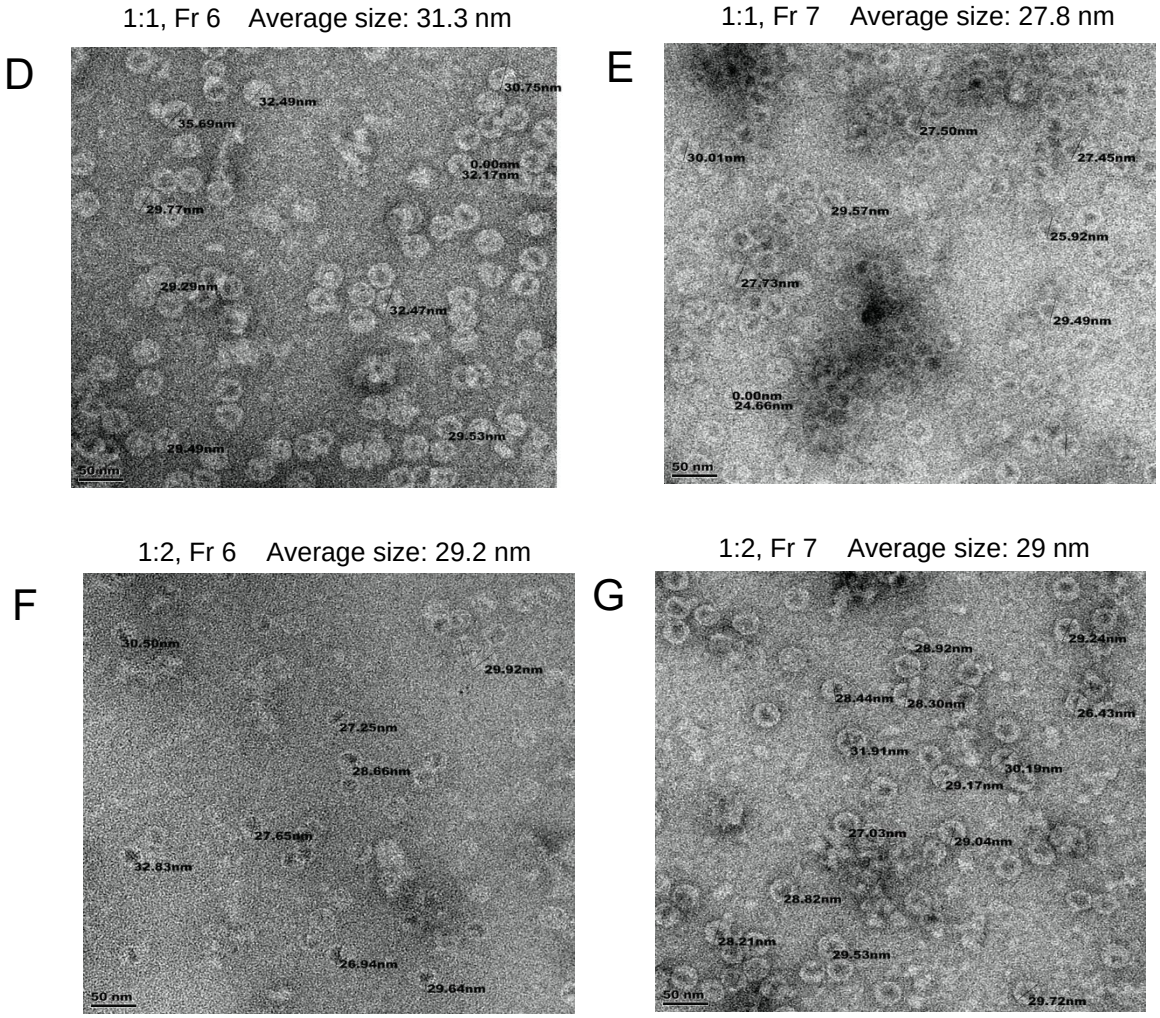

Figure 3.10: Analysis of ST-AP205 VLP and AHSV 5 VP2domSC complex formation following co-purification and detection by western blotting using pre-absorbed guinea pig anti-AHSV 5 (A & B) and polyclonal rabbit anti-ST-AP205 sera (C). (A & B) Coupled complexes of ST-AP205 VLP/VP2domSC indicated by red arrows and arrowheads (16.5 kDa and 48 kDa). Blue arrow indicates uncoupled VP2domSC protein (48kDa). (C) ST-AP205 VLP/VP2domSC complex formation not seen but expected, on area where red arrow is indicating. Detected ST-AP205 proteins conformations namely monomer (16.5 kDa), dimer (33 kDa) and tetramer (66 kDa). Yellow arrows indicate RuBisCO plant protein. Empty pEAQ-*HT* expression vector (-) was used as a negative control. M: PageRuler Plus Prestained Protein Ladder (Fermentas UAB, Vilnius, Lithuania) was used as a molecular weight marker. (D-G) Images by TEM revealed the presence of purified VLPs, 1:1 and 1:2 ratios, fractions 6 - 7. Scale bars: 50 nm.

3.3.3.3.2 Adjusted method of ST-AP205 and AHSV 5 VP2domSC co-purification

After comparing results from the coupling techniques (*in vitro* coupling, co-infiltration) and the co-purification VLP: antigen ratios (1:1, 1:2, and 1:3), co-purification at 1:1 leaf weight ratio was identified as a preferred coupling approach due to the quality and quantity of particles visualised. However, to further increase the yield for the 1:1 VLP: antigen ratio, some adjustments were made to the initial co-purification method.

Coupled ST-AP205:VP2domSC products (16.5 kDa and 48 kDa), at 1:1 leaf weight ratio were observed with pre-absorbed guinea pig anti-AHSV 5 when ST-AP205 and VP2domSC were co-purified using the adjusted conditions (Figure 3.11 A, red arrowheads). Nevertheless, based on the band intensity, the yield of complex formation across fractions 5 – 8 was lower than expected, and also less than observed in the initial co-purification method (Figure 3.10 A & B). Uncoupled VP2domSC (blue arrow, 48kDa) was observed, just below RuBisCO (yellow arrow, 55kDa). However, detection of complex formation (64.5kDa; 16.5 kDa and 48 kDa) was not clearly seen nor distinguished from the ST-AP205 tetramer (66kDa) when polyclonal rabbit anti-ST-AP205 sera was used (Figure 3.11 B).

TEM evaluation indicated the presence of fewer particles with an estimated average diameter of ±29.4 nm per field of view (Figure 3.11 C & D), fraction 7.

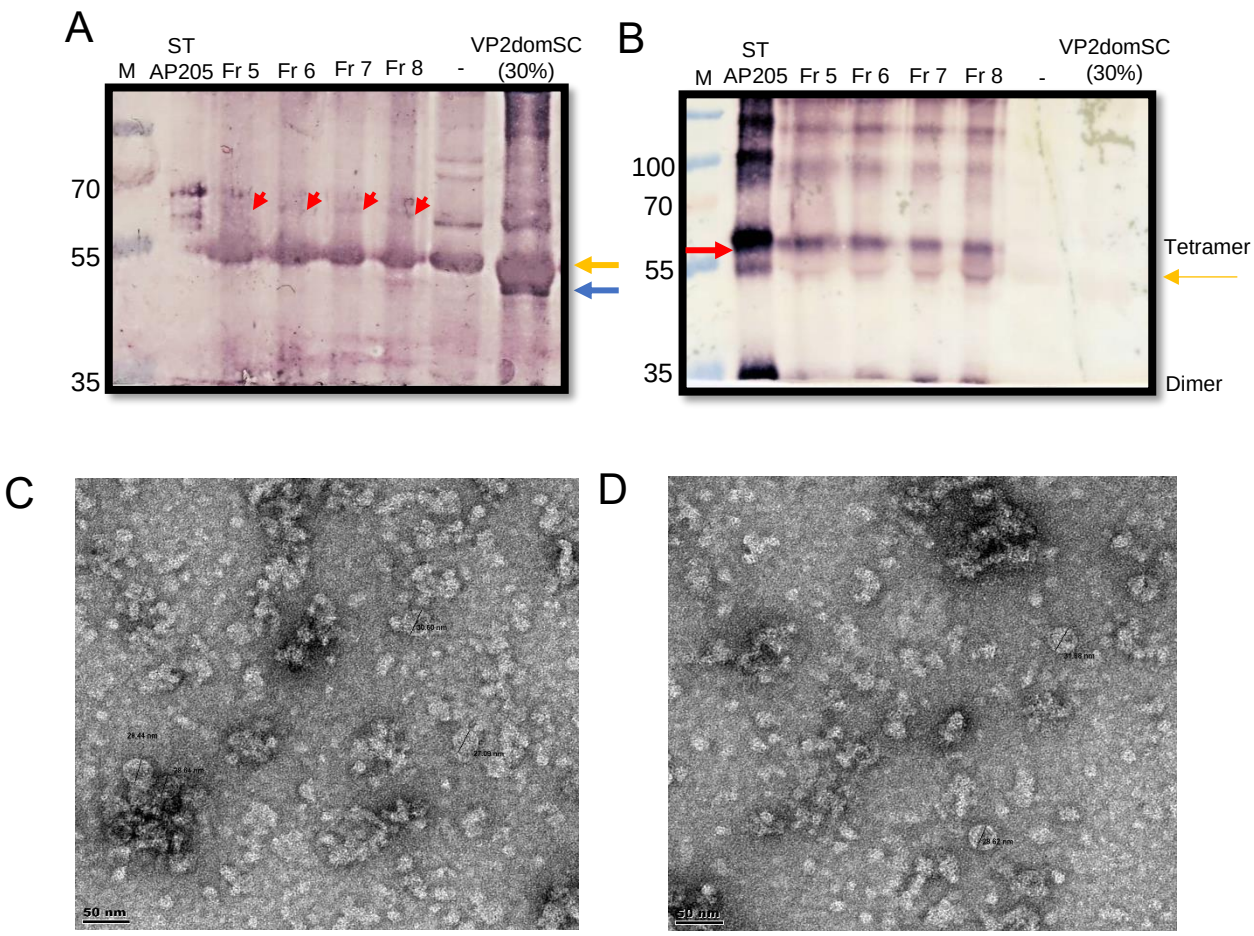

Figure 3.11: Analysis of ST-AP205 VLP and AHSV 5 VP2domSC complex formation following co-purification (1:1) and detection by western blotting (A) and polyclonal rabbit anti-ST-AP205 sera (B). (A) Coupled complexes of ST-AP205 VLP/VP2domSC indicated by red arrowheads (16.5 kDa and 48 kDa). Blue arrow indicates uncoupled VP2domSC protein (48kDa). (B) ST-AP205 VLP/VP2domSC complex formation not seen but expected on area where red arrow is indicating. Detected ST-AP205 proteins conformations namely dimer (33 kDa) and tetramer (66 kDa). Yellow arrows indicate RuBisCO plant protein. Empty pEAQ-*HT* expression vector (-) used as a negative control. M: PageRuler Plus Prestained Protein Ladder (Fermentas UAB, Vilnius, Lithuania) was used as a molecular weight marker. (C & D) Images by TEM revealed the presence of purified VLPs, fraction 7. Scale bars: 50 nm.

3.4: Discussion

Currently, the only registered prophylactic vaccine to control AHSV in endemic African countries is a polyvalent live-attenuated vaccine (LAV) (Verwoerd, 2012). However, due to safety concerns with the LAV, safe and more effective AHSV vaccine approaches are being evaluated such as inactivated virus, use of recombinant VP2 proteins, reverse genetics and most recently virus-like particles (VLPs) (Aksular *et al*., 2018, Dennis *et al*., 2019, Kanai *et al*., 2014, Lulla *et al*., 2017, Lulla *et al*., 2016, Rodríguez *et al*., 2020, Syomin and Ilyin, 2019, Van Rijn *et al*., 2020, Zientara *et al*., 2015).

VLPs are self-assembling particles, which are highly immunogenic and can mimic the structure of the native virus, but are inherently safer as they contain no genetic material. Due to their physical nature, they may also serve as suitable scaffolds for displaying foreign antigens for vaccine use (Thrane *et al*., 2016). Phage AP205 VLPs have been shown to be very useful in the display of antigens, which are fused to either the N- or C-terminus of the VLPs (Pastori et al., 2012, Tissot et al., 2010b). To aid in the display, studies have utilised the SpyTag-SpyCatcher or “plug-and-display” system, a novel conjugation system to display antigens fused to AP205 VLPs (Brune *et al*., 2016, Govasli *et al*., 2019, Janitzek *et al*., 2016, Molina-Cruz *et al*., 2013, Palladini *et al*., 2018, Yenkoidiok-Douti *et al*., 2019). This chapter focuses on utilizing SpyTag-AP205 VLPs to display AHSV serotype 5 VP2dom-SpyCatcher, the main antigenic domain of AHSV 5 VP2, to develop a safe and effective vaccine against AHSV.

Firstly, a scaled-up purification protocol for VP2domSC produced in plants was developed. Several different methods were employed to purify AHSV 5 VP2domSC protein (48kDa) including $(NH_4)_2SO_4$ precipitation, pH precipitation or the use of different buffers. Some recombinant protein was successfully purified, but some protein was lost during purification because the yield of purified antigen was lower than expected, as seen by reduced band intensity (Figure 3.1 – 3.3). Moreover, despite several purification attempts, VP2domSC could not be separated from some contaminating plant protein, RuBisCo (55kDa) in particular.

Purification of plant expressed ST-AP205 VLPs was successfully achieved, by ultracentrifugation through a discontinuous iodixanol density gradient. This was demonstrated by SDS PAGE then Coomassie blue staining and western blot analysis which detected the monomeric (16.5 kDa), dimeric (33 kDa) and tetrameric (66 kDa) forms of the ST-AP205 CP as expected (Figure 3.4 A).

Secondly, an AHSV particle vaccine candidate was developed, consisting of AHSV 5 VP2dom displayed on the outer surface of phage AP205 particles by coupling ST AP205 particles to AHSV 5 VP2domSC protein produced in plants. Three different coupling strategies were investigated to obtain ST-AP205 VLP_AHSV 5 VP2domSC complex formation. The first strategy involved the use of *in vitro* coupling of purified products.

Although the VP2domSC was not as clean as anticipated, it could nevertheless still be coupled to purified ST-AP205 VLPs. Here, complex formation was investigated through two Spy-tagged VLP: SpyCatcher VP2 mixtures, (40:360 µL) and (80:320 µL). Based on band intensity, the 80:320 µL mixture had a higher yield of coupled product (16.5 kDa ST-AP205 monomer + 48 kDa VP2domSC) compared to the 40:360 µL mixture (Figure 3.6 A & B). These results may suggest that an increase in ST-AP205 is necessary to enhance coupling with VP2domSC. Since there are 180 potential ST antigen-binding motifs on ST-AP205 VLPs (Thrane *et al*., 2016), there might have been fewer VLPs available to accommodate the antigens present within the 40:360 µL mixture. This may also explain why there was more uncoupled VP2domSC seen in the 40:360 µL mixture, as opposed to the 80:320 µL mixture, according to band intensity.

Additionally, *in vitro* coupling was also investigated after crude extract containing VP2domSC was mixed with purified ST-AP205 VLPs. Unlike *in vitro* coupling using purified products only, results showed that the yield in this second *in vitro* coupling method was low, with a fainter band on western blot. This may suggest that to achieve *in vitro* coupling, both products to be coupled have to be purified to prevent hindrances during coupling by i.e., superabundant plant proteins like RuBisCo.

It was also hypothesized that coupling might be improved when the two conjugation partners were co-expressed *in planta*. Results showed that there was better conjugation of ST-AP205 to VP2domSC, especially in fraction 8 (Figure 3.8 A) as compared to *in vitro*

coupling of separately purified products, by western blot. This also correlates with work done by Peyret *et al*. (2020), who indicated that *in vivo* coupling was more advantageous than the *in vitro* coupling used in their particular study. They sought to conjugate tandem Hepatitis B core (tHBcAg) VLPs with the model antigen GFP, with the aid of the SpyTag/SpyCatcher system in *Nicotiana benthamiana*. Their results indicated the successful *in vivo* conjugation of tHBcAg-SC and GFP-ST, both in the cytosol and endoplasmic reticulum. Moreover, the *in vivo* system is less time and material consuming.

Further investigations were carried out to determine whether fully formed VP2domSC antigen would couple to ST-AP205 VLPs when the conjugation partners are expressed separately in plants but extracted and purified together by mixing infiltrated leaf material. This may be advantageous over *in planta* coupling methods because each of the conjugation partners would have undergone post-translational modifications before being co-extracted (Röder *et al*., 2017). Here, it was shown that coupling was also successful across all three VLP: antigen coupling fresh leaf weight ratios (1:1, 1:2 and 1:3), by western blot and TEM (Figure 3.10). Although the coupling yield on western blot appeared to be lower than that which was seen *in planta*, based on band intensity, more fully formed and spherical coupled particles were observed by TEM in fraction 6 and 7 (Figure 3.10 D, E &G). Additionally, through this method, the majority of the particles obtained were bigger, with an average size between ±27.8 nm to ±31.3 nm per field of view as compared to the coupled particles obtained by the other coupling methods.

It was interesting to observe a mixed population of the bigger and smaller particles after co-infiltration and co-purification (Figure 3.8 D and 3.10 D-G, respectively). Conjugated particles are assumed to be bigger than uncoupled ST-AP205 VLPs (±28.4 nm, Figure 3.4 C & D). Moreover, it may be suggested that during coupling, some antigen-binding motifs on ST-AP205 are not occupied by the VP2domSC antigens, thereby influencing the size (nm) of the particle i.e., the fewer the number of antigens on the ST-AP205 VLPs, the smaller the size of the particle, and vice versa.

To increase the degree of coupling, attempts were made to optimize the co-purification method e.g., by increasing the incubation time to mature the particles (Marini *et al*., 2019). Surprisingly, the yield of coupled products was lower than expected (Figure 3.11). It may

be suggested that because protein production can be affected by internal (expression cassettes, epigenetic factors) or external (light quality, temperature, humidity) factors (M Twyman *et al*., 2013), the efficiency of desired protein produced may differ, thereby leading to variable results. Additionally, it was also a challenge to distinguish the coupled product from plant host proteins, by western blot. Besides, purification of most plant-produced recombinant proteins is known to be challenging (Schillberg *et al*., 2019).

Although the three coupling techniques were compared according to either band intensity or size and quantity of ST-AP205 VLPs, this may not have been the best way to determine coupling. Further work may look into assessing the coupling efficiency (%) of each method by measuring the band intensities on western blots through gel densitometry of the coupled product over the uncoupled ST-AP205 VLPs and multiplying this by a hundred. This would allow us to know the occupancy of antigens on the surface of the VLPs. It would also be worth repeating some of the coupling experiments i.e., *in vitro* coupling of purified products and co-infiltration, to provide more data to make a more accurate comparison between the coupling techniques. Moreover, an extra purification step might be necessary to separate the coupled particles from the uncoupled protein (Peyret *et al*., 2020, Röder *et al*., 2017).

Chapter 4: General discussion and conclusions

4.1: General discussion

African horse sickness (AHS) is the most lethal infectious disease of horses worldwide. It is mainly prevalent in sub-Saharan Africa, but outbreaks have also occurred in North Africa, Europe and Asia (Howell, 1962, Morales-Briceño, Roy *et al*., 1994b). With a mortality rate of up to 95%, AHS has significant economic consequences in low-income countries especially, as it poses limitations on draft power and transportation. Moreover, AHS poses a major threat to the equine sport and companion animal industries. These concerns have driven research to control the spread of African horse sickness virus (AHSV), the causative agent of AHS.

Currently, the live attenuated vaccine (LAV) used to protect horses against all AHSV serotypes, is the only commercially available vaccine in Africa. Although this vaccine is effective, there are a lot of safety concerns associated with it, including reversion to virulence and reassortment between vaccine and wild virus strains, and it is not possible to differentiate between infected and vaccinated horses (Mellor and Hamblin, 2004, Weyer *et al*., 2016). With this in mind, there has been a growing need to investigate the production of alternative safer and more cost-effective AHS vaccines. This study focused on producing a plant-based virus-like particle (VLP) candidate vaccine to display the major neutralizing epitopes of AHSV serotype 5 outer capsid protein VP2, with a view to ultimately extending the technology to display the corresponding regions of VP2 from the other AHSV serotypes.

The preliminary aim of the study was to design, clone and transiently express this VP2 antigenic region, referred to as AHSV 5 VP2dom, linked to either the SpyTag (ST) or SpyCatcher (SC) peptide in *Nicotiana benthamiana* plants. According to the literature, the region of AHSV 5 VP2 believed to contain the major neutralizing epitopes, stretches from amino acid 211 to 502 (Bentley *et al*., 2000, Manole *et al*., 2012, Martínez-Torrecuadrada and Casal, 1995). Both AHSV 5 VP2domST and AHSV 5 VP2domSC were designed, synthesized and cloned into the pEAQ-*HT* plant transient expression vector. However,

western blot experiments demonstrated that only AHSV 5 VP2domSC was successfully expressed in plants. This was advantageous, as plant-expressed ST-AP205 VLPs, to which the AHSV 5 VP2domSC could be coupled, were available. Following expression of VP2domSC protein, this work then focussed on its purification. However, despite several different attempts to purify the protein, which included $(NH_4)_2SO_4$ precipitation, pH precipitation, and the use of different buffers, separating it from some plant protein contaminants, proved to be a challenge. It is also unfortunate that the yield of VP2domSC protein was substantially reduced during these different purification processes. In order to overcome this problem in the future, other purification methods could perhaps be explored. For example, it may be possible to use nickel affinity chromatography, because the AHSV 5 VP2domSC protein contains a His-tag at its N-terminus. This method was not originally explored as the protein was not detected by anti-His antibodies. It was thought that the reason for this may be the lack of sufficient exposure of the His-tag on the protein to facilitate its binding to the nickel ions (Bolanos-Garcia and Davies, 2006, Debeljak *et al*., 2006). However, this problem could be further explored by, for example, denaturing the protein prior to binding (McCoy, 2020).

The final goal of this study was to couple the plant-produced AHSV 5 VP2domSC to the outer surface of ST AP205 particles. In an attempt to achieve this, three different coupling strategies were tested: firstly, *in vitro* coupling of purified products, secondly, co-infiltration and subsequent *in planta* coupling of expressed protein products, and thirdly, purification of *in vitro* coupled products resulting from the mixing of separately infiltrated leaf tissues. For the first strategy, purified ST-AP205 VLPs were expressed in plants and an attempt was then made to couple them to $(NH_4)_2SO_4$ purified VP2domSC antigens. Coupling was successful using this method. It was interesting to note that increasing the quantity of ST-AP205 VLPs in the reaction, produced a higher yield of coupled product. A higher concentration of ST-AP205 VLPs could ensure full occupancy of the 180 potential antigen-binding motifs on the VLPs (Thrane *et al*., 2016). Coupling of ST-AP205 VLPs to AHSV 5 VP2domSC *in planta* was also successful, and in fact, as observed by western blot analysis, a higher yield of coupled product was demonstrated using this strategy than was shown for *in vitro* coupling of separately purified products.

Furthermore, successful coupling of ST-AP205 VLP to AHSV 5 VP2domSC using the third co-purification strategy was also achieved, although the yield of coupled product did appear to be lower using this coupling method than when coupling was done *in planta* by co-infiltration. Paradoxically, more fully formed coupled particles resulted from the co-purification strategy, as visualised by TEM. Using this strategy, three different VLP: antigen leaf weight ratios (1:1, 1:2 and 1:3) were compared and it was determined that the best coupling resulted when leaves were mixed in 1:1 leaf weight ratio. Unfortunately, despite several attempts to try and increase the ST-AP205 VLP_AHSV 5 VP2domSC yield through co-purification (1:1), it was still lower than expected.

4.2: Conclusion and future work

The technology from this proof-of-concept study can be used as an alternative to developing VLP vaccines for AHSV. This study reports the production of a VLP candidate vaccine displaying the major neutralizing epitopes of AHSV 5 VP2, using the SpyTag/SpyCatcher (ST/SC) platform. This study demonstrated that through the use of 'Plug-and-Display' technology, it is possible to couple a smaller region of AHSV 5 VP2, containing only the immunogenic determinants of that protein, onto AP205 VLPs without cleavage of the coupled protein product as was observed when the full VP2 antigen was used in a previous study (Dennis, 2019). The next step in the study would be to design VP2domSC for the other serotypes, express those in plants and then couple a mixture of VP2domSC proteins to the ST-AP205 VLPs, with the goal of developing a multivalent AHSV display particle vaccine.

Some aspects which could be further explored from this study include:

I. Investigating the expression of AHSV 5 VP2domSC in *E. coli* or yeast for a possible increase in protein yield. Expression in *E. coli* could reduce the time spent on purifying the protein because one of the main problems encountered with the plant-produced VP2domSC was separating it from some contaminating plant protein, RuBisCo in particular. On the other hand,

yeast expression systems are ideal for large-scale production of recombinant proteins and are cheaper than insect or mammalian expression systems because of their quick growth in defined medium. However, the use of yeast expression systems is beyond the scope of the study.

These single-celled eukaryotic organ-isms grow quickly in defined medium, are easier and less expensive to work with than insect or mammalian cells, and are easily adapted to fermentation. Yeast expression systems are ideally suited for large-scale production of recombinant eukaryotic proteins.

II. Immunogenicity testing in animals, particularly guinea pigs or horses to determine a host-specific antibody response and thereafter testing of the serum from vaccinated animals through ELISA.

References

Aksular, M., Calvo-Pinilla, E., Marín-López, A., Ortego, J., Chambers, A. C., King, L. A. & Castillo-Olivares, J. 2018. A single dose of African horse sickness virus (AHSV) VP2 based vaccines provides complete clinical protection in a mouse model. *Vaccine,* 36**,** 7003-7010.

Alberca, B., Bachanek-Bankowska, K., Cabana, M., Calvo-Pinilla, E., Viaplana, E., Frost, L., Gubbins, S., Urniza, A., Mertens, P. & Castillo-Olivares, J. 2014. Vaccination of horses with a recombinant modified vaccinia Ankara virus (MVA) expressing African horse sickness (AHS) virus major capsid protein VP2 provides complete clinical protection against challenge. *Vaccine,* 32**,** 3670-3674.

Alexander, R. A. 1935. Studies on the neurotropic virus of horsesickness. I. Neurotropic fixation. *Onderstepoort Journal of Veterinary Science and Animal Industry,* 4**,** 291-322.

Amelung, S., Nerlich, A., Rohde, M., Spellerberg, B., Cole, J. N., Nizet, V., Chhatwal, G. S. & Talay, S. R. 2011. The FbaB-type fibronectin-binding protein of *Streptococcus pyogenes* promotes specific invasion into endothelial cells. *Cellular Microbiology,* 13**,** 1200-1211.

Baeshen, N. A., Baeshen, M. N., Sheikh, A., Bora, R. S., Ahmed, M. M. M., Ramadan, H. A., Saini, K. S. & Redwan, E. M. 2014. Cell factories for insulin production. *Microbial cell factories,* 13**,** 141.

Barta, A., Sommergruber, K., Thompson, D., Hartmuth, K., Matzke, M. A. & Matzke, A. J. 1986. The expression of a nopaline synthase—human growth hormone chimaeric gene in transformed tobacco and sunflower callus tissue. *Plant Molecular Biology,* 6**,** 347-357.

Belyaev, A. S. & Roy, P. 1993. Development of baculovirus triple and quadruple expression vectors: co-expression of three or four bluetongue virus proteins and the synthesis of bluetongue virus-like particles in insect cells. *Nucleic Acids Research,* 21**,** 1219-1223.

Bentley, L., Fehrsen, J., Jordaan, F., Huismans, H. & Du Plessis, D. H. 2000. Identification of antigenic regions on VP2 of African horsesickness virus serotype 3 by using phage-displayed epitope libraries. *Journal of General Virology,* 81**,** 993-1000.

Bhaskar, P. B., Venkateshwaran, M., Wu, L., Ané, J.-M. & Jiang, J. 2009. Agrobacterium-mediated transient gene expression and silencing: a rapid tool for functional gene assay in potato. *PLoS One,* 4. https://doi.org/10.1371/journal.pone.0005812.

Bolanos-Garcia, V. M. & Davies, O. R. 2006. Structural analysis and classification of native proteins from *E. coli* commonly co-purified by immobilised metal affinity chromatography. *Biochimica et Biophysica Acta (BBA)-General Subjects,* 1760**,** 1304-1313.

Bordon, E., Shope, R. & Murphy, F. 1971. Physiochemical and morphological relationships of some arthropod-borne viruses to bluetongue virus-a new taxonomic group: physiochemical and serological studies. *Journal of General Virology,* 13**,** 261-266.

Boyce, M., Celma, C. C. & Roy, P. 2008. Development of reverse genetics systems for bluetongue virus: recovery of infectious virus from synthetic RNA transcripts. *Journal of virology,* 82**,** 8339-8348.

Brune, K. D., Leneghan, D. B., Brian, I. J., Ishizuka, A. S., Bachmann, M. F., Draper, S. J., Biswas, S. & Howarth, M. 2016. Plug-and-Display: decoration of virus-like particles via isopeptide bonds for modular immunization. *Scientific Reports,* 6**,** 19234.

Burrage, T., Trevejo, R., Stone-Marschat, M. & Laegreid, W. 1993. Neutralizing epitopes of African horsesickness virus serotype 4 are located on VP2. *Virology,* 196**,** 799-803.

Calvo-Pinilla, E., De La Poza, F., Gubbins, S., Mertens, P. P. C., Ortego, J. & Castillo-Olivares, J. 2014. Vaccination of mice with a modified Vaccinia Ankara (MVA) virus expressing the African horse sickness virus (AHSV) capsid protein VP2 induces virus neutralising antibodies that confer protection against AHSV upon passive immunisation. *Virus Research,* 180**,** 23-30.

Calvo-Pinilla, E., De La Poza, F., Gubbins, S., Mertens, P. P. C., Ortego, J. & Castillo-Olivares, J. 2015. Antiserum from mice vaccinated with modified vaccinia Ankara virus expressing African horse

sickness virus (AHSV) VP2 provides protection when it is administered 48 h before, or 48 h after challenge. *Antiviral Research,* 116**,** 27-33.

Castillo-Olivares, J., Calvo-Pinilla, E., Casanova, I., Bachanek-Bankowska, K., Chiam, R., Maan, S., Nieto, J. M., Ortego, J. & Mertens, P. P. C. 2011. A modified vaccinia Ankara virus (MVA) vaccine expressing African horse sickness virus (AHSV) VP2 protects against AHSV challenge in an IFNAR−/− mouse model. *PloS One,* 6. https://doi.org/10.1371/journal.pone.0016503.

Celma, C. C. & Roy, P. 2009. A viral nonstructural protein regulates bluetongue virus trafficking and release. *Journal of Virology,* 83**,** 6806-6816.

Chackerian, B. 2007. Virus-like particles: flexible platforms for vaccine development. *Expert Review of Vaccines,* 6**,** 381-390.

Charlton Hume, H. K., Vidigal, J., Carrondo, M. J., Middelberg, A. P., Roldão, A. & Lua, L. H. 2019. Synthetic biology for bioengineering virus-like particle vaccines. *Biotechnology and Bioengineering,* 116**,** 919-935.

Chen, Q. & Lai, H. 2013. Plant-derived virus-like particles as vaccines. *Human Vaccines & Immunotherapeutics,* 9**,** 26-49.

Chiam, R., Sharp, E., Maan, S., Rao, S., Mertens, P., Blacklaws, B., Davis-Poynter, N., Wood, J. & Castillo-Olivares, J. 2009. Induction of antibody responses to African horse sickness virus (AHSV) in ponies after vaccination with recombinant modified vaccinia Ankara (MVA). *PLoS One,* 4. https://doi.org/10.1371/journal.pone.0005997.

Coetzer, J. & Guthrie, A. 2004. African horse sickness. *Infectious diseases of livestock,* 2**,** 1231-1246.

Dai, X., Xiong, Y., Li, N. & Jian, C. 2019. Vaccine types. *Vaccines-the History and Future.* IntechOpen. DOI: 10.5772/intechopen.84626.

Debeljak, N., Feldman, L., Davis, K. L., Komel, R. & Sytkowski, A. J. 2006. Variability in the immunodetection of His-tagged recombinant proteins. *Analytical Biochemistry,* 359**,** 216-223.

Demissie, G. H. 2013. Seroepidemiological Study of African horse sickness in Southern Ethiopia. *Open Science Repository Veterinary Medicine*. DOI: 10.7392/Research.70081919.

Dennis, S. J., Meyers, A. E., Guthrie, A. J., Hitzeroth, Ii & Rybicki, E. P. 2018a. Immunogenicity of plant-produced African horse sickness virus-like particles: implications for a novel vaccine. *Plant Biotechnology Journal,* 16**,** 442-450.

Dennis, S. J., Meyers, A. E., Hitzeroth, I. I. & Rybicki, E. P. 2019. African Horse Sickness: A Review of Current Understanding and Vaccine Development. *Viruses,* 11**,** 844.

Dennis, S. J., O'kennedy, M. M., Rutkowska, D., Tsekoa, T., Lourens, C. W., Hitzeroth, Ii, Meyers, A. E. & Rybicki, E. P. 2018b. Safety and immunogenicity of plant-produced African horse sickness virus-like particles in horses. *Veterinary Research,* 49**,** 105.

Du Plessis, M., Cloete, M., Aitchison, H. & Van Dijk, A. 1998. Protein aggregation complicates the development of baculovirus-expressed African horsesickness virus serotype 5 VP2 subunit vaccines. *Onderstepoort Journal of Veterinary Research*, 65(4), 321-329.

El Garch, H., Crafford, J., Amouyal, P., Durand, P., Toulemonde, C. E., Lemaitre, L., Cozette, V., Guthrie, A. & Minke, J. 2012. An African horse sickness virus serotype 4 recombinant canarypox virus vaccine elicits specific cell-mediated immune responses in horses. *Veterinary Immunology and Immunopathology,* 149**,** 76-85.

Feenstra, F., Van Gennip, R. G., Maris-Veldhuis, M., Verheij, E. & Van Rijn, P. A. 2014. Bluetongue virus without NS3/NS3a expression is not virulent and protects against virulent bluetongue virus challenge. *Journal of General Virology,* 95**,** 2019-2029.

Fischer, R., Stoger, E., Schillberg, S., Christou, P. & Twyman, R. M. 2004. Plant-based production of biopharmaceuticals. *Current Opinion in Plant Biology,* 7**,** 152-158.

Foged, C., Rades, T., Perrie, Y. and Hook, S., eds. 2015. Subunit vaccine delivery. *Springer*. https://doi.org/10.1007/978-1-4939-1417-3.

Frietze, K. M., Peabody, D. S. & Chackerian, B. 2016. Engineering virus-like particles as vaccine platforms. *Current Opinion in Virology,* 18**,** 44-49.

Garabagi, F., Mclean, M. D. & Hall, J. C. 2012. Transient and stable expression of antibodies in *Nicotiana* species. *Methods in Molecular Biology*, 907, 389-408.

Gordon, S. J., Bolwell, C., Rogers, C. W., Musuka, G., Kelly, P., Guthrie, A., Mellor, P. S. & Hamblin, C. 2017. The sero-prevalence and sero-incidence of African horse sickness and equine encephalosis in selected horse and donkey populations in Zimbabwe. *Onderstepoort Journal of Veterinary Research,* 84**,** 1-5.

Gorman, B. M., Taylor, J. & Walker, P. J. 1983. Orbiviruses. *The Reoviridae,* 287-357.

Goulet, M.-C., Gaudreau, L., Gagné, M., Maltais, A.-M., Laliberté, A.-C., Éthier, G., Bechtold, N., Martel, M., D'aoust, M.-A. & Gosselin, A. 2019. Production of biopharmaceuticals in *Nicotiana benthamiana*–Axillary stem growth as a key determinant of total protein yield. *Frontiers in Plant Science,* 10**,** 735.

Govasli, M. L., Diaz, Y. & Puntervoll, P. 2019. Virus-like particle-display of the enterotoxigenic *Escherichia coli* heat-stable toxoid STh-A14T elicits neutralizing antibodies in mice. *Vaccine,* 37**,** 6405-6414.

Guthrie, A. J., Quan, M., Lourens, C. W., Audonnet, J.-C., Minke, J. M., Yao, J., He, L., Nordgren, R., Gardner, I. A. & Maclachlan, N. J. 2009. Protective immunization of horses with a recombinant canarypox virus vectored vaccine co-expressing genes encoding the outer capsid proteins of African horse sickness virus. *Vaccine,* 27**,** 4434-4438.

Hassan, S., Wirblich, C., Forzan, M. & Roy, P. 2001. Expression and functional characterization of bluetongue virus VP5 protein: role in cellular permeabilization. *Journal of Virology,* 75**,** 8356-8367.

Hatlem, D., Trunk, T., Linke, D. & Leo, J. C. 2019. Catching a SPY: Using the SpyCatcher-SpyTag and related systems for labeling and localizing bacterial proteins. *International Journal of Molecular Sciences,* 20**,** 2129.

Hiatt, A., Caffferkey, R. & Bowdish, K. 1989. Production of antibodies in transgenic plants. *Nature,* 342**,** 76.

Howell, P. 1962. The isolation and identification of further antigenic types of African horsesickness virus. *Onderstepoort Journal of Veterinary Research*, 29, 139-149.

Huang, X., Wang, X., Zhang, J., Xia, N. & Zhao, Q. 2017. *Escherichia coli*-derived virus-like particles in vaccine development. *Nature Partner Journals Vaccines,* 2 (3). https://doi.org/10.1038/s41541-017-0006-8.

Huismans, H., Van Dijk, A. A. & Els, H. J. 1987. Uncoating of parental bluetongue virus to core and subcore particles in infected L cells. *Virology,* 157**,** 180-188.

Janitzek, C. M., Matondo, S., Thrane, S., Nielsen, M. A., Kavishe, R., Mwakalinga, S. B., Theander, T. G., Salanti, A. & Sander, A. F. 2016. Bacterial superglue generates a full-length circumsporozoite protein virus-like particle vaccine capable of inducing high and durable antibody responses. *Malaria Journal,* 15**,** 1-9.

Jennings, G. T. & Bachmann, M. F. 2008. The coming of age of virus-like particle vaccines. *Biological Chemistry,* 389**,** 521-536.

Kanagarajan, S., Muthusamy, S., Gliszczyńska, A., Lundgren, A. & Brodelius, P. E. 2012. Functional expression and characterization of sesquiterpene synthases from *Artemisia annua L*. using transient expression system in *Nicotiana benthamiana*. *Plant Cell Reports,* 31**,** 1309-1319.

Kanai, Y., Van Rijn, P. A., Maris-Veldhuis, M., Kaname, Y., Athmaram, T. & Roy, P. 2014. Immunogenicity of recombinant VP2 proteins of all nine serotypes of African horse sickness virus. *Vaccine,* 32**,** 4932-4937.

Kaname, Y., Celma, C. C., Kanai, Y. & Roy, P. 2013. Recovery of African horse sickness virus from synthetic RNA. *Journal of General Virology,* 94**,** 2259-2265.

Laegreid, W. 1994. Diagnosis of African horsesickness. *Comparative Immunology, Microbiology and Infectious Diseases,* 17**,** 297-303.

Le, C. P., Genin, P., Baines, M. & Hiscott, J. 2000. Interferon activation and innate immunity. *Reviews in Immunogenetics,* 2**,** 374-386.

Li, L., Fierer, J. O., Rapoport, T. A. & Howarth, M. 2014. Structural analysis and optimization of the covalent association between SpyCatcher and a peptide Tag. *Journal of Molecular Biology,* 426**,** 309-317.

Li, S.-F., Gong, M.-J., Zhao, F.-R., Shao, J.-J., Xie, Y.-L., Zhang, Y.-G. & Chang, H.-Y. 2018. Type I interferons: distinct biological activities and current applications for viral infection. *Cellular Physiology and Biochemistry,* 51**,** 2377-2396.

Liebenberg, D., Van Hamburg, H., Piketh, S. & Burger, R. 2015. Comparing the effect of modeled climatic variables on the distribution of African horse sickness in South Africa and Namibia. *Journal of Vector Ecology,* 40**,** 333-341.

Lulla, V., Losada, A., Lecollinet, S., Kerviel, A., Lilin, T., Sailleau, C., Beck, C., Zientara, S. & Roy, P. 2017. Protective efficacy of multivalent replication-abortive vaccine strains in horses against African horse sickness virus challenge. *Vaccine,* 35**,** 4262-4269.

Lulla, V., Lulla, A., Wernike, K., Aebischer, A., Beer, M. & Roy, P. 2016. Assembly of replication-incompetent African horse sickness virus particles: rational design of vaccines for all serotypes. *Journal of Virology,* 90**,** 7405-7414.

Twyman, R. M., Schillberg, S. & Fischer, R. 2013. Optimizing the yield of recombinant pharmaceutical proteins in plants. *Current Pharmaceutical Design,* 19**,** 5486-5494.

Ma, J. K., Drake, P. M. & Christou, P. 2003. Genetic modification: the production of recombinant pharmaceutical proteins in plants. *Nature Reviews Genetics,* 4**,** 794.

Maclachlan, N. J. & Guthrie, A. J. 2010. Re-emergence of bluetongue, African horse sickness, and other orbivirus diseases. *Veterinary Research,* 41**,** 35.

Maclean, J., Koekemoer, M., Olivier, A., Stewart, D., Hitzeroth, I., Rademacher, T., Fischer, R., Williamson, A.-L. & Rybicki, E. 2007. Optimization of human papillomavirus type 16 (HPV-16) L1 expression in plants: comparison of the suitability of different HPV-16 L1 gene variants and different cell-compartment localization. *Journal of General Virology,* 88**,** 1460-1469.

Manning, N. M., Bachanek-Bankowska, K., Mertens, P. P. C. & Castillo-Olivares, J. 2017. Vaccination with recombinant Modified Vaccinia Ankara (MVA) viruses expressing single African horse sickness virus VP2 antigens induced cross-reactive virus neutralising antibodies (VNAb) in horses when administered in combination. *Vaccine,* 35**,** 6024-6029.

Manole, V., Laurinmäki, P., Van Wyngaardt, W., Potgieter, C. A., Wright, I. M., Venter, G. J., Van Dijk, A. A., Sewell, B. T. & Butcher, S. J. 2012. Structural insight into African horsesickness virus infection. *Journal of Virology,* 86**,** 7858-7866.

Maree, S., Maree, F. F., Putterill, J. F., De Beer, T. A., Huismans, H. & Theron, J. 2016. Synthesis of empty African horse sickness virus particles. *Virus Research,* 213**,** 184-194.

Marini, A., Zhou, Y., Li, Y., Taylor, I. J., Leneghan, D. B., Jin, J., Zaric, M., Mekhaiel, D., Long, C. A. & Miura, K. 2019. A universal Plug-and-Display vaccine carrier based on HBsAg VLP to maximize effective antibody response. *Frontiers in Immunology,* 10**,** 2931.

Marín-López, A., Calvo-Pinilla, E., Barriales, D., Lorenzo, G., Benavente, J., Brun, A., Martínez-Costas, J.M. and Ortego, J. 2017. Microspheres-prime/rMVA-boost vaccination enhances humoral and cellular immune response in IFNAR (−/−) mice conferring protection against serotypes 1 and 4 of bluetongue virus. *Antiviral Research*, 142, 55-62.

Marín-López, A., Otero-Romero, I., de la Poza, F., Menaya-Vargas, R., Calvo-Pinilla, E., Benavente, J., Martínez-Costas, J.M. and Ortego, J. 2014. VP2, VP7, and NS1 proteins of bluetongue virus targeted in avian reovirus muNS-Mi microspheres elicit a protective immune response in IFNAR (−/−) mice. *Antiviral Research*, 110, 42-51.

Martínez-Torrecuadrada, J. L. & Casal, J. I. 1995. Identification of a linear neutralization domain in the protein VP2 of African horse sickness virus. *Virology,* 210**,** 391-399.

Martínez-Torrecuadrada, J. L., Díaz-Laviada, M., Roy, P., Sánchez, C., Vela, C., Sánchez-Vizcaíno, J. M. & Casal, J. I. 1996. Full protection against African horsesickness (AHS) in horses induced by baculovirus-derived AHS virus serotype 4 VP2, VP5 and VP7. *Journal of General Virology,* 77**,** 1211-1221.

Martínez-Torrecuadrada, J. L., Langeveld, J. P., Meloen, R. H. & Casal, J. I. 2001. Definition of neutralizing sites on African horse sickness virus serotype 4 VP2 at the level of peptides. *Journal of General Virology,* 82**,** 2415-2424.

Matsuo, E., Celma, C. C., Boyce, M., Viarouge, C., Sailleau, C., Dubois, E., Bréard, E., Thiéry, R., Zientara, S. & Roy, P. 2011. Generation of replication-defective virus-based vaccines that confer full protection in sheep against virulent bluetongue virus challenge. *Journal Of Virology,* 85**,** 10213-10221.

Matsuo, E. & Roy, P. 2009. Bluetongue virus VP6 acts early in the replication cycle and can form the basis of chimeric virus formation. *Journal of Virology,* 83**,** 8842-8848.

Mcintosh, B. M. 1958. Immunological types of horsesickness virus and their significance in immunization. *Onderstepoort Journal of Veterinary Research*. 1958 (27), 465-536

Mellor, P. S. & Hamblin, C. 2004. African horse sickness. *Veterinary Research,* 35**,** 445-66.

Mir-Artigues, P., Twyman, R. M., Alvarez, D., Cerda, P., Balcells, M., Christou, P. & Capell, T. 2019. A simplified techno-economic model for the molecular pharming of antibodies. *Biotechnology and Bioengineering*, 116 (10), 2526-2539.

Molina-Cruz, A., Garver, L. S., Alabaster, A., Bangiolo, L., Haile, A., Winikor, J., Ortega, C., Van Schaijk, B. C., Sauerwein, R. W. & Taylor-Salmon, E. 2013. The human malaria parasite Pfs47 gene mediates evasion of the mosquito immune system. *Science,* 340**,** 984-987.

Morales-Briceño, A. African horse sickness: A practice update. 2020. *Microbiology Research International*, 9 (1), 16-20.

Nandi, S., Kwong, A. T., Holtz, B. R., Erwin, R. L., Marcel, S. & Mcdonald, K. A. 2016. Techno-economic analysis of a transient plant-based platform for monoclonal antibody production. *Monoclonal Antibodies Journal*, 8 (8), 1456-1466.

Nascimento, I. & Leite, L. 2012. Recombinant vaccines and the development of new vaccine strategies. *Brazilian Journal of Medical and Biological Research,* 45**,** 1102-1111.

Nino-Fong, R. & Johnston, J. B. 2008. Poxvirus-based vaccine platforms: getting at those hard-to-reach places. *Future Virology*, 3 (2). https://doi.org/10.2217/17460794.3.2.99.

Noad, R. & Roy, P. 2003. Virus-like particles as immunogens. *Trends in Microbiology,* 11**,** 438-444.

Norkunas, K., Harding, R., Dale, J. & Dugdale, B. 2018. Improving agroinfiltration-based transient gene expression in *Nicotiana benthamiana*. *Plant Methods,* 14**,** 1-14.

Ozawa, Y. 1968. Studies on the properties of African horse-sickness virus. *Japanese Journal of Medical Science and Biology,* 21**,** 27-39.

Ozawa, Y. & Bahrami, S. 1966. African horse-sickness killed-virus tissue culture vaccine. *Canadian Journal of Comparative Medicine and Veterinary Science,* 30**,** 311.

Ozawa, Y., Hazrati, A. & Bahrami, S. 1967. African Horse-Sickness Live and Killed Virus Tissue Culture Vaccine. *Canadian Journal of Comparative Medicine and Veterinary Science*, 30 (11), 311-314.

Paillot, R. 2020. Special Issue "Equine Viruses": Old "Friends" and New Foes? *Viruses*, 12(2), 153.

Palladini, A., Thrane, S., Janitzek, C. M., Pihl, J., Clemmensen, S. B., De Jongh, W. A., Clausen, T. M., Nicoletti, G., Landuzzi, L. & Penichet, M. L. 2018. Virus-like particle display of HER2 induces potent anti-cancer responses. *Oncoimmunology,* 7 (3). DOI: 10.1080/2162402x.2017.1408749.

Pastoret, P. P. & Vanderplasschen, A. 2003. Poxviruses as vaccine vectors. *Comparative Immunology, Microbiology and Infectious Diseases,* 26**,** 343-355.

Pastori, C., Tudor, D., Diomede, L., Drillet, A., Jegerlehner, A., Röhn, T., Bomsel, M. & Lopalco, L. 2012. Virus like particle based strategy to elicit HIV-protective antibodies to the alpha-helic regions of gp41. *Virology,* 431**,** 1-11.

Peyret, H., Ponndorf, D., Meshcheriakova, Y., Richardson, J. & Lomonossoff, G. P. 2020. Covalent protein display on Hepatitis B core-like particles in plants through the *in vivo* use of the SpyTag/SpyCatcher system. *Scientific Reports,* 10**,** 1-13.

Potgieter, A., Cloete, M., Pretorius, P. & Van Dijk, A. 2003. A first full outer capsid protein sequence data-set in the Orbivirus genus (family Reoviridae): cloning, sequencing, expression and analysis of a complete set of full-length outer capsid VP2 genes of the nine African horsesickness virus serotypes. *Journal of General Virology,* 84**,** 1317-1326.

Potgieter, A., Page, N., Liebenberg, J., Wright, I., Landt, O. & Van Dijk, A. 2009. Improved strategies for sequence-independent amplification and sequencing of viral double-stranded RNA genomes. *Journal of General Virology,* 90**,** 1423-1432.

Pujar, N., Low, D. & O'leary, R. 2009. Antibody purification: drivers of change. *Process Scale Purification of Antibodies***,** 407-426.

Robin, M., Page, P., Archer, D. & Baylis, M. 2016. African horse sickness: The potential for an outbreak in disease-free regions and current disease control and elimination techniques. *Equine Veterinary Journal,* 48**,** 659-669.

Röder, J., Fischer, R. & Commandeur, U. 2017. Engineering potato virus X particles for a covalent protein based attachment of enzymes. *Small,* 13 (48). https://doi.org/10.1002/smll.201702151.

Rodríguez, M., Joseph, S., Pfeffer, M., Raghavan, R. & Wernery, U. 2020. Immune response of horses to inactivated African horse sickness vaccines. *BioMed Central Veterinary Research,* 16**,** 1-13.

Roy, P. 2004. Genetically engineered structure-based vaccine for bluetongue disease. *Veterinaria Italiana,* 40**,** 594-600.

Roy, P. 2008. Bluetongue virus: dissection of the polymerase complex. *The Journal of General Virology,* 89**,** 1789.

Roy, P., Bishop, D. H., Howard, S., Aitchison, H. & Erasmus, B. 1996. Recombinant baculovirus-synthesized African horsesickness virus (AHSV) outer-capsid protein VP2 provides protection against virulent AHSV challenge. *Journal of General Virology,* 77**,** 2053-2057.

Roy, P., Bishop, D. H., Leblois, H. & Erasmus, B. J. 1994a. Long-lasting protection of sheep against bluetongue challenge after vaccination with virus-like particles: evidence for homologous and partial heterologous protection. *Vaccine,* 12**,** 805-811.

Roy, P., Mertens, P. P. & Casal, I. 1994b. African horse sickness virus structure. *Comparative Immunology, Microbiology And Infectious Diseases,* 17**,** 243-273.

Rutkowska, D. A., Mokoena, N. B., Tsekoa, T. L., Dibakwane, V. S. & O'kennedy, M. M. 2019. Plant-produced chimeric virus-like particles-a new generation vaccine against African horse sickness. *BioMed Central Veterinary Research,* 15**,** 432.

Rybicki, E. P. 2010. Plant-made vaccines for humans and animals. *Plant Biotechnology Journal,* 8**,** 620-37.

Scacchia, M., Molini, U., Marruchella, G., Maseke, A., Bortone, G., Cosseddu, G. M., Monaco, F., Savini, G. & Pini, A. 2015. African horse sickness outbreaks in Namibia from 2006 to 2013: clinical, pathological and molecular findings. *Veterinaria Italiana,* 51**,** 123-130.

Scanlen, M., Paweska, J., Verschoor, J. & Van Dijk, A. 2002. The protective efficacy of a recombinant VP2-based African horsesickness subunit vaccine candidate is determined by adjuvant. *Vaccine,* 20**,** 1079-1088.

Schillberg, S., Raven, N., Spiegel, H., Rasche, S. & Buntru, M. 2019. Critical analysis of the commercial potential of plants for the production of recombinant proteins. *Frontiers in Plant Science,* 10. https://doi.org/10.3389/fpls.2019.00720.

Shah, K. H., Almaghrabi, B. & Bohlmann, H. 2013. Comparison of expression vectors for transient expression of recombinant proteins in plants. *Plant Molecular Biology Reporter,* 31**,** 1529-1538.

Shen, W.-J. & Forde, B. G. 1989. Efficient transformation of Agrobacterium spp. by high voltage electroporation. *Nucleic Acids Research,* 17**,** 8385.

Shishovs, M., Rumnieks, J., Diebolder, C., Jaudzems, K., Andreas, L. B., Stanek, J., Kazaks, A., Kotelovica, S., Akopjana, I. & Pintacuda, G. 2016. Structure of AP205 coat protein reveals circular permutation in ssRNA bacteriophages. *Journal of Molecular Biology,* 428**,** 4267-4279.

Sijmons, P. C., Dekker, B. M., Schrammeijer, B., Verwoerd, T. C., Van Den Elzen, P. J. & Hoekema, A. 1990. Production of correctly processed human serum albumin in transgenic plants. *Biotechnology Journal,* 8**,** 217.

Singh, S. K., Thrane, S., Janitzek, C. M., Nielsen, M. A., Theander, T. G., Theisen, M., Salanti, A. & Sander, A. F. 2017. Improving the malaria transmission-blocking activity of a Plasmodium falciparum 48/45 based vaccine antigen by SpyTag/SpyCatcher mediated virus-like display. *Vaccine,* 35**,** 3726-3732.

Smith, M. T., Hawes, A. K. & Bundy, B. C. 2013. Reengineering viruses and virus-like particles through chemical functionalization strategies. *Current Opinion in Biotechnology,* 24**,** 620-626.

Spence, R., Moore, N. & Nuttall, P. A. 1984. The biochemistry of orbiviruses. *Archives of virology,* 82**,** 1-18.

Stern, A. W. 2011. African horse sickness. *Compendium: Continuing Education for Veterinarians,* 33**,** E1-5.

Stewart, M., Dubois, E., Sailleau, C., Bréard, E., Viarouge, C., Desprat, A., Thiéry, R., Zientara, S. & Roy, P. 2013. Bluetongue virus serotype 8 virus-like particles protect sheep against virulent virus infection as a single or multi-serotype cocktail immunogen. *Vaccine,* 31**,** 553-558.

Stone-Marschat, M., Moss, S., Burrage, T., Barber, M., Roy, P. & Laegreid, W. 1996. Immunization with VP2 is sufficient for protection against lethal challenge with African horsesickness virus Type 4. *Virology,* 220**,** 219-222.

Studdert, M. 1965. Sensitivity of Bluetongue Virus to Ether and Sodium Deoxycholate. *Proceedings of the Society for Experimental Biology and Medicine,* 118**,** 1006-1009.

Sutter, G. & Moss, B. 1992. Nonreplicating vaccinia vector efficiently expresses recombinant genes. *Proceedings of the National Academy of Sciences,* 89**,** 10847-10851.

Sutter, G., Wyatt, L. S., Foley, P. L., Bennink, J. R. & Moss, B. 1994. A recombinant vector derived from the host range-restricted and highly attenuated MVA strain of vaccinia virus stimulates protective immunity in mice to influenza virus. *Vaccine,* 12**,** 1032-1040.

Syomin, B. & Ilyin, Y. 2019. Virus-like particles as an instrument of vaccine production. *Molecular Biology,* 53**,** 323-334.

Theiler, A. 1921. African horsesickness (pestis equorum). *Scientific Bulletin*, 19, 1-29.

Thrane, S., Janitzek, C. M., Matondo, S., Resende, M., Gustavsson, T., De Jongh, W. A., Clemmensen, S., Roeffen, W., Van De Vegte-Bolmer, M. & Van Gemert, G. J. 2016. Bacterial superglue enables easy development of efficient virus-like particle based vaccines. *Journal of Nanobiotechnology,* 14**,** 30.

Thuenemann, E. C., Meyers, A. E., Verwey, J., Rybicki, E. P. & Lomonossoff, G. P. 2013. A method for rapid production of heteromultimeric protein complexes in plants: assembly of protective bluetongue virus-like particles. *Plant Biotechnology Journal,* 11**,** 839-846.

Tissot, A. C., Renhofa, R., Schmitz, N., Cielens, I., Meijerink, E., Ose, V., Jennings, G. T., Saudan, P., Pumpens, P. & Bachmann, M. F. 2010a. Versatile virus-like particle carrier for epitope based vaccines. *PloS One,* 5. https://doi.org/10.1371/journal.pone.0009809.

Tissot, A. C., Renhofa, R., Schmitz, N., Cielens, I., Meijerink, E., Ose, V., Jennings, G. T., Saudan, P., Pumpens, P. & Bachmann, M. F. 2010b. Versatile virus-like particle carrier for epitope based vaccines. *PLoS One,* 5. https://doi.org/10.1371/journal.pone.0005997.

Van De Water, S. G., Van Gennip, R. G., Potgieter, C. A., Wright, I. M. & Van Rijn, P. A. 2015. VP2 Exchange and NS3/NS3a Deletion in African Horse Sickness Virus (AHSV) in Development of Disabled Infectious Single Animal Vaccine Candidates for AHSV. *Journal of Virology,* 89**,** 8764-72.

Van Gennip, R. G., Van De Water, S. G., Potgieter, C. A. & Van Rijn, P. A. 2017. Structural protein VP2 of African horse sickness virus is not essential for virus replication in vitro. *Journal of Virology,* 91**.** DOI: 10.1128/JVI.01328-16

Van Gennip, R. G., Van De Water, S. G. & Van Rijn, P. A. 2014. Bluetongue virus nonstructural protein NS3/NS3a is not essential for virus replication. *PloS One,* 9. https://doi.org/10.1371/journal.pone.0085788.

Van Rijn, P. A., Maris-Veldhuis, M. A., Boonstra, J. & Van Gennip, R. G. 2018a. Diagnostic DIVA tests accompanying the Disabled Infectious Single Animal (DISA) vaccine platform for African horse sickness. *Vaccine,* 36**,** 3584-3592.

Van Rijn, P. A., Maris-Veldhuis, M. A., Grobler, M., Wright, I. M., Erasmus, B. J., Maartens, L. H. & Potgieter, C. A. 2020. Safety and efficacy of inactivated African horse sickness (AHS) vaccine formulated with different adjuvants. *Vaccine,* 38**,** 7108-7117.

Van Rijn, P. A., Maris-Veldhuis, M. A., Potgieter, C. A. & Van Gennip, R. G. 2018b. African horse sickness virus (AHSV) with a deletion of 77 amino acids in NS3/NS3a protein is not virulent and a safe promising AHS Disabled Infectious Single Animal (DISA) vaccine platform. *Vaccine,* 36**,** 1925-1933.

Van Rijn, P. A., Van De Water, S. G., Feenstra, F. & Van Gennip, R. G. 2016. Requirements and comparative analysis of reverse genetics for bluetongue virus (BTV) and African horse sickness virus (AHSV). *Virology Journal,* 13**,** 119.

Van Zyl, A. R., Meyers, A. E. & Rybicki, E. P. 2016. Transient Bluetongue virus serotype 8 capsid protein expression in *Nicotiana benthamiana*. *Biotechnology Reports,* 9**,** 15-24.

Venter, M., Napier, G. & Huismans, H. 2000. Cloning, sequencing and expression of the gene that encodes the major neutralisation-specific antigen of African horsesickness virus serotype 9. *Journal of Virological Methods,* 86**,** 41-53.

Vermaak, E., Paterson, D. J., Conradie, A. & Theron, J. 2015. Directed genetic modification of African horse sickness virus by reverse genetics. *South African Journal of Science,* 111**,** 1-8.

Verwoerd, D. W. 2012. History of orbivirus research in South Africa. *Journal of the South African Veterinary Association,* 83**,** 1-6.

Von Teichman, B. F., Dungu, B. & Smit, T. K. 2010. *In vivo* cross-protection to African horse sickness Serotypes 5 and 9 after vaccination with Serotypes 8 and 6. *Vaccine,* 28**,** 6505-17.

Voss, A., Niersbach, M., Hain, R., Hirsch, H. J., Liao, Y. C., Kreuzaler, F. & Fischer, R. 1995. Reduced virus infectivity in N. tabacum secreting a TMV-specific full-size antibody. *Molecular Breeding,* 1**,** 39-50.

Wernery, U., Joseph, S., Elizabeth, S. K., Patteril, N., Wernery, R. & Spendrup, S. 2016. Production of an African Horse Sickness killed vaccine containing all 9 serotypes. *Journal of Equine Veterinary Science***,** 39, S101-S102.

Weyer, C. T., Grewar, J. D., Burger, P., Rossouw, E., Lourens, C., Joone, C., Le Grange, M., Coetzee, P., Venter, E. & Martin, D. P. 2016. African horse sickness caused by genome reassortment and reversion to virulence of live, attenuated vaccine viruses, South Africa, 2004–2014. *Emerging Infectious Diseases,* 22**,** 2087.

Yenkoidiok-Douti, L., Williams, A. E., Canepa, G. E., Molina-Cruz, A. & Barillas-Mury, C. 2019. engineering a virus-Like particle as an antigenic platform for a Pfs47-targeted malaria transmission-blocking vaccine. *Scientific Reports,* 9**,** 1-9.

Yu, G., Xian, L., Sang, Y. & Macho, A. P. 2019. Cautionary notes on the use of Agrobacterium-mediated transient gene expression upon SGT 1 silencing in *Nicotiana benthamiana*. *New Phytologist,* 222**,** 14-17.

Zahmanova, G. G., Mazalovska, M., Takova, K. H., Toneva, V. T., Minkov, I. N., Mardanova, E. S., Ravin, N. V. & Lomonossoff, G. P. 2020. Rapid high-yield transient expression of swine hepatitis E ORF2 capsid proteins in *Nicotiana benthamiana* plants and production of chimeric hepatitis E virus-like particles bearing the M2e influenza epitope. *Plants,* 9**,** 29.

Zakeri, B., Fierer, J. O., Celik, E., Chittock, E. C., Schwarz-Linek, U., Moy, V. T. & Howarth, M. 2012. Peptide tag forming a rapid covalent bond to a protein, through engineering a bacterial adhesin. *Proceedings of the National Academy of Sciences,* 109**,** E690-E697.

Zhang, X., Boyce, M., Bhattacharya, B., Zhang, X., Schein, S., Roy, P. & Zhou, Z. H. 2010. Bluetongue virus coat protein VP2 contains sialic acid-binding domains, and VP5 resembles enveloped virus fusion proteins. *Proceedings of the National Academy of Sciences,* 107**,** 6292-6297.

Zientara, S., Weyer, C. T. & Lecollinet, S. 2015. African horse sickness. *Revue Scientifique et Technique*, 34 (2), 315-27.

Appendices

Appendix A: pEAQ-AHSV 5 VP2domain SpyCatcher plasmid map and sequence

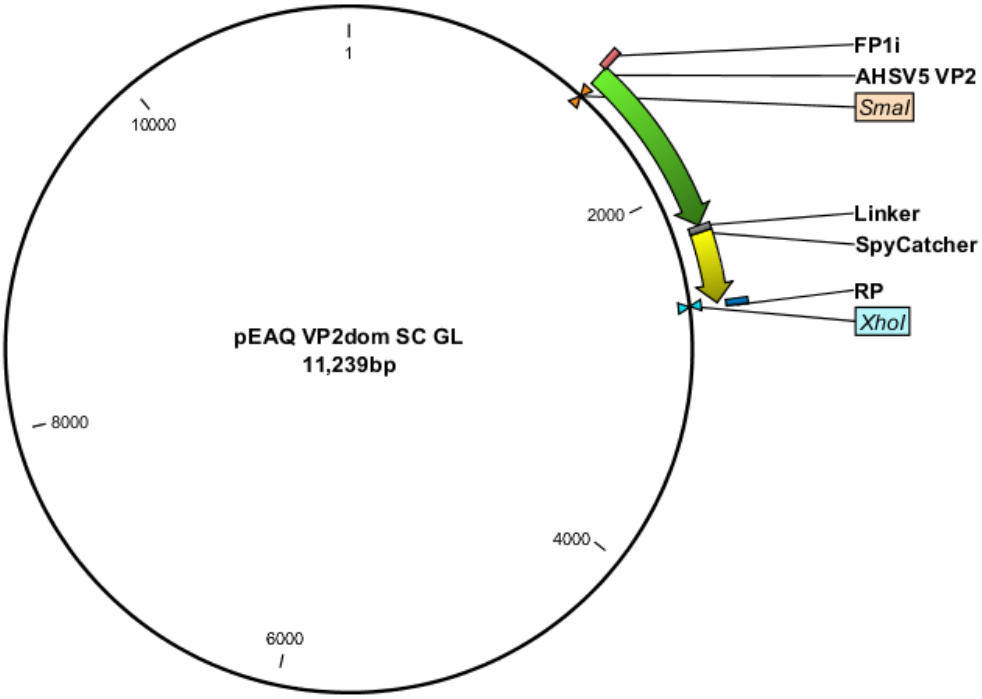

Figure 1. pEAQ-AHSV 5 VP2domSC plasmid map. Construct cloned into pEAQ-*HT* vector using forward primer (FP1i, red) and reverse primer (RP, blue) at 5' *SmaI* and 3' *XhoI* site, respectively. AHSV5 VP2domain (green) is fused to SpyCatcher (yellow) using linker (GGS, grey).

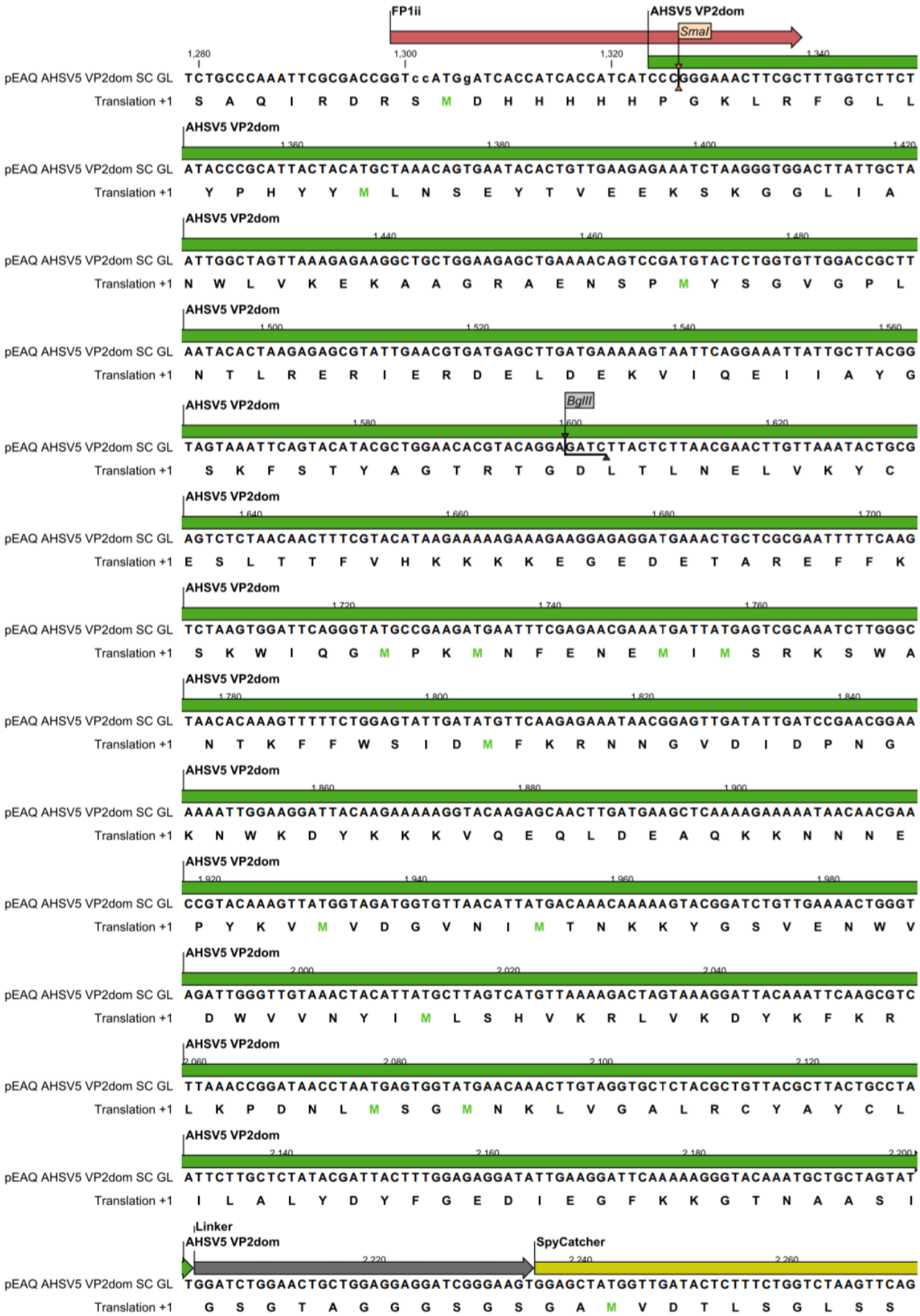
FP1ii
AHSV5 VP2dom
SmaI
pEAQ AHSV5 VP2dom SC GL
Translation +1
AHSV5 VP2dom
BglII
Linker
SpyCatcher

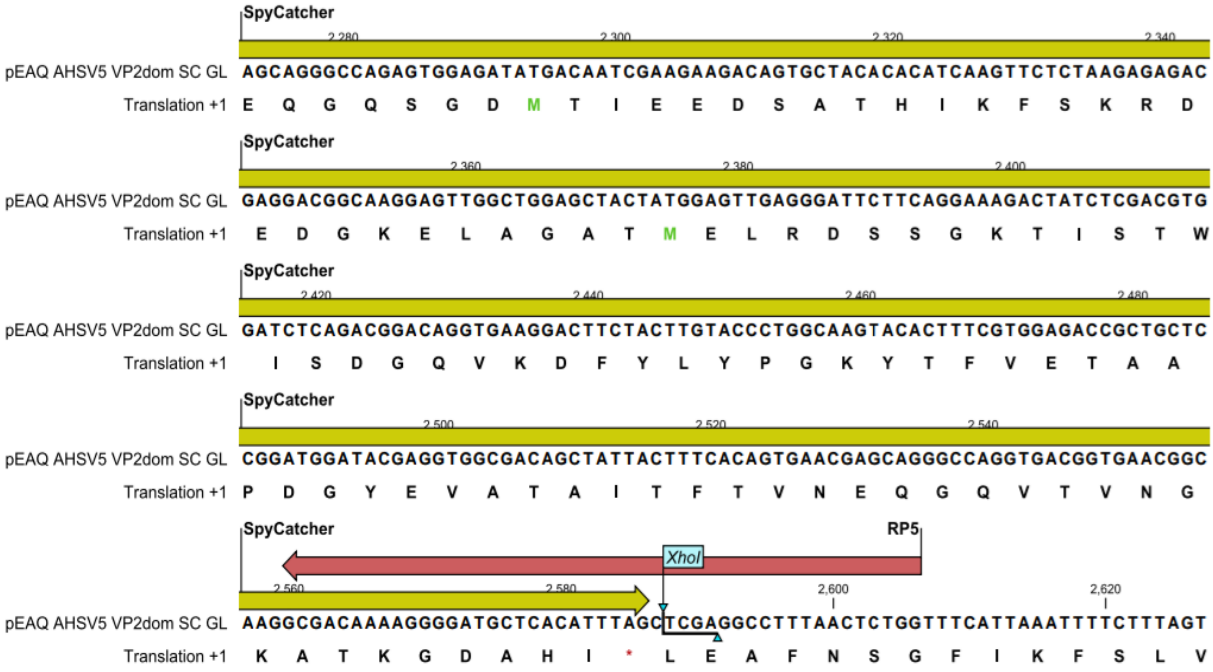

Figure 2. AHSV 5 VP2domSC sequence. Construct cloned into pEAQ-*HT* vector using forward primer (FP1ii) and reverse primer (RP5) at 5' *SmaI* and 3' *XhoI* site, respectively. AHSV5 VP2domain (green) is fused to SpyCatcher (yellow) using linker (GGS, grey).

Appendix B: Supplementary western blots of AHSV 5 VP2domain SpyCatcher protein purification

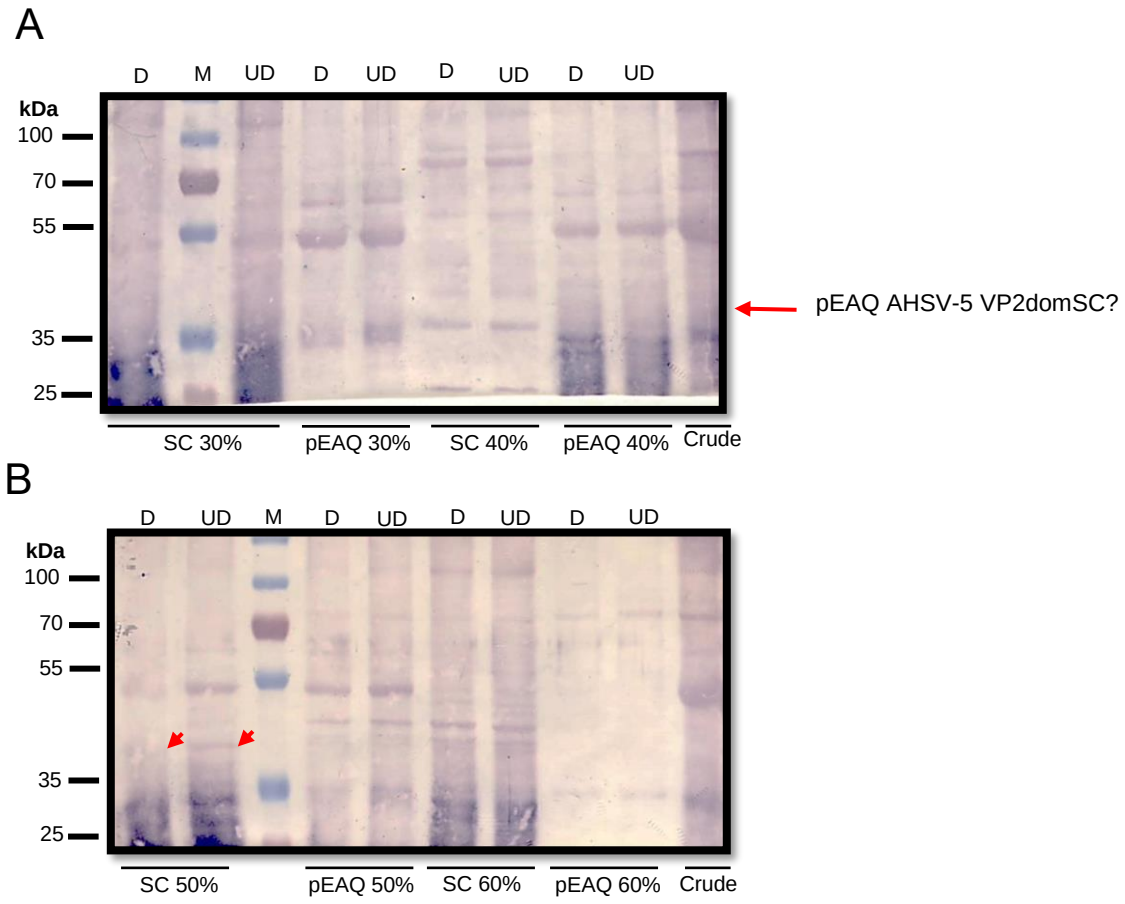

Figure 3: Purification of AHSV5 VP2domSC protein by ammonium sulphate precipitation. (A) 30 – 40% and (B) 50 – 60% $(NH_4)_2SO_4$ precipitation of VP2domSC and pEAQ-*HT*, dialysed (D) and undialysed (UD). Equal volumes of clarified crude plant extract and purified fractions were loaded in each lane. Empty pEAQ-*HT* expression vector was used as a negative control. Guinea pig anti-AHSV 5 sera (1:3000) was used as the primary antibody and AP-conjugated goat anti-guinea pig (1: 5000) sera was used as the secondary antibody to detect crude and purified AHSV-5 VP2domSC protein (SC; 48kDa, red arrowheads. Crude extract from plants infiltrated with the VP2domSC *Agrobacterial* recombinant was used as a positive control. M: PageRuler Plus Prestained Protein Ladder (Fermentas UAB, Vilnius, Lithuania) was used as a molecular weight marker.

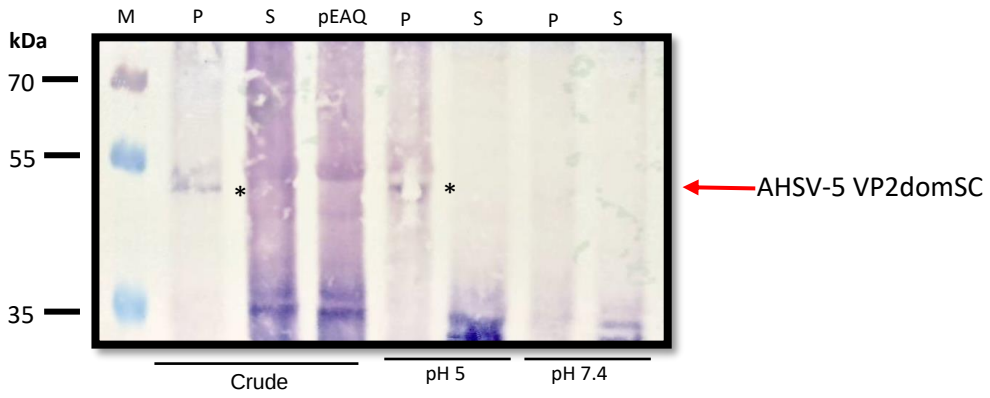

Figure 4: Purification of AHSV 5 VP2domSC protein by pH precipitation. Equal volumes of clarified pellet (P) and supernatant (S) plant crude extract and purified fractions were loaded in each lane. Empty pEAQ-*HT* expression vector was used as a negative control. Guinea pig anti-AHSV 5 sera (1:3000) was used as the primary antibody and AP-conjugated goat anti-guinea pig (1: 5000) sera was used as the secondary antibody to detect AHSV-5 VP2domSC protein (SC; 48kDa, asterisks and red arrow). Crude extract from plants infiltrated with the VP2domSC *Agrobacterial* recombinant was used as a positive control. M: PageRuler Plus Prestained Protein Ladder (Fermentas UAB, Vilnius, Lithuania) was used as a molecular weight marker.